TURUN
YLIOPISTO
UNIVERSITY
OF TURKU

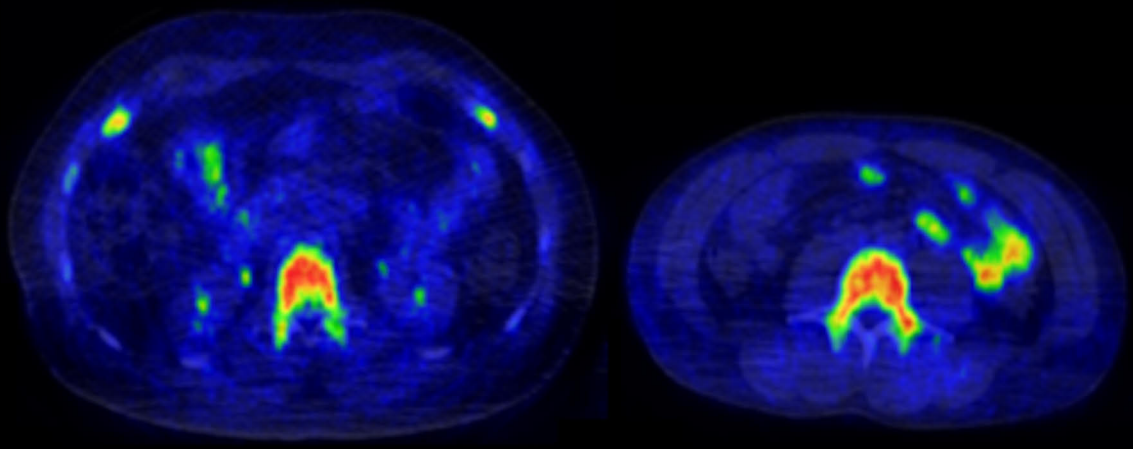

INSULIN SENSITIVITY AND ENDOCANNABINOID FUNCTION AS RISK FACTORS FOR OBESITY

Positron Emission Tomography Studies of Insulin Sensitivity and CB1 Receptors

Laura Pekkarinen

TURUN YLIOPISTON JULKAISUJA – ANNALES UNIVERSITATIS TURKUENSIS
SARJA – SER. D OSA – TOM. 1767 | MEDICA – ODONTOLOGICA | TURKU 2023

TURUN
YLIOPISTO
UNIVERSITY
OF TURKU

INSULIN SENSITIVITY AND ENDOCANNABINOID FUNCTION AS RISK FACTORS FOR OBESITY

Positron emission tomography studies of insulin sensitivity and CB1 receptors

Laura Pekkarinen

TURUN YLIOPISTON JULKAISUJA – ANNALES UNIVERSITATIS TURKUENSIS
SARJA – SER. D OSA – TOM. 1767 | MEDICA – ODONTOLOGICA | TURKU 2023

University of Turku

Faculty of Medicine
Department of Internal Medicine
Doctoral Programme in Clinical Research
Turku PET Centre
Turku, Finland

Supervised by

Professor Pirjo Nuutila, MD, PhD
Turku PET Centre
University of Turku and
Department of Endocrinology
Turku University Hospital
Turku, Finland

Professor Lauri Nummenmaa, PhD
Turku PET Centre
University of Turku
Turku, Finland

Reviewed by

Professor Hubert Preissl, Dr
Institute for Diabetes Research and
Metabolic Diseases of the
Helmholtz Center Munich
University of Tübingen
Tübingen, Germany

Docent Sanni Söderlund, MD, PhD
Endocrinology, Abdominal Center
Meilahti Hospital, Helsinki, Finland
Research Program for Clinical and
Molecular Metabolism
University of Helsinki
Helsinki, Finland

Opponent

Docent Kirsi Timonen, MD, PhD
Department of Clinical Physiology and
Nuclear Medicine at Hospital Nova
Wellbeing Services County of Central Finland
Jyväskylä, Finland

The originality of this publication has been checked in accordance with the University of Turku quality assurance system using the Turnitin OriginalityCheck service.

Cover image by Laura Pekkarinen. [^{18}F]FMPEP-d_2 PET image of one high and one low obesity risk subject.

ISBN 978-951-29-9574-5 (PRINT)
ISBN 978-951-29-9575-2 (PDF)
ISSN 0355-9483 (Print)
ISSN 2343-3213 (Online)
Painosalama, Turku, Finland 2023

To my family

UNIVERSITY OF TURKU
Faculty of Medicine
Internal Medicine
Turku PET Centre
LAURA PEKKARINEN: Insulin Sensitivity and Endocannabinoid Function as Risk Factors for Obesity. Positron Emission Tomography Studies of Insulin Sensitivity and CB1 Receptors.
Doctoral Dissertation, 155 pp.
Doctoral Programme in Clinical Research
December 2023

ABSTRACT

Obesity is a chronic disease with epidemic proportions, and it causes serious threats for human health and wellbeing. Obesity results from long-term positive energy balance, and is characterized by excessive fat accumulation. Insulin action in the brain regulates feeding behaviour and whole-body energy balance in interplay with peripheral metabolic organs. In addition, endocannabinoid system in brain and periphery modulates appetite and energy homeostasis.

Obesity is associated with increased brain insulin-simulated glucose uptake (BGU), which is turn is linked with impaired insulin suppression of hepatic glucose production (EGP) and adipose tissue lipolysis. Subjects with obesity also exhibit lower endocannabinoid type 1 receptor (CB1R) availability in brain and abdominal adipose tissue. It remains unsolved, whether these alterations are present already before the development of obesity.

The aim of this thesis was to examine whether brain and peripheral tissue insulin sensitivity and CB1R availability are altered already in pre-obese state. We studied healthy non-obese young men with either high or low obesity risk using positron emission tomography. Tissue glucose uptake was quantified with a glucose analogue radiotracer [^{18}F]FDG during hyperinsulinemic-euglycemic clamp, and CB1R availability with CB1R inverse agonist radioligand [^{18}F]FMPEP-d_2 . Insulin-stimulated BGU was increased in high as compared to low obesity risk subjects, and it was associated with decreased whole-body glucose uptake and increased insulin-suppressed EGP and serum free fatty acid levels. Familial obesity risk was associated with increased BGU. Abdominal adipose tissue CB1R availability was lower in high than low obesity-risk subjects, and associated with enlarged mass and decreased insulin sensitivity of abdominal adipose tissue. Lower cerebral CB1R availability was associated with decreased whole-body insulin sensitivity, enlarged visceral adipose tissue mass and higher levels of circulating endocannabinoids.

Altogether, these results show that altered brain insulin action and crosstalk with periphery, as well as dysregulated endocannabinoid signalling may precede obesity.

KEYWORDS: Insulin sensitivity, glucose uptake, endogenous glucose production, cannabinoid type 1 receptor, obesity, brain, adipose tissue, positron emission tomography

TURUN YLIOPISTO
Lääketieteellinen tiedekunta
Sisätautioppi
Turun PET-keskus
LAURA PEKKARINEN: Insuliiniherkkyys ja endokannabinoidijärjestelmän toiminta lihavuuden riskitekijöinä. Positroniemissiotomografiatutkimuksia insuliiniherkkyydestä ja CB1-reseptoreista.
Väitöskirja, 155 s.
Turun kliininen tohtoriohjelma
Joulukuu 2023

TIIVISTELMÄ

Lihavuus on pitkäaikainen sairaus, jonka esiintyvyys on saavuttanut epidemian mittasuhteet. Lihavuus aiheuttaa vakavan uhan terveydelle. Lihavuus on seurausta pitkäaikaisesta positiivisesta energiatasapainosta, ja sitä luonnehtii liiallinen kehon rasvamäärä. Aivojen insuliinisignalointi säätelee syömistä ja energiatasapainoa vuorovaikutuksessa ääreiskudosten kanssa. Myös aivojen ja ääreiskudosten endokannabinoidijärjestelmä vaikuttaa ruokahaluun ja energiatasapainoon.

Lihavuuteen liittyy kohonnut aivojen glukoosinotto insuliinialtistuksen aikana, mikä on yhteydessä heikentyneeseen glukoosin tuotannon ja rasvakudoksen rasvojen pilkkoutumisen estoon insuliinin vaikutuksesta. Lihavuuteen liittyy myös alentunut tyypin 1 endokannabinoidireseptorien (CB1R) saatavuus aivoissa ja vatsarasvassa. Ei kuitenkaan tiedetä, esiintyykö näitä muutoksia jo ennen lihavuuden kehittymistä.

Väitöskirjan tavoitteena oli selvittää, onko aivojen ja ääreiskudosten insuliiniherkkyydessä ja CB1R-saatavuudessa muutoksia ennen lihavuuden kehittymistä. Tutkimme positroniemissiotomografian avulla terveitä, ei-lihavia ihmisiä, joilla lihomisriski on joko suuri tai pieni. Kudosten glukoosinotto määritettiin [^{18}F]FDG-glukoosimerkkiaineen avulla hyperinsulineemisen-euglygeemisen clamp-tutkimuksen aikana, ja CB1R-saatavuus [^{18}F]FMPEP-d_2 -merkkiaineen avulla. Aivojen insuliinistimuloitu glukoosinotto oli suurempi suuren kuin pienen lihomisriskin henkilöillä, ja se oli yhteydessä pienentyneeseen kehon glukoosinottoon sekä suurentuneeseen glukoosin tuotantoon ja seerumin vapaiden rasvahappojen määrään. Perhetaustaan liittyvä lihomisriski oli yhteydessä aivojen suurentuneeseen glukoosinottoon. Vatsarasvan CB1R-saatavuus oli alhaisempi suuren kuin pienen lihomisriskin henkilöillä, ja liittyi vatsarasvan suurempaan määrään ja alentuneeseen insuliiniherkkyyteen. Aivojen alhaisempi CB1R-saatavuus liittyi alentuneeseen kehon insuliiniherkkyyteen sekä suurempaan sisäelinrasvan ja verenkierron endokannabinoidien määrään.

Tulokset osoittavat, että muutokset aivojen insuliinisignaloinnissa ja vuorovaikutuksessa ääreiskudosten kanssa sekä endokannabinoidijärjestelmän säätelyhäiriö voivat edeltää lihavuutta.

AVAINSANAT: Insuliiniherkkyys, glukoosin soluunotto, glukoosin tuotto, tyypin 1 kannabinoidireseptori, lihavuus, aivot, rasvakudos, positroniemissiotomografia

Table of Contents

Abbreviations

[^{18}F]FDG	[^{18}F]fluoro-D-glucose
[^{18}F]FMPEP-d_2	(3R,5R)-5-(3-([^{18}F]fluoromethoxy-d2)phenyl)-3-((R)-1-phenylethyl)amino)-1-(4-(trifluoromethyl)phenyl)-pyrrolidin-2-one
1-AG	1-arachidonoylglycerol
2-AG	2-arachidonoylglycerol
AA	Arachidonic acid
AEA	Anandamide
AgRP	Agouti-related peptide
ApoA1	Apolipoprotein A1
ApoB	Apolipoprotein B
ARC	Arcuate nucleus
BAT	Brown adipose tissue
BBB	Blood-brain-barrier
BGU	Brain glucose uptake
CART	Cocaine- and amphetamine-regulated transcript
CB1R	Cannabinoid receptor type 1
CB2R	Cannabinoid receptor type 2
CNS	Central nervous system
CSF	Cerebrospinal fluid
CT	Computed tomography
DEA	Docosatetraenoyl ethanolamide
DIO	Diet-induced obese
DMH	Dorsomedial hypothalamic nucleus
DMN	Default-mode network
EGP	Endogenous glucose production
ECS	Endocannabinoid system
FFA	Free fatty acid
FDR	False discovery rate
FFM	Fat-free mass
fMRI	Functional magnetic resonance imaging

FUR	Fractional uptake rate
GIR	Glucose infusion rate
GlycA	Glycoprotein acetyls
GU	Glucose uptake
HFD	High-fat diet
HR	High-risk group
hs-CRP	High-sensitivity C-reactive protein
HU	Hounsfield unit
IR	Insulin receptor
K_i	Fractional uptake
LC	Lumped constant
α-LEA	α-linolenic acid
γ-LEA	γ-linolenic acid
LH	Lateral hypothalamic nucleus
LR	Low-risk group
Matsuda-ISI	Insulin sensitivity index by Matsuda
MRI	Magnetic resonance imaging
α-MSH	α-melanocyte-stimulating hormone
MUFA	Monounsaturated fatty acids
NALS	N-arachidonoyl-L-serine
NPY	Neuropeptide Y
OGTT	Oral glucose tolerance test
PET	Positron emission tomography
POMC	Pro-opiomelanocortin
PUFA	Polyunsaturated fatty acid
PVH	Paraventricular nucleus
Rd	Rate of glucose disappearance
ROI	Regions of interest
RWAT	Retroperitoneal adipose tissue
SAT	Subcutaneous adipose tissue
SPM	Statistical parametric mapping
TAC	Time-activity curve
T2D	Type 2 diabetes
VAT	Visceral adipose tissue
VOI	Volume of interest
VMH	Ventromedial hypothalamic nucleus
V_T	Volume distribution
WAT	White adipose tissue

List of Original Publications

This dissertation is based on the following original publications, which are referred to in the text by their Roman numerals:

I Kantonen, T., Pekkarinen, L., Karjalainen, T., Bucci, M., Kalliokoski, K., Haaparanta-Solin, M., Aarnio, R., Dickens, A. M., von Eyken, A., Laitinen, K., Houttu, N., Kirjavainen, A. K., Helin, S., Hirvonen, J., Rönnemaa, T., Nuutila, P., & Nummenmaa, L. (2022). Obesity risk is associated with altered cerebral glucose metabolism and decreased μ-opioid and CB1 receptor availability. International journal of obesity (2005), 46(2), 400–407. https://doi.org/10.1038/s41366-021-00996-y.

II Pekkarinen, L., Kantonen, T., Rebelos, E., Latva-Rasku, A., Dadson, P., Karjalainen, T., Bucci, M., Kalliokoski, K., Laitinen, K., Houttu, N., Kirjavainen, A. K., Rajander, J., Rönnemaa, T., Nummenmaa, L., & Nuutila, P. (2022). Obesity risk is associated with brain glucose uptake and insulin resistance. European journal of endocrinology, 187(6), 917–928. https://doi.org/10.1530/EJE-22-0509

III Pekkarinen, L., Kantonen, T., Oikonen, V., Haaparanta-Solin, M., Aarnio, R., Dickens, A. M., von Eyken, A., Latva-Rasku, A., Dadson, P., Kirjavainen, A. K., Rajander, J., Kalliokoski, K., Rönnemaa, T., Nummenmaa, L., & Nuutila, P. (2023). Lower abdominal adipose tissue cannabinoid type 1 receptor availability in young men with overweight. Obesity (Silver Spring, Md.), 31(7), 1844–1858. https://doi.org/10.1002/oby.23770

1 Introduction

Worldwide, obesity is recognized as a chronic disease that increases the risk for other non-communicable diseases, cancers and premature mortality [Bray et al., 2017; EASO, 2015; Jastreboff et al., 2019]. Obesity results from a long-term positive energy balance and is characterized by excess energy stored as fat in adipocytes enlarged in size and number, and as ectopic fat in other organs. The global obesity epidemic causes a serious burden to individuals and communities as worldwide over 650 billion adult have obesity [WHO, 2021]. Therefore, effective tools for preventing and treating obesity are needed, and to reach this, it is essential to understand the complex mechanisms in the pathogenesis of obesity.

Multiple neural and neuroendocrine circuits at central and peripheral levels coordinate appetite, food intake and energy expenditure in interplay with environment and genes [Wilson & Enriori, 2015]. Common obesity thus results from defective interaction between the brain and peripheral metabolic organs, and central resistance to nutritionally relevant signals arising from periphery. Disruption in the fine-tuned regulation of energy balance predisposes to excess eating and weight gain [Oussaada et al., 2019; Timper & Brüning, 2017; Wilson & Enriori, 2015].

Insulin in the brain acts as a satiety signal suppressing appetite particularly for palatable food [Kullmann, Kleinridders, et al., 2020]. In addition to regulation of eating behaviour, brain insulin action has several effects on whole-body metabolism. These include energy expenditure and thermogenesis [Sanchez-Alavez et al., 2010; Spiegelman & Flier, 2001], white adipose tissue and liver lipid metabolism [Scherer et al., 2021], control of blood glucose level by modulating hepatic endogenous glucose production (EGP) [Lewis et al., 2021] and potentially peripheral tissue glucose uptake [Heni et al., 2017], and cognitive performance [Dutta et al., 2022]. Impaired insulin action in the brain, “brain insulin resistance”, in turn is linked with disturbances in central and peripheral metabolism, and has been recognized as central characteristic of obesity [Kullmann, Kleinridders, et al., 2020].

Positron emission tomography (PET) with a labelled glucose analogue radiotracer 2- deoxy-2-[^{18}F]fluoro-D-glucose ([^{18}F]FDG) allows detecting brain insulin sensitivity *in vivo*. Previous studies have demonstrated increased insulin-stimulated brain glucose uptake (BGU) in subjects with obesity [Rebelos et al., 2021;

Tuulari et al., 2013] and impaired glucose tolerance [J. W. Eriksson et al., 2021; Hirvonen et al., 2011; Latva-Rasku et al., 2018] as compared to lean and insulin sensitive subjects. However, it is not known whether altered brain insulin signalling is present already in subjects with overweight and risk factors for developing obesity.

Endocannabinoid system (ECS), consisting of two G-protein-coupled receptors, cannabinoid type 1 and type 2 (CB1R and CB2R, respectively), their endogenous ligands and ligand-metabolizing enzymes, has a central role in the control of energy homeostasis [Silvestri & Di Marzo, 2013]. CB1Rs are widely expressed in brain regions controlling feeding behaviour and energy balance [Di Marzo et al., 2009] and in peripheral tissues, including white and brown adipose tissue, skeletal muscle, endocrine pancreas and gastrointestinal tract [Matias, Petrosino, et al., 2008]. In the brain, activation of CB1Rs stimulate appetite and food intake in interaction with dopaminergic and opioidergic signalling pathways [Silvestri & Di Marzo, 2013]. In addition, the central ECS modulates peripheral metabolism including thermogenesis [Cota et al., 2003] hepatic EGP and white adipose tissue lipid metabolism [O'Hare et al., 2011]. Peripheral ECS modulates metabolic functions locally, and has central role especially in white adipose tissue and liver metabolism [Silvestri & Di Marzo, 2013]. Obesity and associated metabolic disorders are characterized by ECS dysregulation with altered CB1R availability and endocannabinoid levels in tissues and in circulation. CB1R antagonism in turn reduces food intake, body weight and improve the signs of metabolic disorders [Quarta et al., 2011; Silvestri & Di Marzo, 2013]. Withdrawal of the first CB1R inverse agonist Rimonabant (SR141716) from market due to neuropsychiatric side effects, has led to investigate new therapeutic approaches in order to control the overactive ECS in obesity[Simon & Cota, 2017].

ECS function can be studied *in vivo* by quantifying tissue CB1R availability with PET and an CB1R inverse agonist radioligand [3R,5R]-5-[3-methoxy-phenyl]-3-[{R}-1-phenyl-ethylamino]-1-[4-trifluoro-methyl-phenyl]-pyrrolidin-2-one ([^{18}F]FMPEP-d_2). The radioligand binds to CB1Rs that are not occupied with their natural ligands. A previous study from our centre showed lower CB1R availability in the brain and abdominal adipose tissue depots of healthy males with obesity as compared to lean males [Lahesmaa et al., 2018].

The aim of the present thesis is to investigate brain and peripheral tissue insulin sensitivity and endocannabinoid receptors, and their associations with the risk of developing obesity using PET imaging.

2 Review of the Literature

2.1 Obesity – definition, prevalence and incidence

Obesity is a chronic disease defined as excessive fat accumulation in adipose tissue due to energy imbalance, presenting a significant risk for health [Bray et al., 2017]. Obesity can be classified using body mass index (BMI) - body weight in kilograms divided by the square of height in meters (kg/m^2) – as BMI ≥ 30 kg/m^2 defined as obesity [WHO, 2021]. While BMI does not take into account body composition, waist circumference is an additional measurement of abdominal obesity. Waist circumference ≥ 88 cm for women and ≥ 102 cm for men is considered to associate with significant health consequences [Jensen et al., 2014].

The prevalence of obesity has increased worldwide, and today, there are more people living with obesity than with underweight in all areas except Sub-Saharan Africa and South Asia [World Obesity, 2023]. In 2016, 13% of adults aged 18 years or older had obesity accounting for 650 million people [WHO, 2021] (**Figure 1**).

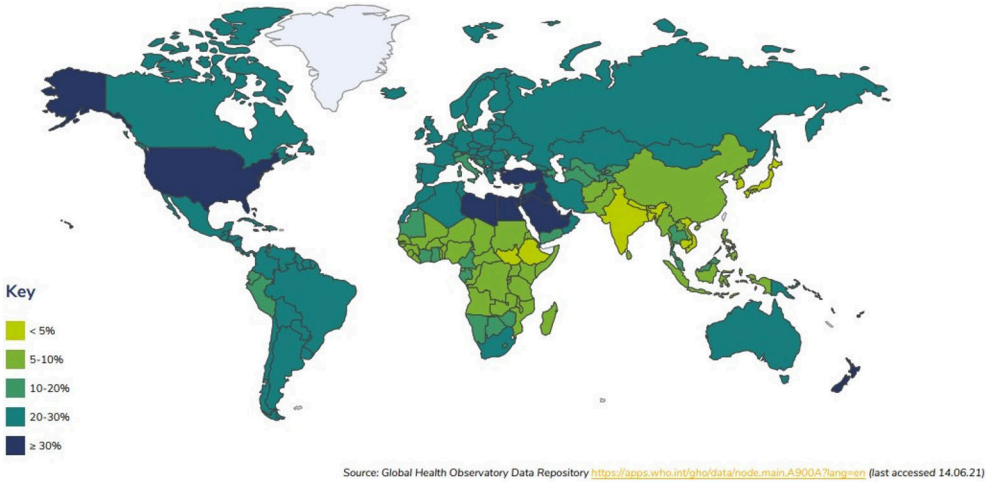

Figure 1. Estimates of prevalence of obesity (BMI ≥ 30 kg/m²) in adults in 2016. The figure is reprinted with permission from World Obesity Federation, London as originally published by The World Obesity Federation.

Between 1980 and 2015, the prevalence of obesity has doubled in 73 countries, and continuously increased in most other countries. The increase has been similar between males and females in all age groups being highest during early adulthood [Afshin et al., 2017]. In Finland in 2017, 17% of men and 19% of women aged 18-29 years had obesity, while in the age group of > 30 years the prevalence of obesity was 26% for men and 28% for woman. Also, 46% of adults have abdominal obesity. [FinTerveys2017, 2018] The estimates suggest that global level of obesity will be on the rise: in 2035, 23% of men and 27% of women may be affected by obesity [World Obesity, 2023]. Country-specific data and trends in obesity and its economic impact are available at https://www.worldobesity.org/.

Obesity related non-communicable diseases, including type 2 diabetes (T2D), cardiovascular diseases (CVDs) and non-alcoholic fatty liver disease impairs both quality of life and life expectancy [Bray et al., 2017; Pereira-Miranda et al., 2017]. Above BMI 25 kg/m^2, each 5 kg/m^2 increasing in BMI associates with about 30% higher overall mortality, and 40% higher vascular, 120% diabetic, 60% kidney disease and 80% liver disease [Whitlock et al., 2009]. Also, abdominal adiposity, when adjusted for BMI, presents an independent risk for premature death [Pischon et al., 2008]. Overweight and obesity are estimated to be responsible for 5.0 million deaths and 160 million disability-adjusted life-years globally in 2019 [Chong et al., 2023].

2.2 Central and peripheral regulation of energy homeostasis

Two complementary pathways, homeostatic and reward-driven pathways regulate food intake, glucose metabolism and energy expenditure. The homeostatic signals ensures that food intake meets the energy demand. The reward-driven, or hedonistic regulation in turn, drives motivation to acquire and consume calories regardless of energy requirement [Lutter & Nestler, 2009; Myers et al., 2021]. The interplay of the neural and peripheral processes and environmental and lifestyle factors is schematically presented in **Figure 2**.

Homeostatic signals encompass vagal afferent signals and circulating hormones and metabolites from the peripheral tissues and organs supplying information about nutritional status to brain centres that coordinate the adaptive chances in food intake, energy expenditure and storage [Lenard & Berthoud, 2008; Roh et al., 2016; Wilson & Enriori, 2015]. The gustatory system, gastrointestinal tract, pancreas, adipose tissue, liver and muscle are the main peripheral components participating in the energy homeostasis. They are in bidirectional communication with the brain through neural circuits, hormones and metabolites. The peripheral signals affecting energy balance include for instance leptin, insulin, amylin, ghrelin, cholecystokinin, peptide

YY, glucagon-like peptide-1 (GLP-1), somatostatin, glucose, fatty acids and amino acids [Lenard & Berthoud, 2008; Myers et al., 2021; Roh et al., 2016; Wilson & Enriori, 2015]. Leptin signalling represents long-term control mechanism, while leptin is secreted by white adipocytes in proportion to the amount of stored fat. Insulin, secreted by pancreatic β-cells in response to circulating nutrients, [Fu et al., 2013] is likewise comparable to fat stores, and also tissue insulin sensitivity [Brochu et al., 2000]. In addition, endocannabinoids participate in the regulation on appetite and food intake by modulating central neurons via activation of cannabinoid receptors. This is, at least partly mediated by feeding-regulated hormones, especially leptin and ghrelin (Silvestri, and Marzo, 2013).

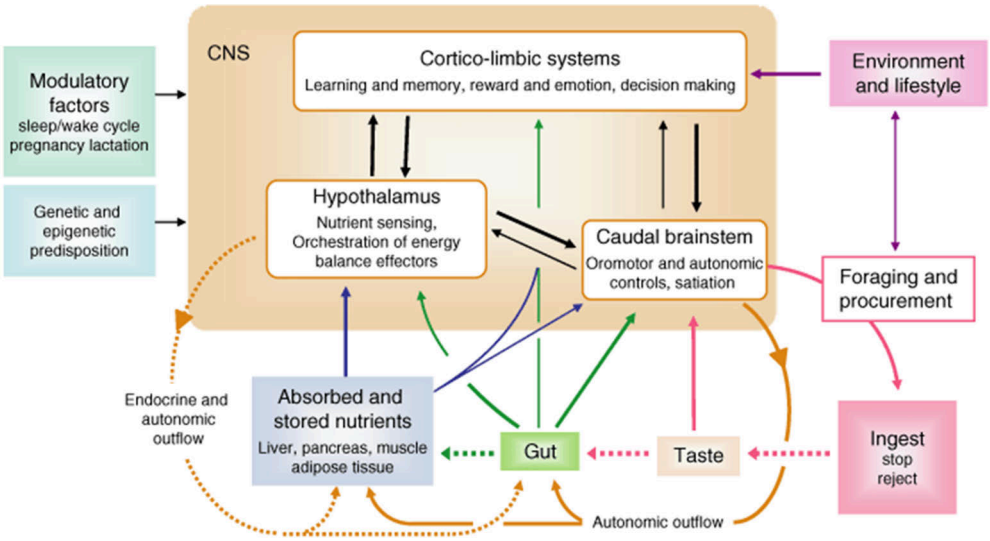

Figure 2 A schematic diagram showing major components of the peripheral and central systems involved in energy balance regulation, and control of food intake, and the interaction with environment and genes. Reprinted with permission from publisher, © Wiley, as originally published by Lenard and Berthoud, 2008.

The hindbrain is the first brain structure to receive information from the gustatory cells and gastrointestinal tract through the gustatory and vagal afferents. The hypothalamus and the specific regions within it such as arcuate (ARC) and paraventricular (PVH) nuclei in turn, has a central role in integrating information originated from peripheral organs via circulating hormones, metabolites and neural circuits. This nutritional information is then processed in the context of other internal and external information. The optimal adaptive responses are finally implemented through behavioural, autonomic and endocrine output pathways [Lenard & Berthoud, 2008].

The hypothalamic ARC contains anorexigenic (appetite-suppressing) pro-opiomelanocortin (POMC)-expressing POMC and cocaine- and amphetamine-regulated transcript (CART) neurons that promote the release of α-melanocyte-stimulating hormone (α-MSH), and the orexigenic (appetite-stimulating) neuropeptide Y (NPY) and agouti-related peptide (AgRP)-expressing NPY/AgRP neurons. These neurons project to second-order neurons in the hypothalamus and in the hindbrain resulting in a response on energy intake an expenditure [Myers et al., 2021; Timper & Brüning, 2017; Wilson & Enriori, 2015]. PVH neurons control sympathetic outflow to peripheral organs leading to increased fatty acid oxidation and lipolysis and secrete hormones having catabolic actions, including thyrotropin-releasing hormone and corticotrophin-releasing hormone, and destruction of PVH leads to hyperphagia and obesity [Roh et al., 2016]. POMC/CART and NPY/AgRP neurons express receptors for peripheral hormones, including leptin and insulin [Kleinridders et al., 2014; Timper & Brüning, 2017; Wilson & Enriori, 2015]. Other hypothalamic nuclei that are essential in energy balance regulation include dorsomedial hypothalamic (DMH), ventromedial hypothalamic (VMH) and lateral hypothalamic (LH). Destruction of the DMH and VMH results in hyperphagia, hyperglycemia and obesity [Roh et al., 2016]. Neurons within the LH links the hypothalamus with brain areas associated with reward and motivation, and with areas in brainstem associated with visceral sensory input. Destruction of LH in turn, results in hypophagia and weight loss. Hypothalamic neurons are connected to nucleus solitary tract (NTS) in the hindbrain. In addition to receiving satiety signals from periphery, NTS neurons produce appetite-regulating peptides GLP-1, NPY and POMC [Lenard & Berthoud, 2008; Roh et al., 2016; Timper & Brüning, 2017].

At fasting, low circulating and stored fuel levels are signalled to the brain by elevated ghrelin and low levels of other gut hormones, and a decrease in leptin. As a result, NPY/AgRP neurons are activated leading to feeding behaviour, a reduction in energy expenditure, energy storage, increased hepatic EGP, and release of AgRP that prevents the anorexigenic effects of POMC/CART neurons. In postprandial state, ghrelin levels decrease, leptin and insulin increase and gastrointestinal hormones secreted in response to ingested nutrients, project to ARC. This leads to inhibition of NPY/AgRP neurons and stimulation of POMC/CART neurons. POMC/CART activation results also from direct effect of glucose and fatty acids. As a result, food intake and hepatic EGP decreases while energy expenditure increases. In addition, seeing and tasting tempting foods activates POMC/CART and inhibit NPY/AgRP neurons [Timper & Brüning, 2017; Wilson & Enriori, 2015]. Hypothalamic endocannabinoid levels increase at fasting and decrease at postprandial state due to changes in the hormonal signals [Silvestri & Di Marzo, 2013]. In basal state between the meals, energy homeostasis is mostly dependent on input from leptin [Myers et al., 2010].

Cortico-limbic reward system contributes to cognitive and emotional aspect in feeding. Hedonic aspects of appetite is regulated by hunger, taste, food cues, and palatable food [Berthoud, 2004; Kleinridders & Pothos, 2019]. Opioid and endocannabinoid (ECS), as well dopamine system, are involved in the hedonic control of food intake [Berthoud, 2004; Silvestri & Di Marzo, 2013]. The homeostatic signals interact with the reward pathway. For instance, leptin suppress feeding, and insulin decreases the desire for high-fat or high-sugar food by acting on the dopaminergic neurons in the reward circuitry [Könner et al., 2009; Lutter & Nestler, 2009; Timper & Brüning, 2017].

2.3 The Pathogenesis of obesity

The constitutive cause of obesity is a long-term positive energy balance: energy intake exceeding energy expenditure [Haslam & James, 2005]. Appetite, food intake, and energy expenditure are coordinated by neural and neuroendocrine circuits at central and peripheral levels in interplay with environment and genes [Oussaada et al., 2019; Timper & Brüning, 2017; Wilson & Enriori, 2015]. This intrinsic system controlling energy balance is sensitive to disturbances that can unsettle energy homeostasis predisposing to obesity [Myers et al., 2021; Roh et al., 2016]. The overall pathogenesis of obesity is complex and not yet fully understood. Obesity involves several components regulating energy homeostasis: dysregulated interplay of brain and peripheral signals, pathological overeating and low physical activity in a genetically prone person [Oussaada et al., 2019; Timper & Brüning, 2017; Wilson & Enriori, 2015].

2.3.1 Impaired crosstalk between the brain and periphery

Altered hypothalamic function or defective sensing of peripheral signals in hypothalamic neurons, particularly leptin and insulin is associated with high-fat diet, positive energy balance, and obesity [Könner & Brüning, 2012; Kullmann et al., 2015; Roh et al., 2016]. Brain insulin resistance can result from several mechanism, for instance, decreased blood-brain-barrier (BBB) transport of insulin to the brain or impaired insulin signalling because of overfeeding and hypothalamic inflammation. Central insulin resistance in turn, further promotes increased appetite, overnutrition and weight gain [Könner & Brüning, 2012; Scherer et al., 2021]. Hypothalamic inflammation and gliosis – reactive inflammatory response of glial to cell damage – are suggested causal factors of diet-induced obesity. Obesogenic diet among genetically prone persons may induce inflammatory reaction in hypothalamic nuclei involved in energy balance regulation. This in turn, may lead to neuronal dysfunction favouring increased food intake and energy stores [Sewaybricker et al., 2023].

In addition, dysregulation of reward circuits is a hallmark of obesity. Dopamine D_2 receptor availability in subjects with obesity is proportional to their BMI [Wang et al., 2001], and increased reactivity to food reward in limbic system in subjects with obesity [Stoeckel et al., 2008]. While ECS participates in the energy balance regulation in the central and peripheral levels by modulating both homeostatic and hedonic pathways, dysregulation of this system associates with obesity. The overall action of the ECS is to promote energy intake and storage, but when energy-dense, highly palatable food is abundant, it favours development of obesity [Silvestri & Di Marzo, 2013]. The ECS is more thoroughly discussed in later chapters.

2.3.2 Environment and lifestyle

The modern environment characterized by high availability of energy dense, palatable food, increased presence of food cues with reduced level of physical activity favours weight gain. In this obesogenic environment, the hedonic regulation is prone to override the homeostatic pathway increasing the consumption of palatable food regardless of energy requirement [Lutter & Nestler, 2009; Myers et al., 2021]. In preclinical studies with rodents, gliosis and structural changes in the hypothalamic ARC, are stimulated by hypercaloric diet rich with saturated fat and simple carbohydrates, and are associated with hyperphagia and weight gain. In humans, this association is not yet proven, although neuroimaging studies and postmortem histopathological analyses have served evidence of hypothalamic gliosis associated with obesity [Sewaybricker et al., 2023].

Total body energy expenditure consists of resting metabolic rate, activity-related energy expenditure and diet-induced thermogenesis (energy dissipated in the absorption, metabolism and storage of nutrients). Studies examining energy expenditure in obesity suggest lower activity-related energy expenditure, but not resting metabolic rate or diet-induced thermogenesis, as a contributor to weight gain [Oussaada et al., 2019]. Sedentary lifestyle and low physical activity promote weight gain and ectopic fat [Jebb & Moore, 1999; Kujala et al., 2022; Leskinen et al., 2009], although conflicting results exists [Hill et al., 2012].

BMI in childhood and youth correlates positively with BMI in adulthood [Juhola et al., 2011]. Also low family income predisposes to obesity later in life [Juonala et al., 2011]. Furthermore, family history of obesity and T2D increases the risk for overweight and obesity adulthood [Anjana et al., 2009; Cederberg et al., 2015]. Other environmental and societal factors that have been linked to the development of the obesity pandemic are powerful marketing of calorie-rich food, low socioeconomic status, gut microbiota, circadian rhythm and stress [Blüher, 2019; Oussaada et al., 2019; Qayyum et al., 2009].

2.3.3 Genetic factors

Several genes associated with severe, early-onset obesity have been identified [Loos & Yeo, 2022]. These monogenic causes of obesity are however rare, accounting only approximately 7.3% of childhood-onset obesity [Kleinendorst et al., 2018]. Common, multifactorial, obesity is typically polygenic, in which the phenotype is caused by several polymorphisms, witch account only a minor effect on BMI. Over 750 single-nucleotide polymorphisms have found to be associated with BMI [Locke et al., 2015]. This genetic predisposition is not deterministic for obesity. Instead, environmental and lifestyle factors modify heritability estimates [Loos & Yeo, 2022; Silventoinen & Konttinen, 2020]. However, the monogenic and polygenic obesity share the same biology as the pathology lies in the brain neural circuits, for instance in genes coding for leptin-melanocortin pathway and pathways controlling the hedonic aspect of food intake [Loos & Yeo, 2022].

2.4 Insulin action in energy and glucose metabolism

Insulin is the main regulator of body glucose, lipid and amino acid metabolism. Following plasma glucose rise after food ingestion, insulin secretion by pancreatic β cells is stimulated. The resulted hyperinsulinemia leads to suppression of EGP and stimulation of glucose uptake (GU) and utilization in peripheral tissues. In addition, insulin stimulates energy storage by stimulating glycogen synthesis, lipogenesis, protein synthesis and by inhibiting lipolysis, glycogenolysis and protein catabolism [Norton et al., 2022; M. C. Petersen & Shulman, 2018; Saltiel & Kahn, 2001]. In the brain, insulin signalling regulates appetite, eating behaviour and whole-body energy homeostasis through several mechanism by coordinating the organ interplay [Kullmann, Kleinridders, et al., 2020; Scherer et al., 2021].

2.4.1 Insulin secretion and signalling

High surrounding glucose concentration is the main regulator of insulin secretion from pancreatic β cells. In addition to insulin secretion, glucose increases insulin gene transcription, and translation and transcription of insulin mRNA [Weiss et al., 2000]. Amino acids, free fatty acids, and other hormones and neurotransmitters can modulate the insulin secretion too. The effect of plasma amino acids at their physiological concentrations is however small, and they only potentiate the effect of glucose. Circulating free fatty acids can exert a long-term positive effects at physiological levels on the responsiveness of β cells, but at pathological levels induce β cell dysfunction [Henquin, 2021]. Incretins are peptide hormones secreted by enteroendocrine cells in the gut in response to nutrient absorption. Glucose-

dependent insulinotropic polypeptide (GIP) and glucagon-like peptide-1 (GLP-1) amplify insulin secretion initiated by hyperglycaemia [Nauck & Meier, 2018]. Somatostatin is produced in in many locations in the body. Majority of circulating somatostatin originate from gastrointestinal track, and a small proportion from pancreatic δ cells. Somatostatin has an inhibitory effect on insulin secretion. Also leptin, secreted by white adipocytes, may have a long-term inhibitory effect on insulin secretion. Parasympathetic nervous system can enhance insulin secretion, while sympathetic system has an inhibitory effect. Long-term endogenic, as well exogenic hypercortisolism, may lead to hypersecretion of insulin, while as a short-term the effect is inhibitory [Henquin, 2021].

Insulin exerts its actions by binding to insulin receptors (IR), or in lesser extent to closely related insulin-like growth factor-1 (IGF-1R) receptor, on the plasma membrane of target cells (**Figure 3**). This initiates a cascade of phosphorylation events leading to activation of phosphatidylinositol 3-kinase (PI3K)/ protein kinase B (Akt) pathway. Of three Akt isoforms, Akt2 is predominant in insulin-sensitive tissues and mediates most of insulin´s metabolic actions [Boucher et al., 2014; M. C. Petersen & Shulman, 2018]. The low frequency partial loss-of-function p.P50T/Akt2 variant is associated with reduced insulin sensitivity in several peripheral tissues, and also in brain [Latva-Rasku et al., 2018].

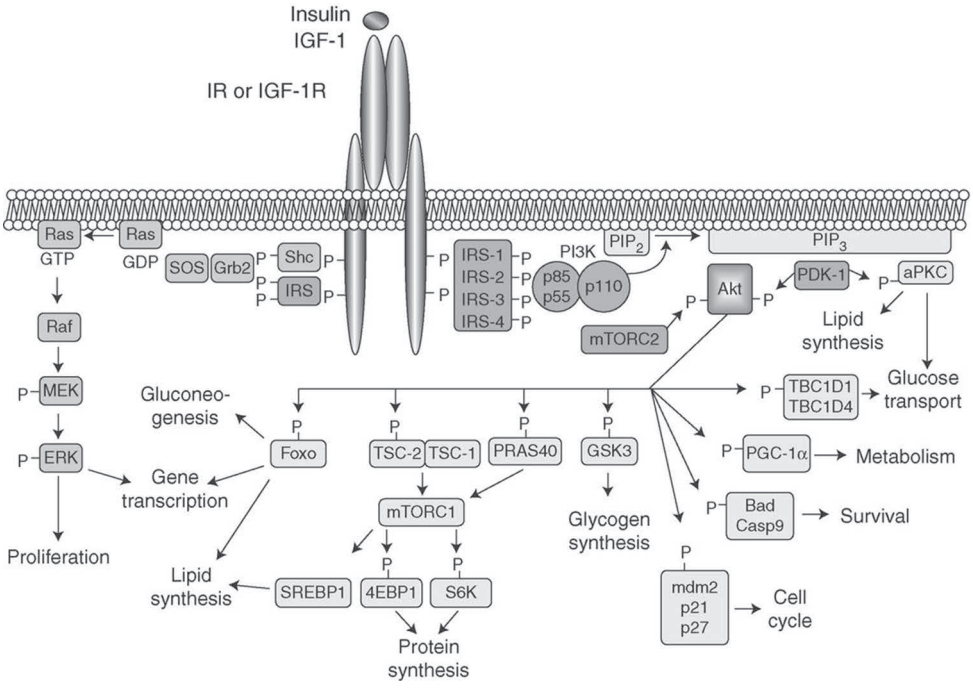

Figure 3. Insulin signalling pathways. Reprinted with permission from publisher, © Cold Spring Harbor Laboratory Press, as originally published by Boucher at al., 2014.

Activated Akt allows multiple adjacent downstream reactions that leads to insulin response in the plasma membrane. Phosphorylation of TBC1D4 and TBC1D1 by Akt mediates insulin-stimulated tissue GU by stimulating the translocation of the transporter GLUT4 from intracellular stores to the plasma membrane [Boucher et al., 2014; M. C. Petersen & Shulman, 2018; Saltiel & Kahn, 2001]. Phosphorylation of glycogen synthase kinase 3 (GSK3) in turn results in glycogen synthesis in liver. Akt induced activation of mechanistic target of rapamycin complex 1 (mTORC1) leads to enhanced protein synthesis as well as increased lipid synthesis both in liver and in white adipose tissue (WAT). Inactivation of transcription factors of the Forkhead box O (Foxo) by Akt results in decreased expression of gluconeogenic genes, and suppression of EGP in liver. Suppression of gluconeogenesis, and liver fatty acid oxidation is facilitated by phosphorylation of PGC-1α [Boucher et al., 2014]. In addition, inactivation on Foxo results decreased expression of lipogenic genes leading to reduced hepatic very-low-density lipoprotein (VLDL) and triglyceride production [Boucher et al., 2014; M. C. Petersen & Shulman, 2018; Sparks & Dong, 2009]. Inhibition of lipolysis in WAT comprises of several Akt-dependent events as well [Norton et al., 2022].

2.4.2 Insulin action on peripheral tissue metabolism in normal physiology

2.4.2.1 Skeletal muscle

In skeletal muscle, insulin action contributes primarily to GU and glycogen synthesis. Hyperinsulinemia increases skeletal muscle GU up to 10-fold compared to fasting state [Norton et al., 2022]. In basal postprandial state, skeletal muscle is responsible for 30-40% of total systemic glucose disposal. The insulin stimulated GU is mediated via recruitment of GLUT4 to the plasma membrane of myocytes. Once entered to myocytes, glucose is phosphorylated to glucose-6-phoshate by hexokinase II. Insulin-stimulated pathway downstream to glucose-6-phoshate can either drift to glycolysis or glycogen synthesis, of which the latter predominates at postprandial state. While glycogen synthesis is allowed by GSK3 inhibition by Akt, insulin also suppresses glycogen breakdown by inhibin glycogen phosphorylase. Insulin also participates to skeletal muscle protein metabolism. Insulin suppresses proteolysis and stimulates protein synthesis [Norton et al., 2022; M. C. Petersen & Shulman, 2018].

2.4.2.2 White adipose tissue

The effect of insulin in WAT is anabolic: insulin suppresses lipolysis, stimulates GU and adipogenesis by promoting triglyceride synthesis. At postprandial state, insulin inhibits the release of non-esterified fatty acids (NEFA) into circulation and to other tissues [Norton et al., 2022]. Long-term impairment of insulin action to suppress WAT lipolysis and chronic exposure to increased level of circulating NEFAs can lead to impaired insulin action in multiple tissues and compensatory increase in insulin secretion, which is further disturbed by the "lipotoxic" effect on insulin secretion of β cells. Ultimately this can lead to development of T2D. Insulin-suppressed WAT lipolysis is indirectly involved in the suppression on hepatic EGP though reduction of substrate and energy availability for hepatic gluconeogenesis [M. C. Petersen & Shulman, 2018; Wajchenberg, 2000].

Insulin-stimulated GU into WAT is facilitated by GLUT4 [M. C. Petersen & Shulman, 2018]. At postprandial state, the GU into WAT account for 5-10% of glucose disposal [Virtanen et al., 2002]. However, fat depots largely differ according to their metabolic characteristics such as lipid composition, secreted factors, and sensitivity to sympathetic and hormonal control of lipolysis, lipogenesis and GU [Wajchenberg, 2000]. Higher metabolic activity measured as GU has been shown in visceral (VAT) than in abdominal subcutaneous (SAT) adipose tissue both *in vivo* and *in vitro* [Christen et al., 2010; Virtanen et al., 2002]. Excess amount of visceral adipose tissue associates with systemic insulin resistance and metabolic risk factors stronger than abdominal adipose tissue, while femoral subcutaneous adipose tissue can even have a have a protective role [Fox et al., 2007; Goodpaster et al., 2005; Zhang et al., 2015].

Insulin promotes adipogenesis in adipocytes by providing glucose for the formation of glycerol-3-phosphate (G3P) with which fatty acids esterify into acyl-CoA to be used in glycerolipid synthesis. Insulin also stimulates the activity of lipoprotein lipase (LPL), which acts on endothelium to release fatty acids from circulating triglycerides to be taken up to adipocyte. Furthermore, insulin promotes *de novo* lipogenesis, which proportion of the adipocyte lipid synthesis is however small [M. C. Petersen & Shulman, 2018].

2.4.2.3 Brown adipose tissue

Brown adipose tissue, located mainly in supraclavicular and paravertebral depots in adults, is capable to produce heat because of large number of mitochondria and expression of uncoupling protein -1 (UCP1). Although fatty acids are likely the main substrates for BAT energy utilization, glucose is an important nutrient in BAT. BAT cells express GLUT1 and insulin-responsive GLUT4 transporters, of which GLUT4 are shown to be more abundant in BAT than in WAT [Orava et al., 2011; Ramage et

al., 2016]. Under cold-exposure, BAT GU is up to eightfold higher than that if skeletal muscle accounting for 1% of whole-body glucose disposal [Carpentier et al., 2018]. Insulin can stimulate BAT GU up to fivefold independent of blood flow. It seems that cold induced thermogenesis increases BAT GU by increasing perfusion, while insulin-stimulated GU is not dependent on increased blood flow [Orava et al., 2011].

2.4.2.4 Liver

Insulin action in the liver regulates hepatic glucose and lipid metabolism via direct and indirect mechanisms. During the fasting state, low circulating insulin and high glucagon level increase hepatic EGP. Following glucose ingestion and rise in plasma insulin and decline in glucagon levels, hepatic EGP decreases, GU, glycogen and protein synthesis, and also the synthesis and storage of lipids increases [Norton et al., 2022; M. C. Petersen & Shulman, 2018; Titchenell et al., 2017].

Insulin from the pancreatic β cell is secreted into the portal vein, and liver removes 50% of the insulin secreted into circulation. Inhibition of hepatic EGP by insulin takes place rapidly, and is mediated directly through suppression of glycogenolysis. Suppression of gluconeogenesis is less sensitive to insulin. Indirect effect on insulin on gluconeogenesis is mediated through suppression of WAT lipolysis and a decrease in fatty acid availability for gluconeogenesis. Under normal physiological conditions, the direct inhibition of gluconeogenesis is most prominent and predominate in fed state, whereas the indirect insulin action predominates under fasting [Norton et al., 2022; M. C. Petersen & Shulman, 2018].

Number of inputs, such as arterial-portal vein glucose gradient, fatty acids, amino acids, insulin and neural mediators modulate the uptake of glucose into hepatocytes. Hyperinsulinemia or hyperglycaemia themselves are not sufficient to enhance hepatic GU. However, delivery of glucose to liver via oral-enteral-portal vein route, and elevated insulin concentration increases the hepatic GU [Moore et al., 2012]. Glucose enters to hepatocyte through GLUT2 transporters [Thorens, 2015]. The liver takes up approximately one third of the glucose load after a meal, thus limiting postprandial hyperglycaemia [Moore et al., 2012]. In the hepatocytes, glucose is converted to glucose-6-phosphate (G6P) by glucokinase (GCK), of which transcription insulin increases. G6P, glucose and insulin stimulate glycogen synthase leading to glycogen formation [Radziuk & Pye, 2002].

Insulin action in hepatic lipid metabolism is likewise anabolic. In postprandial state, insulin promotes lipid storage in the hepatocytes by increasing *de novo* lipogenesis, increases the uptake of triglyceride from circulation, suppresses fatty acid oxidation and decreases the export of VLDL. Insulin-stimulated protein synthesis in hepatocytes is mediated via Akt induced activation of mTORC1 activity [Norton et al., 2022; M. C. Petersen & Shulman, 2018].

2.4.3 Brain insulin signalling

2.4.3.1 Insulin transport and receptors

Insulin enters the brain across the BBB via saturable receptor-mediated transport [Banks et al., 2012; King & Johnson, 1985]. Insulin concentration in the cerebrospinal fluid (CSF) is approximately 25% of that in blood, and increases proportionally after ingestion of meal or with peripheral insulin infusion [Woods et al., 2003]. However, if serum level of insulin is high enough to result in hypoglycaemia, the CNS insulin acts in counter-regulatory manner to restrain hypoglycaemia. Several factors and conditions affect the rate of insulin transport, including brain region, hyperglycaemia, triglycerides, starvation, obesity, T2D, inflammatory conditions and neurodegenerative diseases [Banks et al., 2012; Scherer et al., 2021]. Insulin can also enter the brain via rapid, passive extravasation through the median eminence (ME), located directly below the mediobasal hypothalamus and adjacent to ARC. This route allows insulin a straight access to interact with the orexigenic and anorexigenic neurons [Beddows & Dodd, 2021].

IRs, and also IGF-1Rs, are expressed throughout the brain in most cell types. The highest density of IRs is found in the hypothalamus, olfactory bulb, hippocampus, cerebral cortex and cerebellum [Banks et al., 2012; Havrankova et al., 1978; Plum et al., 2005]. The IR density is higher in neurons than in glial cells, of which 20-40% express IRs, and the density decreases with age [Banks et al., 2012; Scherer et al., 2021]. Astrocytes, the most abundant glia cells in the brain and located between vessels and neurons, are involved in nutrient sensing and the central regulation of systemic metabolism. Astrocytic insulin signalling plays a key role in regulating hypothalamic neuronal responses in order to adequately respond to changes in systemic glucose availability. In mice, astrocyte-specific loss of IRs led to impaired neuronal glucose sensing, reduced glucose and insulin levels in CSF and decreased brain GU. The mice lacking astrocytic IRs are unable to increase or decrease feeding in response to glucose deprivation or hyperglycaemia [García-Cáceres et al., 2016]. Insulin binding to its receptor activates the PI3K/Akt signalling pathway, leads to activation of ATP-sensitive potassium (K_{ATP}) channel and modulation of synaptic plasticity, gene expression and neuronal excitability. [Beddows & Dodd, 2021; Plum et al., 2005].

2.4.3.2 The hypothalamic and extrahypothalamic targets of insulin

Hypothalamic NPY/AgRP and POMC/CART neurons in the ARC are the primarily targets of central insulin through which insulin signals in the brain. In postprandial state, IR activation in NPY/AgRP neurons results in decreased transcription of

orexigenic NPY and AgRP. Insulin binding to POMC/CART neurons on the other hand, leads upregulation of anorexigenic α-MSH and activation of melanocortin 4 receptors (MC4R) [Kleinridders et al., 2014; Plum et al., 2005]. The action of insulin in hypothalamic neurons is interconnected with leptin signalling. In addition to ARC, IR signalling in VMH and LH neurons modulates energy balance regulation [Timper & Brüning, 2017]. Hypothalamic IR activation in astrocytes controls glucose and insulin transport from circulation to brain and regulates glucose-induced activation of hypothalamic POMC neurons [García-Cáceres et al., 2016].

IRs are expressed also in the dopaminergic neurons in the reward circuit, where insulin act to decrease the motivation to consume food [Kullmann, Kleinridders, et al., 2020; Timper & Brüning, 2017]. Furthermore, intranasal (IN) administration of insulin improves the functional connectivity in dopaminergic neurons, which has found to associate with decreases in hunger and food desire. Central insulin resistance in turn, associated with increased craving of palatable food [Kullmann, Kleinridders, et al., 2020]. However, nutritional status and diet can modulate the effects of insulin on dopaminergic neurons. Food restriction has been shown to enhance and obesogenic diet decrease the dopamine release [Stouffer et al., 2015]. The effect of insulin in dopaminergic signalling might also be sex-dependent [Kullmann, Kleinridders, et al., 2020].

Insulin action is essential for synaptic plasticity and functional connectivity in the default-mode network (DMN), which participates self-referential processing and evaluation of one's internal mental and physiological state [Kleinridders et al., 2014; Kullmann et al., 2016]. The DMN comprises of precuneus/posterior cingulate cortex, lateral temporal cortex, prefrontal regions and hippocampus [Broyd et al., 2009; Kullmann, Kleinridders, et al., 2020]. The prefrontal regions receive interoceptive and exteroceptive signals stimulus via afferent input from other brain areas such as hypothalamus, striatum and limbic system, and correspond to execution of adequate behaviour. The lateral prefrontal cortex is involved in the inhibitory control of eating, while the orbitofrontal cortex and anterior cingulate cortex participates decision-making according to reward [Kullmann et al., 2016]. Hippocampal processing, important in learning and memory, is also modulated by insulin [Banks et al., 2012; Kleinridders et al., 2014; Kullmann et al., 2016]. Insulin regulates the activity of N-methyl-D-aspartate (NMDA), α-amino-3-hydroxy-5-methyl-4-isoxazolepropionic acid (AMPA) and type A γ-aminobutyric acid (GABA) receptors in the hippocampus (Kleinridders et al., 2014). In the fusiform gyrus, a brain region nearby hippocampus within the temporal lobe, insulin suppresses the neural activity in response to visual food cues [Kullmann et al., 2016].

2.4.3.3 Brain glucose metabolism and relation to insulin signalling

The brain consumes 100-150 g glucose per day [Cahill et al., 1966] accounting for 20% of the whole-body oxygen consumption at rest [Rolfe & Brown, 1997]. Under normal physiological conditions, glucose is the main energy source for the brain. During prolonged fasting however, ketone bodies, produced by hepatic mitochondria from fatty acids, are the major energy source for brain [White & Venkatesh, 2011] along with lactate [Deitmer et al., 2019; Koepsell, 2020].

Glucose transport into central nervous system (CNS) is facilitated in non-active manner, mainly by saturable, high-affinity GLUT1 transporters in capillaries and brain cells (**Figure 4**) Additionally, GLUT3, GLUT4 and the sodium-glucose cotransporter 1 (SGLT1) in small brain capillaries may participate in local glucose transport across the BBB. The facilitated diffusion of glucose occurs independent of insulin, down the concentration gradient between glucose in blood and the brain interstitium.

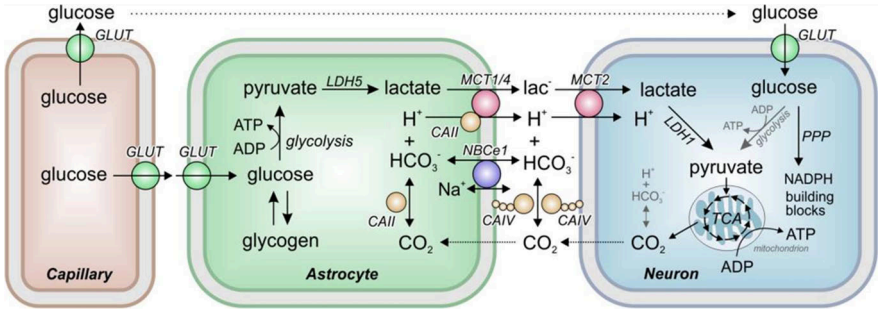

Figure 4 Glucose transport and metabolism in brain and the astrocyte-neuron lactate shuttle. GLUT1 transporters mediate glucose transport across the capillary endothelial cells to central nervous system downstream to glucose concentration gradient. The GU into astrocytes is mediated mainly by GLUT1. Inside the astrocytes, glucose is metabolized to pyruvate in glycolysis and then converted to lactate, or stored as glycogen. The lactate is shuttled from astrocytes to neurons, where it is converted to pyruvate and transferred for citric acid cycle in mitochondria for aerobic energy production. GU into neurons is facilitated mainly by high-affinity GLUT3 transporters, and in hypothalamus also by GLUT2 and insulin-responsive GLUT4 transporters. Inside the neurons glucose is utilized in the production of energy in glycolytic or pentose phosphate pathway (Deitmer et al., 2019; Koepsell, 2020). Reprinted with permission from Deitmer et al. 2019.

GU into neurons is mainly mediated by high-affinity and high-efficacy GLUT3 transporters. However, hypothalamic nuclei participating in the regulation of food intake and energy homeostasis express also low affinity GLUT2 and insulin-responsive GLUT4 transporters. It is proposed that GLUT2 are involved in the regulation of food intake and the central regulation of glucose homeostasis [Koepsell, 2020]. In rodents, reduced GLUT2 expression has been shown to link

with increased food intake and altered expression of orexigenic and anorexigenic neuropeptides [Bady et al., 2006]. In humans, genetic variation of GLUT2 associated with increased daily consumption of sugars [Eny et al., 2008].

The role of hypothalamic GLUT4 transporters in the whole-body energy and glucose homeostasis is essential, and brain GLUT4 and insulin signalling are mutually related [Koepsell, 2020; Ren et al., 2015; Reno et al., 2017]. GLUT4 is often coexpressed with IRs, and insulin, as well as leptin, stimulates GLUT4 translocation to the plasma membrane [Koepsell, 2020]. Neuronal IR knockout mice (NIRKO) have expressed significantly reduced hypothalamic GLUT4 expression, impaired hypothalamic neuronal response to hypoglycaemia, and blunted glucose-responsiveness in specific glucose-sensing neurons, but unaltered brain GU [Diggs-Andrews et al., 2010]. Mice with selective knockout of brain GLUT4 in turn were glucose intolerant, showed impaired suppression of EGP and GU into brain, and impaired response to hypoglycaemia, which was associated with reduced hypothalamic neuronal activation [Reno et al., 2017]. Likewise, mice with selective ablation of hypothalamic GLUT4 neurons also exhibited increased hepatic gluconeogenic gene expression and hepatic lipid content. In addition, the GLUT4 neuron ablated mice showed signs of negative energy balance, including decreased food intake and body weight, and increased energy expenditure [Ren et al., 2015].

In neurons, glucose is metabolized in the glycolytic pathway into pyruvate, which is further metabolized in the citric acid cycle in mitochondria, or is converted in lactate [Deitmer et al., 2019; Koepsell, 2020]. In addition, neurons receive energy in the form of lactate generated and supplied by astrocytes. This astrocyte –neuron lactate shuttle operates in accordance to neuronal activity. Lactate transferred to neurons is converted to pyruvate for aerobic energy production in mitochondria (**Figure 4**.) [Deitmer et al., 2019]. GU into astrocytes is mediated mainly by GLUT1, but also GLUT2, GLUT3 and insulin-responsive GLUT4 transporters. In addition to providing energy for neurons, astrocytes are capable to store glucose as glycogen [Deitmer et al., 2019; Koepsell, 2020].

2.4.4 Physiological effects of brain insulin action

2.4.4.1 Regulation of feeding behaviour

Insulin acts as a satiety signal for brain suppressing appetite for especially palatable foods. The primarily targets of insulin are the hypothalamic anorexigenic and orexigenic neurons, as also dopaminergic neurons in the reward system [Timper & Brüning, 2017; Wilson & Enriori, 2015]. The effect of central insulin action on food intake was first demonstrated in mice [Debons et al., 1970] and baboons [Woods & Porte, 1975] and after that with numerous other species [Kullmann et al., 2016;

Scherer et al., 2021]. In humans, IN insulin administration can be used for studying the central insulin action [Dhuria et al., 2010; Schmid et al., 2018] with only minor uptake into circulation [Born et al., 2002]. IN insulin administration increases the feeling of satiety, decreases food intake [Benedict et al., 2008; Jauch-Chara et al., 2012; Krug et al., 2018] and also body adiposity [Hallschmid et al., 2004], although conflicting findings exist [Krug et al., 2018]. Anorexigenic response to IN insulin might depend on sex, BMI and the nutritional state. In response to IN insulin administration, men has showed greater reductions in weight, adipose tissue and food intake than woman [Benedict et al., 2008; Hallschmid et al., 2004], and subjects with obesity no significant reduction in weight as compared to lean subjects [Hallschmid et al., 2008]. IN insulin administration in postprandial but not in fasted state was followed by decreased appetite and food intake [Hallschmid et al., 2012].

Furthermore, IN administered insulin enhances functional connectivity between brain areas associated with metabolic and cognitive processes, and this effect is paralleled with suppression of appetite and reduction in the amount of VAT [Kullmann, Heni, et al., 2017]. For instance, by controlling memory processes about previously eaten food and satiety signals hippocampus can inhibit subsequent food intake [Coppin, 2016]. Modification of olfaction by insulin may also affect calorie intake. Hyperinsulinemia during euglycemia [Ketterer et al., 2011] as well as intracerebroventricular [Aimé et al., 2012] and IN administration of insulin [Brünner et al., 2013] has been found to decrease olfactory detection, which associated with decreased food craving in rats [Aimé et al., 2012].

In addition, cerebral insulin may suppress appetite and food intake by increasing cerebral energy content as observed as increased levels of high-energy phosphate compounds assessed with magnetic resonance spectroscopy (MRS) after IN insulin administration [Jauch-Chara et al., 2012]. Likewise, insulin-stimulated chances in cerebral metabolites in frontal and temporal brain regions were observed with MRS, and this correlated with high whole-body insulin sensitivity. It is thus possible that low whole-body insulin sensitivity might associate with impaired neuronal metabolism [Karczewska-Kupczewska et al., 2013].

2.4.4.2 Regulation of energy expenditure and thermogenesis

The brain controls energy metabolism via adjusting basal metabolic rate, physical activity and adaptive thermogenesis [Spiegelman & Flier, 2001]. Thermogenesis occurs mainly via BAT, and also in beige adipocytes located within WAT depots, and is under central regulation and dependent on sympathetic outflow. Hypothalamus receives thermal signals from periphery and activates signalling pathway to induce BAT thermogenesis [Roh et al., 2016]. In addition, hormones and nutrients such as insulin, leptin and glucose have an influence on BAT activity

[Cannon & Nedergaard, 2004]. Data on brain insulin action on thermogenesis are mainly based on murine models. Intracerebral administration of insulin induces BAT activation [Bamshad et al., 1999; Müller et al., 1997], which was demonstrated also as increased BAT GU with positron emission tomography (PET) imaging [Sanchez-Alavez et al., 2010]. Mice lacking brain IRs in turn, displayed a decrease in body temperature under cold exposure indicating a failure in thermogenesis [Kleinridders et al., 2014]. Central administration of MC4R and melanocortin 3-receptor (MC3R) agonist had a stimulatory effect on BAT thermogenesis via enhanced sympathetic outflow, indicating the role of central melanocortin receptors in BAT thermogenesis [Brito et al., 2007]. In humans, IN insulin administration increased energy expenditure at postprandial state as measured with indirect calorimetry [Benedict et al., 2011].

2.4.4.3 White adipose tissue lipolysis and lipogenesis

In addition to direct effects, insulin controls WAT metabolism indirectly through brain insulin signalling [Scherer et al., 2021]. Insulin infused to mediobasal hypothalamus suppressed lipolysis and increased the expression of lipogenic proteins. The suppression of lipolysis is mediated via suppression of sympathetic outflow independent of peripheral insulin signalling. Also, increased lipolysis and decreased *de novo* lipogenesis have been demonstrated with mice lacking neuronal IRs [Scherer et al., 2011]. Similarly, mice with IR inactivation in all tissues, including the brain, exhibited greater loss of WAT mass and hypoleptinemia due to uncontrolled lipolysis as compared to mice with IR inactivation only in peripheral tissues demonstrating the essential role of brain insulin action in regulating adipose tissue metabolism [Koch et al., 2008]. The sympathetic nervous outflow to WAT has been shown to colocalize with MC4Rs [Song et al., 2005] and being associated with the control of WAT lipolysis [Brito et al., 2007]. Mice lacking IRs in POMC neurons, show impaired suppression on WAT lipolysis indicating an impaired indirect insulin action in WAT. The hepatic EGP however was not reduced in these mice. Deletion of IRs in AgRP neurons did not alter the rate of WAT lipolysis, but impaired the suppression of hepatic EGP [Shin et al., 2017]. Central administration of insulin stimulated fatty acid uptake into WAT under conditions of hyperinsulinemic-euglycemic clamp by activation of central K_{ATP} channels, independent of activation of insulin or leptin signalling pathways in WAT [Coomans, Geerling, et al., 2011]. In humans, IN insulin administration suppressed circulating FFA levels and the rate of appearance of deuterated glycerol, indicating suppression of lipolysis, without changes in lipolytic protein expression or changes in plasma insulin levels [Iwen et al., 2014].

2.4.4.4 Regulation of hepatic glucose and lipid metabolism

Hypothalamic insulin signalling modulates the hepatic EGP in addition to the direct insulin effect (**Figure 5**). In rodents, administration of insulin into the third cerebral ventricle suppresses hepatic EGP independent of circulating insulin or other glucoregulatory hormone levels. Also, blocking the binding on insulin to central IRs leads to impaired ability of circulating insulin to suppress EGP [Obici, Feng, et al., 2002; Obici, Zhang, et al., 2002]. While the insulin signalling cascade involves activation of K_{ATP} channel, inhibition of the channels by central infusion of sulfonylurea prevents the physiological suppression of EGP during an insulin clamp [Obici, Zhang, et al., 2002; Pocai et al., 2005].

Similarly, activation of hypothalamic K_{ATP} channels results in decreased hepatic EGP, with reduced expression of hepatic gluconeogenic enzymes [Pocai et al., 2005]. AgRP neurons in the hypothalamus and the dorsal vagal complex are recognized as an essential sites of central insulin signalling regulating the hepatic EGP [Filippi et al., 2012; Könner et al., 2007]. In addition, resection of the efferent, but not afferent, hepatic branch of vagus nerve fibres abolished the effect of centrally administered insulin on hepatic EGP suggesting that efferent vagal input from brain to liver is required for the proper action of brain-liver-axis [Pocai et al., 2005]. Central insulin signalling suppresses the hepatic efferents resulting in an increase in hepatic interleukin 6 (IL-6) secretion leading to subsequent activation of transcription 3 (STAT3) in hepatocytes and reductions in gluconeogenic enzyme expression [Könner et al., 2007]. Indirect effect of central insulin signalling on hepatic EGP is mediated via suppression of adipose tissue lipolysis and reduced FFA and glycerol fluxes to liver [Koch et al., 2008], and possibly reduced pancreatic glucagon secretion [Paranjape et al., 2010].

Somatostatin clamp studies in dogs with insulin infused either via portal or peripheral vein and administering insulin centrally, has demonstrated the direct effect of insulin to suppress EGP to overcome that of central insulin. This finding was verified when controlling the indirect insulin effect to suppress lipolysis and glucagon secretion. Central hyperinsulinemia was shown to activate hypothalamic Akt and hepatic STAT3 accompanied by reduced gluconeogenic enzyme expression, while central administration of PI3K inhibitor reversed these actions [Ramnanan et al., 2011].

In humans, under euglycemic clamp with somatostatin, administration of IN insulin demonstrated late suppression of EGP, occurring between 180-360 min after insulin administration [Dash et al., 2015], as shown also with oral diazoxide [Esterson et al., 2016; Kishore et al., 2011]. However, earlier, 100–120 min, decreases in EGP have been reported as well [Heni et al., 2017]. Increases in the rate of glucose infusion rate 15 min after IN insulin administration (in order to maintain euglycemia during hyperinsulinemic-euglycemic clamp) as well as improvement in

the insulin sensitivity has been demonstrated [Heni, Wagner, et al., 2014]. Liver transplantation enables the study of hepatic denervation in humans. No significant difference in the glucoregulatory indices was observed between the liver transplant and control group [Schneiter et al., 2000]. It is thus assumed, that the effect of central insulin on hepatic EGP is limited, and only potentiates the action of systemic insulin [Scherer et al., 2021].

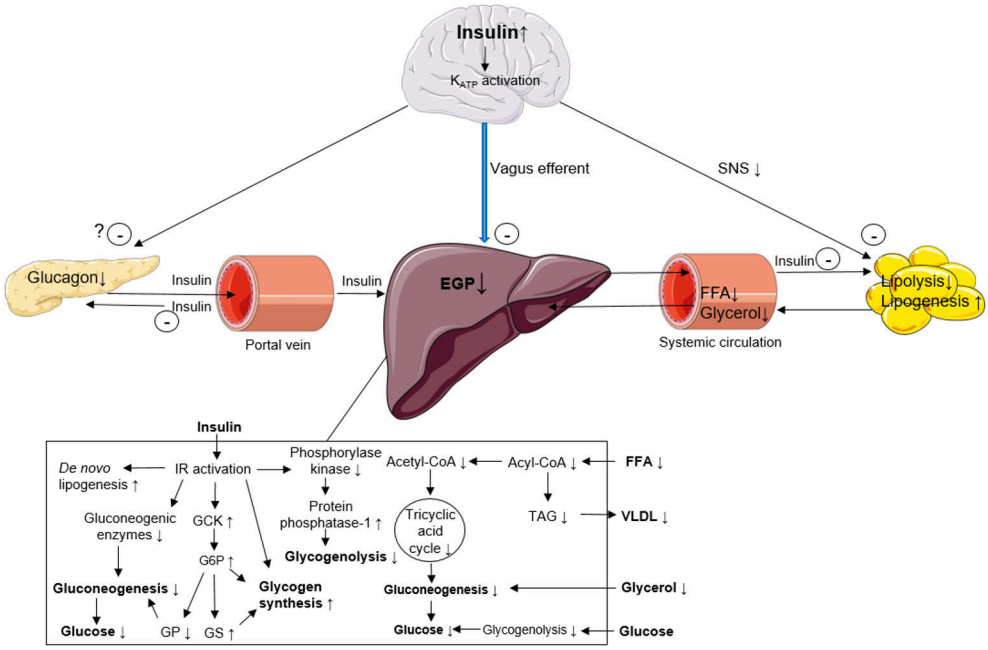

Figure 5 Direct hepatic and extrahepatic insulin suppression of hepatic endogenous glucose production (EGP). In the liver, insulin suppresses glycogenolysis and gluconeogenesis and enhance glycogen synthesis. Acute activation of hepatic IRs stimulate glycogen synthesis, whereas chronic results in downregulation of gluconeogenic enzymes, upregulation of glucokinase (GCK), and an increase in glucose-6-phosphate (G6P) and glycogen synthase (GS) levels leading to glycogen formation. G6P inhibits glycogen phosphorylase (GP) decreasing thus glucose production. Inhibition of phosphorylase kinase and activation of protein phosphatase by insulin results in suppression of glycogenolysis. Peripheral and central insulin act via decreased sympathetic nervous system (SNS) outflow to suppress WAT lipolysis and stimulate lipogenesis resulting in decreased free fatty acid (FFA) and glycerol flux to liver. Reduced FFA flux to liver inhibits intrahepatic triacylglycerol (TAG) accumulation and very-low-density lipoprotein (VLDL) secretion. Peripheral and potentially central insulin suppress pancreatic glucagon secretion, and central insulin action may suppress pancreatic insulin secretion. Activation of ATP-sensitive potassium (KATP) channels mediate central insulin action via vagal efferents to liver. Modified from Lewis et al., 2021. Based on Petersen & Shulman, 2018; Roden & Shulman, 2019 and Lewis et al., 2021. Illustrated partly using Servier Medical Art; https://smart.servier.com/, provided by Servier, licensed under a Creative Commons Attribution 3.0 Unported license.

Controversy exists about the effect of central insulin on adipose tissue lipolysis in humans. Suppression of lipolysis assessed by circulating FFA levels and the rate of appearance of deuterated glycerol in fasting state after IN insulin have been reported [Iwen et al., 2014] as well as transient decrease in FFA levels in postprandial state [Benedict et al., 2011]. With diazoxide during euglycemic clamp with somatostatin no chances in FFA levels were found [Esterson et al., 2016; Kishore et al., 2011]. Decreased FFA flux into the liver as a result of suppressed lipolysis and increased lipogenesis by insulin leads to decrease in hepatic triacylglycerol (TAG) content and VLDL secretion [Scherer et al., 2011]. Central insulin signalling in contrast results in enhanced hepatic VLDL secretion thus decreasing hepatic lipid content as demonstrated in rats with intracerebroventricular [Scherer et al., 2016], and in humans with IN administration of insulin [Gancheva et al., 2015]. Also, mice lacking central IRs showed decreased hepatic lipid secretion, whereas mice with peripheral loss of IRs exhibited increased hepatic lipid export [Scherer et al., 2016]. It is suggested that the opposing effect of central insulin balances the direct insulin action on liver [Scherer et al., 2021].

2.4.4.5 Brain insulin action and peripheral insulin sensitivity

Evidence points towards that brain insulin action modulates peripheral insulin sensitivity, although controversies exists. In mice, central administration of K_{ATP} channel inhibitor reduced the insulin-stimulated GU of muscle, but not heart or WAT, and reduced the inhibitory effect of insulin on hepatic EGP [Coomans, Biermasz, et al., 2011]. Central delivery of a MC4R agonist enhanced the insulin action measured as increased GU and glucose infusion rate and inhibition of EPG, while the receptor antagonist had opposing effects [Obici et al., 2001]. However, a study with centrally administered insulin antagonists, insulin or insulin agonist did not show a change in the glucose disposal, although suppression of EGP was either impaired or increased [Obici, Zhang, et al., 2002]. Also, intracerebroventricular insulin infusion [Filippi et al., 2012] and central K_{ATP} channel activation [Pocai et al., 2005] increased the glucose infusion rate needed to maintain euglycemia, which was due to suppression of EGP instead of increased GU. The different results regarding the GU has been by some authors explained by the use of differing insulin levels or duration of fast before the clamp study [Parlevliet et al., 2014].

In humans, IN insulin administration improved systemic insulin sensitivity as estimated by the homeostatic model assessment for insulin resistance (HOMA-IR), and this correlated with an increase in hypothalamic activity measured with functional magnetic resonance imaging (MRI) [Heni et al., 2012]. Improvement in whole-body insulin sensitivity after IN insulin was found also during a hyperinsulinemic-euglycemic clamp, detected as higher glucose infusion rate to

maintain euglycemia and higher insulin sensitivity index. Also these findings correlated with the chance in hypothalamic activity in functional MRI [Heni, Wagner, et al., 2014].

CNS modulates pancreatic insulin, and also glucagon secretion via autonomic output according to circulating and brain interstitial fluid glucose concentration [Faber et al., 2020]. Early studies with dogs have found evidence of the central insulin action in the control on pancreatic insulin secretion, while insulin delivery into CSF was followed by an increase in peripheral insulin secretion [Chen et al., 1975]. Later studies have not found this effect consistently [Scherer et al., 2011, 2016]. In mice, maternal HFD feeding during lactation led to impaired formation of hypothalamic POMC and AgRP projections and parasympathetic innervation of pancreas in offspring, which in turn was associated with obesity and insulin resistance. POMC-specific IR inactivation in offspring prevented the impaired axonal projections and the subsequent metabolic disturbances, demonstrating the contributing effect of defective hypothalamic insulin signalling induced by maternal HFD during lactation [Vogt et al., 2014].

When hypothalamic insulin sensitivity in humans was determined as decreased hypothalamic blood flow after IN insulin delivery, the hypothalamic insulin sensitivity was found to associate with decreased pancreatic insulin secretion [Kullmann, Fritsche, et al., 2017]. [^{18}F]FDG PET study showed a positive correlation with BGU and basal insulin secretion rate and total insulin output in non-diabetic subjects but not in subjects with T2D. Potentiation of insulin secretion associated positively with BGU in non-diabetic, but negatively in subjects with T2D. The results points towards the brain´s contribution of insulin secretion independently of insulin sensitivity [Rebelos et al., 2020]. According to neuronal mapping, the glucose sensing neurons of ARC that express GCK enzyme appears to be essential for pancreatic insulin secretion. Inhibition of these neurons resulted in impaired insulin secretion and glucose intolerance [Rosario et al., 2016]. Also MC4Rs that bind α-MSH derived from POMC neurons seem to have a role in regulating insulin level. Deletion of these receptors in the dorsal vagal complex, a brainstem region integrating afferent and efferent signals, has found to result in hyperinsulinemia and insulin resistance independently of changes in weight and glucose homeostasis [Berglund et al., 2014]. In addition, perturbation of hypothalamic GLUT4 expressing neurons has found to associate with hyperglycaemia and decreased insulin secretion [Ren et al., 2015]. The brain modulates the counterregulatory responses to hypoglycaemia [Bolli & Fanelli, 1999]. Based on studies with mice, it is suggested that hypothalamic insulin signalling might modulate glucagon secretion from the pancreatic α-cells under fasting and hypoglycaemia [Paranjape et al., 2010].

2.5 Obesity and insulin resistance

2.5.1 Mechanisms of obesity-induced insulin resistance

Insulin resistance is defined as inability of target tissues to adequately respond to insulin effect [M. C. Petersen & Shulman, 2018]. Obesity-related insulin resistance contributes to both defect in IRs and insulin signal transduction. The pathophysiology of systemic insulin resistance is chronic overnutrition, which promotes ectopic lipid accumulation in skeletal muscle and liver, and adipose tissue hypertrophy and hyperplasia resulting in tissue-specific and systemic insulin resistance [M. C. Petersen & Shulman, 2018]

Skeletal muscle insulin resistance is considered to precede the hepatic and adipose tissue insulin resistance and pancreatic β-cell failure [DeFronzo & Tripathy, 2009; K. F. Petersen et al., 2007]. Because of the large proportion of postprandial glucose disposal, skeletal muscle insulin resistance has a marked significance in whole-body glucose turnover. The defect in insulin signalling cascade in myocyte has been located at the proximal level as decreased IRs and PI3K/Akt binding, GLUT4 translocation and glycogen synthesis [M. C. Petersen & Shulman, 2018]. Instead of glycogen synthesis in skeletal muscle, the ingested carbohydrates are converted to hepatic *de novo* lipogenesis resulting in increased VLDL secretion and plasma triglyceride level, and reduced plasma high-density lipoproteins [K. F. Petersen et al., 2007]. Elevated FFA and triglyceride content in myocytes favours lipid synthesis and further impairs the insulin signal transduction events and insulin-stimulated GU resulting in lipid-induced insulin resistance. Suggested mediators of lipid-induced insulin signalling impairment include fatty acid metabolite diacylglycerol (DAG), fatty acyl-coenzyme A (fatty acyl-CoA), ceramides, and incomplete mitochondrial fatty acid oxidation that produces reactive oxygen species and acylcarnitine [Kahn et al., 2006; M. C. Petersen & Shulman, 2018; Roden & Shulman, 2019].

WAT insulin resistance is associated with decreased adipocyte IR content, signalling cascade activity and decreased GU. WAT expansion due to chronic nutrient oversupply is accompanied with homeostatic stress, increased adipocyte death, macrophage recruitment and increased production of molecules including hormones and inflammatory cytokines that promote low-grade inflammation. WAT dysfunction plays a central role in the development of systemic insulin resistance. Impaired suppression of lipolysis and decreased lipogenesis stimulate increased glycerol and FFA flux to other tissues. These changes favour ectopic lipid accumulation and impairment of insulin signalling [Kahn et al., 2006; M. C. Petersen & Shulman, 2018; Roden & Shulman, 2019]. Abnormal WAT mitochondrial function associates with decreased whole-body insulin sensitivity via decreased

secretion of bioactive factors and increased production of lactate. VAT, as compared to SAT expresses higher lipolytic activity and lower rate of lipogenesis. Thus the liver is via portal delivery exposed to larger amounts of lipid metabolites than the peripheral tissues [Bódis & Roden, 2018].

Increased glycerol and FFA flux to liver stimulates hepatic gluconeogenesis, triglyceride and TAG accumulation, and formation of lipotoxic metabolites and proinflammatory mediators that inhibit insulin signalling. If continuing, these changes are associated with non-alcoholic fatty liver disease (NAFLD). Suppression of insulin-stimulated GU and glycogen synthesis results in rise in plasma glucose level. In addition, overnutrition induced ER stress stimulates hepatic *de novo* lipogenesis impairing hepatic insulin signalling. Increased lactate flux from WAT further enhances liver insulin resistance by inducing hepatic gluconeogenesis [M. C. Petersen & Shulman, 2018; Roden & Shulman, 2019].

Tissue-specific changes in insulin resistance results in postprandial and fasting hyperglycaemia followed by compensatory rise in β-cell insulin secretion and β-cell mass. Insulin secretion can increase up to fivefold to that of insulin sensitive subjects´, while the β-cell mass is increased about 50% in subjects with obesity related insulin resistance. The resultant hyperinsulinemia induces downregulation of the number of IRs and the intracellular insulin signalling promoting insulin resistance. Chronic hyperglycaemia and elevated FFA levels impair the adaptive response of β-cells that results in a decline in insulin synthesis, secretion and defective intracellular insulin signalling, and ultimately the development of T2D [Kahn et al., 2006; Roden & Shulman, 2019].

2.5.2 Tissue-specific changes in insulin resistance

Insulin resistance results in tissue-specific manifestations that further modulate tissue communication. In skeletal muscle, insulin resistance is manifested as impaired insulin-stimulated GU and glycogen synthesis, increased FFA uptake derived from WAT lipolysis, and accumulation of ectopic fat. Increased skeletal muscle FFA availability impairs mitochondrial function and enhances lipotoxic signalling. In WAT, insufficient suppression of lipolysis and impaired lipogenesis with subsequent release of FFAs and glycerol, and decreased insulin-stimulated GU and low-grade inflammation takes place. Hepatic glycolysis and gluconeogenesis are enhanced, and net glycogen synthesis and GU decreased under insulin resistant conditions. Skeletal muscle insulin resistance increases glucose delivery to the liver. This, in association with hyperinsulinemia and increased FFA and glycerol flux from the unsuppressed lipolysis in WAT, promotes triglyceride and hepatic ectopic fat formation, lipotoxic signalling and impaired control of glycogen synthesis and gluconeogenesis. Upregulated *de novo* lipogenesis leads to increased VLDL

production. Obesity and HFD feeding that associates with systemic insulin resistance, leads to BAT dysfunction. This BAT "whitening" is characterized by diminished vascularity, loss of mitochondrial function and number, lipid droplet accumulation, impaired thermogenic response and decreased BAT GU (Shimizu et al., 2014). As a consequence of these dysregulated processes, insulin secretion compensatory increases restoring normoglycaemia. With persistent stimulus, and acquired and inherited factors, failure of β-cell insulin secretion and progression to T2D may occur [Roden & Shulman, 2019; Samuel & Shulman, 2016].

2.5.3 Brain insulin resistance

Mechanisms of brain insulin resistance are not fully understood. According to a theory, brain insulin resistance is a physiological adaptation to maintain systemic euglycaemia under conditions with scarce availability of nutrients and warmth; increased WAT lipolysis and hepatic EGP met the increased substrate utilization ensuring the survival. In the modern world with abundant food supply and sedentary lifestyle in turn, the brain insulin resistance is thought to serve as disadvantage response contributing in systemic insulin resistance [Scherer et al., 2021].

Accumulating evidence points to diet-induced inflammation of hypothalamus as a contributing mechanism for brain insulin resistance. This in turn leads to defective interaction with the periphery promoting dysregulation of energy homeostasis and obesity [Jais & Brüning, 2017; Kullmann et al., 2016; Seong et al., 2019]. The most examined nutrients in the pathogenesis of hypothalamic inflammation are lipids, especially long-chain saturated fatty acids (SFA). These lipid species cross the BBB and accumulate in the hypothalamus resulting in activation of inflammatory pathways and inhibition of insulin, and also leptin signalling [Jais & Brüning, 2017; Seong et al., 2019]. In rodent models, high-fat diet (HFD) feeding induces hypothalamic inflammation characterized by increased expression of proinflammatory cytokines and inflammatory response, and impaired anorexigenic insulin signalling [De Souza et al., 2005].

In rodent models, the onset of central inflammatory process is rapid. Hypothalamic inflammatory signalling is evident only after few days of HFD consuming before the onset of peripheral inflammation or substantial changes in weight [Thaler et al., 2012; Waise et al., 2015]. The effect of HFD on markers of inflammation resolves within the first few weeks suggesting a neuroprotective response. However, with prolonged HFD feeding, the hypothalamic inflammatory response and neuronal injury reappears [Thaler et al., 2012]. .Accordingly, post-mortem brain tissue analysis in humans has revealed hypothalamic inflammatory changes in subjects with obesity, with the degree of changes correlating with BMI [Baufeld et al., 2016].

Various cell types are involved in the HFD-induced hypothalamic inflammation. Reactive gliosis, the recruitment, proliferation and morphological chances of astrocytes and microglia in response to injury, and subsequent impairment in the function of NPY/AgRP and POMC/CART neurons are the key events in hypothalamic inflammation. In addition, impaired BBB function in response to HFD contributes to the development of hypothalamic inflammation. Activated microglia accumulated in the hypothalamus produce proinflammatory cytokines such as TNF-α, IL-1β and IL-6 [De Souza et al., 2005; Jais & Brüning, 2017]. Similarly, astrocytes gathered in the hypothalamus in response to HFD feeding produce inflammatory factors. The underlying molecular mechanisms recognized involve the Toll-like receptor 4 (TLR4), ceramide and protein kinase C (PKC), and ER stress pathways (**Figure 6**). The subsequent insulin resistance leads to defective activation of anorexigenic signals and suppression of orexigenic signals promoting increased food intake and positive energy balance.

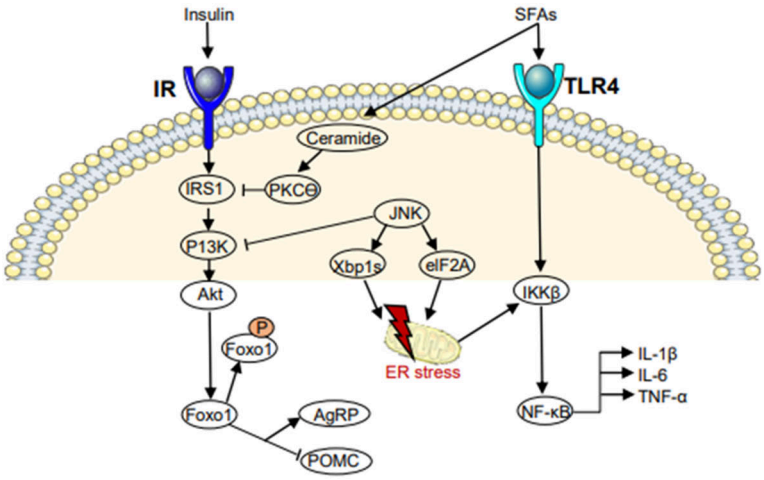

Figure 6 Molecular mechanisms inducing hypothalamic inflammation and insulin resistance. Insulin binding to insulin receptor (IR) activates PI3K/Akt signalling pathway leading to Foxo1 phosphorylation and increased anorexigenic tone via induced POMC and suppressed orexigenic NPY/AgRP gene expression. Binding of saturated fatty acids (SFA) to Toll-like receptor 4 (TLR4) activates inhibitor of kappa B kinase beta (IKKβ) complex and nuclear factor kappa (NF-κB) leading to expression of proinflammatory cytokines. TLR4 activation induces also activation of c-Jun N-terminal kinase (JNK) that inhibits insulin signalling and induces endoplasmic reticulum (ER) stress. ER stress in turn activates the IKKβ and NF-κB promoting inflammation. Induction of ceramides by palmitic acid leads to translocation of protein kinase CΘ (PKCΘ) to the plasma membrane of NPY/AgRP neurons, resulting in inhibition of insulin receptor substrate 1 (IRS1) and insulin signalling cascade. Based on Seong et al., 2019. Illustrated partly using Servier Medical Art; https://smart.servier.com/, provided by Servier, licensed under a Creative Commons Attribution 3.0 Unported license.

Other cell types involved in the neuroinflammation are pericytes, tanycytes and monocytes. Chronic HFD feeding leads to loss of hypothalamic neurons, and reductions in synaptic inputs, activity and plasticity. In addition to hypothalamus, hippocampus, various cortical regions, brainstem and amygdala have been shown to be affected by the obesity-related inflammation. In addition to HFD, the neuroinflammation in these structures is induced by a western diet rich both in fat and carbohydrates, and high intake of sucrose [Dorfman & Thaler, 2015; Guillemot-Legris & Muccioli, 2017; Jais & Brüning, 2017; Seong et al., 2019].

2.5.4 Assessing brain changes associated with obesity with neuroimaging

Neuroimaging studies have demonstrated hypothalamic inflammation also in humans with obesity. Increased gliosis was observed in the mediobasal hypothalamus in subjects with obesity as compared to normal-weight subjects in MRI analysis, and the degree of gliosis did not correlate with age or gender [Thaler et al., 2012]. Also, obesity-related low-grade systemic inflammation associated with reduced integrity of brain structures involved in feeding behaviour, and also with reduced volume of brain regions involved in reward system [Cazettes et al., 2011]. A study using diffusion tensor imaging (DTI), a MRI-based technique that provides information about brain microstructural injury, revealed a positive correlation between BMI, body fat mass, systemic insulin resistance, impaired cognitive performance and the degree of hypothalamic injury [Puig et al., 2015]. Similarly, decreased white matter integrity, which was interpreted to represent axonal loss and measured with DTI, associated with obesity-related systemic inflammation and impaired working memory [Repple et al., 2018]. Furthermore, metabolic syndrome and insulin resistance has found to associated with reduced cortical grey matter volume and thickness assessed with MRI, and the effect was due to insulin resistance per se [Lu et al., 2021]. In numerous studies obesity has found to be linked with lower grey matter volume and cortical thickness [Kullmann et al., 2016].

Further evidence on the relationship of obesity and central insulin resistance in humans has accumulated with magnetoencephalography (MEG), functional MRI (fMRI) and PET studies. MEG showed an increase in spontaneous and stimulated cerebrocortical activity during hyperinsulinemic-euglycemic clamp in lean subjects but not with subjects with obesity, and the increase in the cortical activity correlated negatively with BMI and percent body fat [Tschritter et al., 2006]. Also, insulin-mediated cortical activity correlated negatively with VAT mass, intrahepatic lipid content and serum SFA concentrations suggesting a link between circulating SFA and defective insulin action in the brain [Tschritter et al., 2009]. Data from fMRI

studies have revealed obesity-related changes in brain responses to food stimulus in brain areas related to food processing and reward. After food exposure, subjects with obesity showed greater brain responses than lean subjects, even when satiated [Connolly et al., 2013; Filbey et al., 2012; Heni, Kullmann, et al., 2014].

Finally, PET studies investigating brain insulin signalling have revealed increased insulin-stimulated BGU in humans and animal with obesity as compared to lean subjects [Bahri et al., 2018; Tuulari et al., 2013], and attenuation in BGU after bariatric surgery induced weight loss coupled with enhanced peripheral insulin sensitivity [Tuulari et al., 2013]. Also, subjects with impaired glucose tolerance showed increased BGU under insulin stimulation when compared to healthy subjects [Boersma et al., 2018; J. W. Eriksson et al., 2021; Hirvonen et al., 2011; Latva-Rasku et al., 2018]. Similarly, a large scale cohort analysis showed a negative correlation between the insulin-stimulated BGU and whole-body insulin sensitivity [Rebelos et al., 2021].

2.5.4.1 Brain insulin resistance and dysregulation of peripheral tissues

Brain insulin resistance has been found to associate with metabolic alterations in peripheral tissues, feeding behaviour and also in cognitive functions (**Figure 7**). Although it is unknown whether the brain insulin resistance is a cause or the consequence of these changes, it acknowledged that the brain participates in the interorgan communication regulating systemic insulin sensitivity and energy homeostasis [Kullmann, Kleinridders, et al., 2020; Scherer et al., 2021].

Overnutrition and excess dietary fat correlate with hypothalamic inflammation and resistance to circulating anorexic signals. The subsequent insulin, as well as leptin resistance results in disrupted neuronal interplay with impaired activation of POMC/CART and suppression of NPY/AgRP neurons and decreased MC4R signalling. This further promotes appetite and food intake, and decreases energy expenditure via reduced secretion of thermogenic hormones such as thyrotropin- (TRH) and corticotrophin-releasing hormone (CRH) and increased secretion of anti-thermogenic melanin-concentrating hormone (MCH) [Jais & Brüning, 2017; Seong et al., 2019]. The following positive energy balance leads to weight gain maintaining the cycle. Evidence of the association of impaired brain insulin signalling and reduced BAT metabolism has gained from studies with mice and humans [Benedict et al., 2011; Sanchez-Alavez et al., 2010]. Also, BAT activity is blunted in subjects with obesity as compared to lean subjects. This has been demonstrated as lower BAT GU rate under cold and insulin stimulation with [^{18}F]FDG PET, with the BAT GU correlating positively with whole-body insulin sensitivity [Orava et al., 2013].

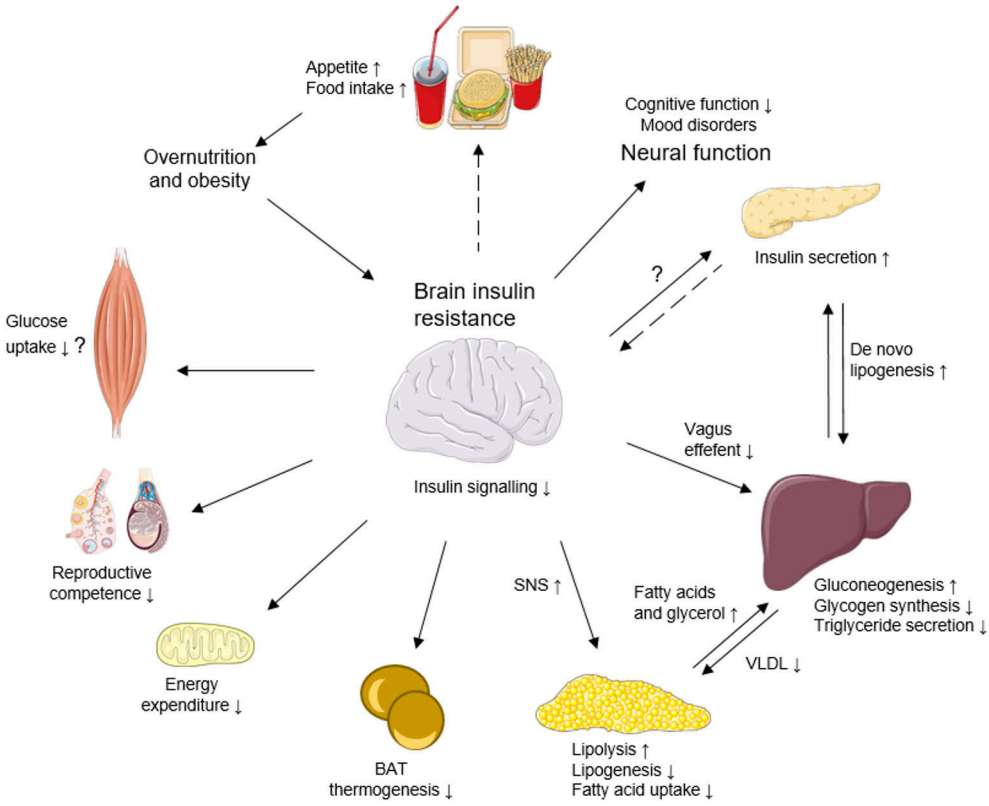

Figure 7 Brain insulin resistance and its metabolic and neural impacts. Chronic overnutrition and obesity induce brain insulin resistance leading to impaired metabolic functions in peripheral tissues, increased food intake, and a decline in cognitive functions and mood disorders. Dashed lines indicate impaired insulin effect. BAT, brown adipose tissue; SNS, sympathetic nervous system; VLDL, very-low-density lipoprotein. Based on Kullmann et al., 2016, Heni et al., 2017 and Scherer et al., 2021. Illustrated partly using Servier Medical Art; https://smart.servier.com/, provided by Servier, licensed under a Creative Commons Attribution 3.0 Unported license.

Brain insulin action inhibits lipolysis and promotes lipogenesis in WAT, and during brain insulin resistance, these effects are impaired, via increased sympathetic outflow to WAT. The resultant increase in FFA and glycerol flux to liver provide substrate for hepatic gluconeogenesis [Scherer et al., 2011]. Central insulin resistance results in impaired hepatic vagal nerve suppression of hepatic EGP by decreasing gluconeogenic enzyme expression and stimulating glycogen synthesis [Lewis et al., 2021]. The decreased central insulin action and simultaneous peripheral hyperinsulinemia promotes hepatic *de novo* lipogenesis, and reduces hepatic triglyceride and VLDL secretion [Scherer et al., 2016].

The relationship and potential causality between brain and skeletal muscle insulin resistance is more controversial. In a study with juvenile obese, Western diet

fed pigs, signs of impaired insulin signalling and action were detected in brain and WAT, but not in skeletal muscle, suggesting that impairments in the brain and WAT insulin signalling may precede that in skeletal muscle, or the brain might be more vulnerable to metabolic perturbations [Olver et al., 2018].

In addition, impaired brain insulin signalling has been found to associate with premature cognitive decline, Alzheimer´s disease and related dementias and behavioural disorders [Kullmann et al., 2016]. Murine models have demonstrated hypogonadotropic hypogonadism and reduced fertility due to hypothalamic-pituitary-gonadotropin axis dysfunction as a result of impaired central insulin signalling [Brüning et al., 2000; Manaserh et al., 2019].

2.6 Endocannabinoid system

2.6.1 Cannabinoid receptors and their ligands

The ECS modulates appetite, food intake and energy balance, in addition to other physiological and cognitive processes [Silvestri & Di Marzo, 2013]. The ECS consists of two G-protein-coupled receptors, cannabinoid type 1 and type 2 (CB1R and CB2R, respectively), their endogenous ligands and ligand-metabolizing enzymes [Di Marzo et al., 2009]. CB1Rs are widely expressed in the CNS, including the neurons involved in the energy balance regulation. In peripheral tissues, CB1Rs are abundant in tissues controlling energy homeostasis, such as gastrointestinal tract, adipose tissue, liver, skeletal muscle, and endocrine pancreas [Silvestri & Di Marzo, 2013]. CB2Rs in turn are mostly located in immune cells, were they modulate cytokine release [Pertwee, 2006]. Although CB1Rs are considered to be the primary cannabinoid receptors responsible for metabolic regulation, CB2Rs might have role in the energy homeostasis control [Silvestri & Di Marzo, 2013].

The most studied endogenous ligands, endocannabinoids (EC) are anandamide (AEA) and 2-arachidonoylglycerol (2-AG). All ECs are derivates from the cell membrane long chain polyunsaturated fatty acid (PUFA) arachidonic acid. ECs are produced after cell stimulation “on demand” and released to their target cannabinoid receptor [Silvestri & Di Marzo, 2013]. Intracellular EC degradation is facilitated mainly by fatty acid amide hydrolase (FAAH) and monoacylglycerol lipase (MAGL) [Muccioli, 2010]. The precursors of the EC metabolizing enzymes derive from phospholipids, whose levels are influenced by dietary omega-3 and omega-6 PUFAs, especially arachidonic acid and docosahexaenoic acid (DHA) [Di Marzo, 2008a].

After released from the cell, ECs bind to cannabinoid receptors, and are then rapidly taken into the cell resulting in an activation of signal transduction pathway, and followed by intracellular degradation. The outcome is a modulation of

neurotransmitter release within the nervous system and multiple biological actions in peripheral tissues [Silvestri & Di Marzo, 2013].

2.6.2 Central endocannabinoid system and the regulation of energy balance

In the CNS, ECS stimulates appetite and food consumption by modulating both homeostatic and hedonic pathways. CB1Rs are widely expressed in the olfactory bulb, several cortical regions and basal ganglia, thalamic and hypothalamic nuclei, cerebellar cortex, and brainstem nuclei [Pagotto et al., 2006]. A brainstem structure outside the BBB, area postrema (AP), might be an important structure for EC signalling as well [Quarta et al., 2011]. The hypothalamic CB1Rs have been found to colocalize with neuropeptides that modulate food intake. ECs are released from the depolarized post-synaptic neuron to activate the presynaptic CB1Rs resulting in either increased stimulation of orexigenic or inhibition of anorexigenic neurons. Leptin controls negatively central ECS tone [Gatta-Cherifi & Cota, 2016], while hypothalamic insulin seems to have no effect on hypothalamic EC levels [Matias, Vergoni, et al., 2008].

Although the main effect of EC signalling in the brain is orexigenic, CB1Rs in the forebrain GABAergic neurons mediate hypophagic actions via reduced inhibitory transmission. It is proposed, that the opposing effects of the ECS in different brain structures reflects the fine-tuned control of neuronal network for the regulation of feeding behaviour [Bellocchio et al., 2010]. As the CB1R signalling may vary upon the specific brain region and presence of hormones such as leptin, ghrelin and glucocorticoids, it may depend on diet consumed as well. Accordingly, mice lacking hypothalamic VMH CB1Rs were hypophagic when exposed to food after prolonged fast, but hyperphagic when exposed to HFD [Cardinal et al., 2014].

The homeostatic pathways in the hypothalamus interact with the reward system. Activation of CB1Rs in the mesolimbic system, nucleus accumbens and ventral tegmentum area affects the hedonistic aspects of feeding by promoting the motivation to consume highly palatable food, especially high caloric food rich in fat and sugar [Tarragon & Moreno, 2017]. This takes place in interaction with the dopaminergic and opioidergic pathways [Silvestri & Di Marzo, 2013]. In addition, activation of CB1Rs in the afferent and efferent brainstem neurons are thought to modulate the vagal output to periphery and thus regulate energy metabolism according to the anorexigenic or orexigenic gastric peptides and gastrointestinal load in relation to eating or fast [Quarta et al., 2011].

Besides the control of eating behaviour, the central ECS participates in the control of thermogenesis. Hypothalamic CB1Rs are suggested to regulate neuronal input to BAT [Cota et al., 2003] and BAT thermogenesis [Richard et al., 2009].

Hypothalamic EC signalling modulates peripheral metabolism also by regulating hepatic EGP and WAT metabolism. Central CB1R activation induce hepatic insulin resistance independent of hepatic insulin signalling, whereas blockade of the central CB1Rs in HFD fed insulin resistant rats restored the hepatic insulin sensitivity. Also, central CB1R stimulation led to impaired suppression of WAT lipolysis under insulin-stimulation that was reversed by the blockage of these receptors. It was suggested that elevated central ECS tone suppresses hypothalamic insulin sensitivity, which in turn correspondence the peripheral metabolic alterations [O'Hare et al., 2011].

In addition to being located on the neuronal membrane, CB1Rs have been detected in the mitochondrial membrane, where they participate in the regulation of neuronal energy metabolism [Bénard et al., 2012]. Furthermore, CB1Rs are expressed in astrocytes on their plasma membrane and in mitochondria. ECS signalling seems to modulate several essential astrocytic functions, such as calcium signalling, which is further linked with the release of gliotransmitters and inflammation [Eraso-Pichot et al., 2023]. Interestingly, activation of mitochondrial CB1Rs in astrocytes led to decreased glycolytic production of lactate, which in turn associated with impaired neuronal metabolic state and altered social behaviour in mice. It was concluded, that mitochondrial CB1Rs regulate glycolysis and lactate production in astrocytes to ensure the metabolic homeostasis of neurons [Jimenez-Blasco et al., 2020].

2.6.3 Peripheral endocannabinoid system and energy metabolism

ECS regulates metabolic functions in several peripheral tissues, including the WAT, BAT, liver, endocrine pancreas and skeletal muscle. CB1R activation on WAT has lipogenic actions and associates with adipocyte differentiation. CB1R stimulation in WAT promotes fatty acid and glucose uptake, *de novo* lipogenesis, adipocyte differentiation, reduces lipolysis, and impairs mitochondrial biogenesis and cold-induced browning. In BAT, ECS activation results in decreased fatty acid uptake, thermogenesis and mitochondrial biogenesis. The overall effect of ECS signalling in adipose tissue is thus to favour energy storage. These actions are mediated by the direct binding of circulating ECs to adipocyte CB1Rs, central ECS signalling and modulation of sympathetic outflow to adipose tissue [Jung et al., 2022; Quarta et al., 2011]. In addition, EC biosynthesis in WAT seems to be under negative control of insulin and central leptin signalling [Matias et al., 2006].

Activation of hepatic CB1Rs promotes lipogenesis and lipid accumulation via upregulation of lipogenic enzymes and *de novo* lipogenesis [Osei-Hyiaman et al., 2005]. In addition, hepatic CB1R activation is associated with impaired glucose tolerance, presumably through inhibition of insulin signalling within hepatocytes

[Silvestri & Di Marzo, 2013]. In pancreatic β-cells, CB1R stimulation have found to enhance basal and glucose-stimulated release of insulin, as also insulin signalling [Gatta-Cherifi & Cota, 2016]. In pancreatic α-cells, stimulation of CB1Rs enhance glucagon release. It is suggested that the altered hormone secretion from the pancreas after CB1R stimulation do not however account for the alterations in plasma glucose level, which is rather affected by modulations in skeletal muscle and liver insulin sensitivity [Di Marzo, 2008b].

In myocytes, ECS seems to regulate the insulin signalling pathways downstream the IR leading to reduced translocation of GLUT4 and decreased basal and insulin-stimulated GU into myocytes. In addition, CB1R stimulation inhibits mitochondrial biogenesis and impairs skeletal muscle oxidative metabolism [Silvestri & Di Marzo, 2013].

2.6.4 Endocannabinoid system in obesity

Obesity and related metabolic disorders are characterized by dysregulation of the ECS. As a manifestation, increased EC biosynthesis and EC levels within the brain, peripheral tissues, circulation, and also altered CR1R expression has been detected in both rodents and humans [Gatta-Cherifi & Cota, 2016; Quarta et al., 2011]. Also, increased circulating EC levels are found to correlate positively with BMI, waist, body fat percentage, VAT and SAT masses, plasma triglyceride, insulin sensitivity, and negatively with high-density lipoprotein (HDL) cholesterol. Weight loss in turn is followed by a decrease in the EC levels. As the EC levels are increased in tissues, including the VAT, in subjects with obesity, they show decreased EC levels in SAT. This is suggest to reflect an imbalance of the ECS tone favouring fat accumulation to VAT depots [Quarta et al., 2011]. It is also observed that the circulating EC levels change according to the phase of eating in both lean subjects and subjects with obesity [Gatta-Cherifi & Cota, 2016] and the content of food consumed, especially the amount and quality of fat, and the duration of HFD [Matias, Petrosino, et al., 2008].

Some discrepancy exists regarding the CB1R expression rate in obesity. HFD fed [Yan et al., 2007] and obese rats [Bensaid et al., 2003] showed increased CB1R expression in WAT, while in humans with obesity, a trend toward a decreased CB1R levels with increased EC levels in VAT were observed [Matias et al., 2006]. Similarly, subjects with obesity displayed lower CB1R gene expression in abdominal SAT and VAT than lean subjects [Bennetzen et al., 2011; Blüher et al., 2006; Engeli, 2008; Sarzani et al., 2009], and weight loss was followed by an increase in the CB1R expression rate [Bennetzen et al., 2011]. EC degrading enzyme and CB1R expression in abdominal SAT both has been found to correlate negatively with circulating EC levels suggesting a negative feedback loop regulation [Engeli et al., 2005]. HFD consumption alters skeletal muscle CB1R expression in rodent

models of obesity, and the altered ECS tone might promote muscle insulin resistance [Silvestri & Di Marzo, 2013]. Accordingly, pharmacological blockade of skeletal muscle CB1Rs lead to an increase in the muscle GU [Liu et al., 2005]. Similarly, in diet-induced obese (DIO) rats, downregulation of central CB1Rs in several extrahypothalamic regions but not in the hypothalamus has been shown. Interestingly, especially intake of highly palatable food associated with the CB1R density in these extrahypothalamic regions, suggesting a link between these receptors and diet-induced obesity [Harrold et al., 2002]. Varying results of the relation of EC metabolizing enzymes in obesity has been found, expression the enzymes being differently affected depending also the WAT depot [Bennetzen et al., 2011; Blüher et al., 2006; Engeli et al., 2005].

Whether the deregulated ECS tone is a cause or the consequence of obesity has not been established [Gatta-Cherifi & Cota, 2016]. As obesity is characterized by insulin and leptin resistance, it seems that these disturbances are linked with the elevated ECS tone in both central and peripheral tissues [D'Eon et al., 2008; Di Marzo, 2008c; Di Marzo et al., 2001; Matias et al., 2006; Tam et al., 2012]. Impaired hypothalamic leptin signalling in obesity associates with elevated hypothalamic EC levels, which in turn might contribute to peripheral metabolic dysregulations including excess fat accumulation [Di Marzo et al., 2001]. Likewise, it is suggested that the central ECS upregulation hinders hypothalamic insulin sensitivity and the insulin effect on peripheral tissue metabolism, which can predispose to systemic metabolic dysregulation and obesity [Quarta et al., 2011]. Obesity-related ECS activation associates with increased expression of TNF-α, which in turn drives ECS activation, and thus creates a potential cycle between adipose tissue inflammation, ECS overactivity and weight gain [Kempf et al., 2007]. Impaired WAT and BAT mitochondrial oxidative activity due to ECS overactivity may in part contribute to decreased whole-body energy metabolism and favour weight gain [Quarta et al., 2011]. In addition, genetic variability in the CB1R coding gene, the CNR1 in humans has found to associate with BMI, insulin resistance and dyslipidaemia [Baye et al., 2008] and also visceral adiposity [Bordicchia et al., 2010]. Similarly, AEA degrading enzyme polymorphism is linked with obesity phenotype related to cardiometabolic risk with higher levels of circulating AEA [Martins et al., 2015], and interestingly, increased reward-related brain activity [Hariri et al., 2009].

2.6.5 Endocannabinoid system as a target to treat obesity

While the ECS regulates energy balance at several levels it provides a potential target to treat obesity and associated metabolic disturbances. Initial studies with rodents demonstrated that the first selective CB1R inverse agonist Rimonabant (SR141716) [Rinaldi-Carmona et al., 1994] reduced food intake and weight [Colombo et al.,

1998]. Accordingly, clinical trials revealed reductions in body weight and adiposity, as also improvements in lipid and glucose homeostasis in humans. Severe neuropsychiatric side effects forced the Rimonabant to be withdrawn from clinical use [Sam et al., 2011], and since then approaches to modulate the peripheral ECS has been investigated [Simon & Cota, 2017].

Peripherally restricted CB1R inverse agonist JD5037 was shown to reduce appetite, body weight, insulin resistance and hepatic steatosis in DIO mice, and the appetite and weight reduction were mediated by reversion of hypothalamic leptin resistance by the JD5037 [Tam et al., 2012, 2017]. Also, DIO mice treated with peripherally restricted CB1R antagonist AM6545 was found to be hypophagic and showed sustained weight loss and improvements in glucose homeostasis, plasma lipid profile and hepatic lipid content [Cluny et al., 2010; Tam et al., 2010]. Peripheral CB1R antagonist BPR0912 induced weight loss irrespective of food intake in DIO mice. In addition, chronic treatment with BPR0912 resulted in an activation of hormone-sensitive lipase (HSL), the key lipolytic enzyme in WAT, and induced upregulation of lipolytic and lipid oxidation promoting genes in DIO mice. Also, BPR0912 induced upregulation of mitochondrial UCP1 in BAT and WAT, and enhanced thermogenesis. As in previous studies, an increase in leptin sensitivity was the suggested the underlying mechanism in these effects. Upregulation of β2-adrenoreceptor in both WAT and BAT observed in DIO mice treated with BPR0912 was suggested to explain the observed improvements in insulin sensitivity and in part the loss in body weight, as β2-adrenoreceptor activation stimulates mitochondrial function, insulin-dependent GU and GLUT4 translocation. [Hsiao et al., 2015].

As the neuropsychiatric adverse effects of Rimonabant were suggested to result from the inverse agonism of the compound [Meye et al., 2013], CB1R neutral antagonist, such as AM4113, has been found to induce weight loss without increases in anxiety and depressive-like behaviour in mice [Gueye et al., 2016]. Several studies in rodents have demonstrated AM4113 treatment induced suppression of appetite and food intake accompanied with reduction in body weight [Chambers et al., 2007; Cluny et al., 2011; Sink et al., 2008], which was primarily contributed by reduced fat mass, but unaltered circulating glucose and lipid levels [Cluny et al., 2011]. In addition, endogenous allosteric ligands such as the steroid hormone pregnenolone, hemopressin, and an urea derivative PSNCBAM-1 have shown to reduce food intake and body weight in animal studies [Simon & Cota, 2017].

Inhibition of the biosynthesis of ECs by modulating the dietary lipid composition has provided promising results both in animals and humans. Diet enriched in omega-3 and limited with omega-6 PUFAs has shown improvements in lipid profile, body composition accompanied with reduced circulating EC levels in subjects with obesity and dyslipidaemia [Berge et al., 2013; Naughton et al., 2016].

3 Aims

The aim of the thesis was to investigate whether alterations in brain and peripheral tissue insulin sensitivity and endocannabinoid system associates with obesity risk in the early adulthood. It is widely acknowledged that obesity is associated with brain insulin resistance manifested as increased insulin-stimulated brain glucose uptake, and alterations in the endocannabinoid system tone. It remains unresolved whether the alterations are present already in the pre-obese state, and whether they link with risk factors for obesity.

The specific questions addressed in this thesis were:

I. Is cerebral glucose uptake increased in healthy young subjects in pre-obese state?

II. Is brain glucose uptake associated with whole-body and peripheral tissue insulin sensitivity already in early adulthood?

III. Are central and peripheral CB1R availabilities associated with obesity risk factors including overweight and increased body adiposity, insulin resistance, low physical activity and familial risk factors?

4 Materials and Methods

The study protocol was reviewed and approved by the Ethics Committee of the Hospital District of Southwest Finland. All participants provided their written informed consent prior to participating in the clinical study (NCT03106688). The studies were conducted in accordance with the principles of the Declaration of Helsinki. Volunteers were recruited via newspaper advertisements, university-hosted email lists and bulletin boards.

4.1 Study subjects

A group of 19 healthy subjects were recruited to the high-risk (HR) and 22 to the low-risk (LR) group according to common obesity risk factors (BMI, leisure time physical exercise and parental risk factors). Inclusion criteria to the HR group was male sex, age of 20–35 years, BMI 25-30 kg/m^2, leisure time physical exercise < 4 hours per week and maternal or paternal overweight or obesity or T2D. Inclusion criteria for LR group were male sex, age 20–35 years, BMI 18.5–24.9 kg/m^2, leisure time physical exercise > 4 hours per week and no parental overweight or obesity or T2D. Exclusion criteria for both groups were any chronic disease or medication that could affect glucose metabolism or neurotransmission, eating disorder, smoking tobacco, abusive use of alcohol or narcotics, and prior participation in PET studies or other significant prior exposure to radiation.

Clinical screening, consisting of physical examination, anthropometric measurements, electrocardiography (ECG), routine laboratory tests, a 2-hour oral 75-g glucose tolerance test, urine drug screening and medical history inquiry were performed before inclusion to the study. In study I and II, the sample consisted of 19 HR and 22 LR subjects, and in study III, 16 HR and 21 LR subjects. The basic characteristics of the subjects´ are described in **Table 1**.

The familial obesity risk scoring applied in study I, consisted of subject´s report of parental overweight, obesity and T2D; one point from such condition in one parent and two point from both parents, total score ranging from 0 to 4.

Table 1 Basic characteristics of the study subjects. HR, high-risk; LR, low-risk. Data presented as mean ± SD.

Study	Risk group	n	Age (years)	BMI (kg/m^2)	Radiotracer
I	HR	19	27 ± 4	27.1 ± 1.9	[^{11}C]carfentanil [^{18}F]FMPEP-d_2 [^{18}F]FDG
	LR	22	23 ± 3	21.9 ± 2.0	
II	HR	19	27 ± 4	27.1 ± 1.9	[^{18}F]FDG
	LR	22	23 ± 3	21.9 ± 2.0	
III	HR	16	28 ± 4	27.3 ± 1.9	[^{18}F]FMPEP-d_2 [^{18}F]FDG
	LR	21	23 ± 3	22.1 ± 2.0	

4.2 PET studies

4.2.1 Principles of PET

PET is a non-invasive imaging technique which allows quantitative in vivo measurement of physiological and biochemical processes such as metabolism, blood flow and neurotransmitter systems. PET is based on a positron decay of radionuclides that are used to label compounds of special biological interest

PET uses of cyclotron-produced, short half-life and positron rich radionuclides that decay by positron emission. The emitted positrons rapidly lose their kinetic energy in tissue, and subsequently annihilate with a nearby electron. The annihilation process results in two photons that are emitted in opposite directions, both carrying energy of 511 keV. The photons emitted are recorded in coincidence detection by a PET scanner containing an imaging ring of radiation detectors (**Figure 8**). The line between the two detectors is called the line of response (LOR), and during a PET scan, data from numerous LORs at different angles are collected. The number of counts measured by a detector is proportional to the radioactivity along the LOR. The raw data, consisting of coincidence events of all angles, is represented as sinogram, which is ultimately reconstructed into cross-sectional images. The PET data can be collected as dynamic or static sequence. The dynamic time frames provide information about the changes in tissue activity concentration over time course, and enables modelling and calculations of the rates of radiotracer transportation between blood and tissue compartments. Static data acquisition comprises of a single frame, scanned usually later after tracer injection, and can be used when the radiotracer concentration in circulation and tissues are expected to be more stable [Cherry & Dahlbom, 2006; Turkington, 2001].

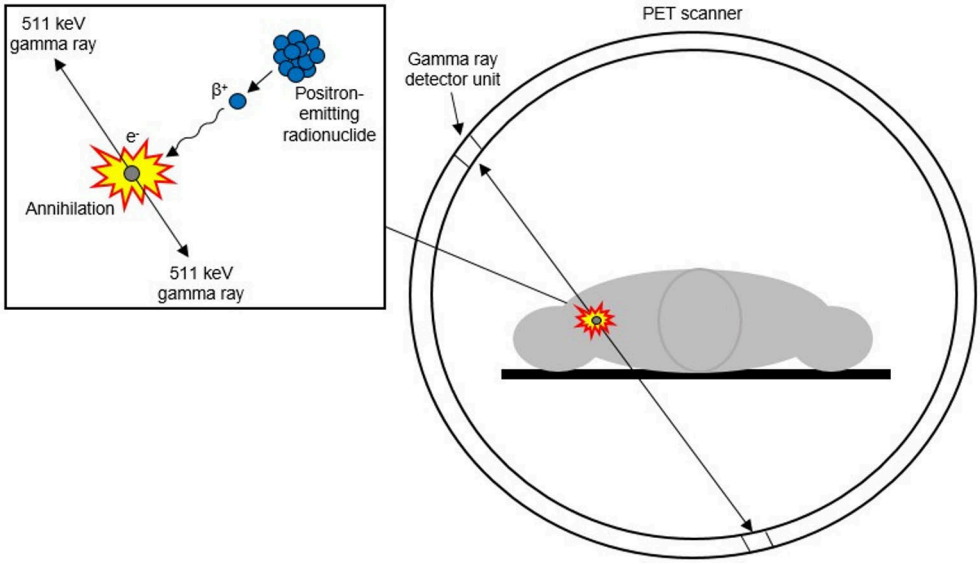

Figure 8 A schematic illustration of positron-electron annihilation producing two 511 keV photons leaving in opposite directions, and detection of the coincidence event by the PET scanner. Modified from van der Veld et al., 2013.

While the quality of images is degraded by such factors as dead time (missing photon detection due to increased rate of photons hitting a detector), decay (the decay of the radionuclide after radioligand injection, and the decrease of radioactivity during the PET scan) and photon attenuation (the loss of detection of coincidence due to photon absorption in the body), they should be corrected before or during image reconstruction. Correction for decay and dead time can be done automatically, while the attenuation correction is performed by modelling using low-dose CT images acquired before the start of PET scans. [Cherry & Dahlbom, 2006; Turkington, 2001].

4.2.2 Radiochemistry

Radionuclides were produced in the cyclotrons of Åbo Akademi University and Turku PET Centre, and radiotracers were synthesized in the Radiopharmaceutical Chemistry Laboratory of the Turku PET Centre.

[^{18}F]FDG was used to quantify tissue glucose uptake in Studies I-III. [^{18}F]FDG is a glucose analogue, with a hydroxyl group at the C-2- position in the glucose molecule substituted by a fluorine-18 (halflife 109.8 min) radionuclide. [^{18}F]FDG is widely use in the determination of regional glucose utilization by tissues and organs. As glucose, [^{18}F]FDG enters the cell via GLUT transporters, and then either rapidly undergoes a phosphorylation by hexokinase into [^{18}F]FDG-6-phosphate ([^{18}F]FDG-

6-P) [Bessell et al., 1972] or is transported back to circulation. Further metabolites such as 2-[^{18}F]-fluoro-2-deoxy-6-phosphogluconate ([^{18}F]FDG-6-PG1) and 2-[^{18}F]-Fluoro-2-deoxy-6-phospho-d-gluconolactone ([^{18}F]FDG-6-PGL) appears later, 90 min after [^{18}F]FDG injection with extent varying from tissue to tissue. Likewise, these metabolites accumulate inside the cell [Bender et al., 2001]. Because of the fluorine-18 substituting the hydroxyl group in the C-2 position, the [^{18}F]FDG-6-P does not enter the glycolytic pathway [Horton et al., 1973] nor glycogen synthesis [Bender et al., 2001], and is not transported back to blood. Because of low expression of glucose-6P-phosphatase in other tissues than liver and kidney [van Schaftingen & Gerin, 2002], dephosphorylation of [^{18}F]FDG-6-P is limited, and the [^{18}F]FDG-6-P gets trapped in inside the cell until the positron decay of fluorine-18. This forms the basis of the measurement of the glucose consumption of a tissue by modelling [^{18}F]FDG uptake with PET data [Phelps et al., 1979]. Comparing hyperinsulinemic-euglycemic clamp with [^{18}F]FDG PET study, tissue-specific GU rates can be assessed *in vivo* [Nuutila et al., 1992]. [^{18}F]FDG was produced using FASTlab synthesis platform (GE Healthcare) according to a modified method of Hamacher et al [Hamacher et al., 1986] and Lemaire et al [Lemaire et al., 2002]. Radiochemical purity was > 98%.

[^{18}F]FMPEP-d_2 was used to measure tissue CB1R availability in studies I and III. [^{18}F]FMPEP-d_2 is an inverse agonist of CB1Rs, and has high affinity and selectivity for CB1Rs [Donohue et al., 2008]. [^{18}F]FMPEP-d_2 passes the BBB, and demonstrates high uptake in brain making it suitable for the measurement of brain CB1R availability [Hirvonen, 2015; Terry, Hirvonen, Liow, Zoghbi, et al., 2010]. In a dosimetry study, of the peripheral organs that were visually identified from the PET images, the uptake of [^{18}F]FMPEP-d_2 was highest in the liver, followed by the lungs, small intestine, kidneys, heart and spleen, gallbladder, lumbar vertebrae and urinary bladder. While [^{18}F]FMPEP-d_2 is excreted in urine and bile, it is not applicable for the measurement of CB1R availability in the liver, intestine or urinary bladder [Terry, Hirvonen, Liow, Seneca, et al., 2010]. Binding of [^{18}F]FMPEP-d_2 to CB1Rs in BAT but not in WAT was detected in rats [O. Eriksson et al., 2015]. In humans, CB1R availability in BAT under cold exposure was upregulated as detected with [^{18}F]FMPEP-d_2 PET imaging, and the binding of [^{18}F]FMPEP-d_2 in WAT, and also in brain, was lower in subjects with obesity as compared to lean participants [Lahesmaa et al., 2018] suggesting that [^{18}F]FMPEP-d_2 is eligible for quantifying the availability of peripheral CB1Rs. The binding of [^{18}F]FMPEP-d_2 d2 to it´s receptors may depend on the level of the natural ligands endocannabinoids competing the receptor binding [Takkinen et al., 2018]. The radiotracer was produced as described previously [Lahdenpohja et al., 2020]. Radiochemical purity was > 95%.

4.2.3 PET image acquisition

The PET studies were performed at the Turku PET Centre on separate days. The subjects were instructed to abstain from caffeine, alcohol and physical exercise on the PET scan days and the day before each scan. All studies were done in room temperature. During all the PET scans, the subjects were positioned in a supine position with their heads strapped to the scan table to prevent head movement. To obtain arterialized venous blood samples, the arm used for blood sampling was heated with a hot water bottle. Plasma radioactivity was measured with an automatic γ-counter (Wizard 1480 3", Wallac, Turku, Finland). The subjects were clinically monitored by physician throughout the scans.

4.2.3.1 [^{18}F]FDG PET scan with hyperinsulinemic–euglycemic clamp

The [^{18}F]FDG scans were performed with the GE Discovery (Discovery 690 PET/CT, GE Healthcare) PET camera after a 12-h overnight fast. Hyperinsulinemic–euglycemic clamp was applied along with the PET imaging to measure whole-body insulin sensitivity (**Figure 9**) [DeFronzo et al., 1979; Nuutila et al., 1992].

Subjects laid in a supine position and one cannula was inserted in an antecubital vein for insulin and glucose infusion and for radiotracer injection, and one in the contralateral antecubital vein for blood sampling. After collecting fasting laboratory samples, the clamp was started. Insulin (Actrapid, Novo Nordisk A/S, Bagsvaerd, Denmark) was administered in a primed continuous manner at the rate of 40 mU/m2 /min after first 7 min of priming with higher doses. Euglycemia, (plasma glucose level 5.0 ± 0.5 mmol/L) was maintained with a variable rate of 20% glucose infusion based on plasma glucose measurements taken every 5 to 10 minutes. Plasma insulin was measured at fasting and every 30 min to ascertain adequate insulin level during the clamp, and serum FFA at fasting and every 60 min to study the suppression on lipolysis. Whole-body insulin sensitivity, indexed by the M value was calculated as the average of 20-min intervals between 60-160 min during steady euglycemia using following formula:

$$M = GIR - UC - SC \quad (1)$$

where GIR is the glucose infusion rate expressed in μmol per kg of body weight or per kg fat-free mass (kg_{FFM}) UC is the urinary glucose excretion rate, and SC is the space correction accounting for the changes in the glucose level in the glucose space [DeFronzo et al., 1979].

The subjects were transferred to the PET/CT scanner. A scout CT was acquired for attenuation correction. After reaching steady euglycemia (80 ± 13 min from the start of the insulin infusion), a single bolus of 156 ± 10 MBq of [^{18}F]FDG was injected intravenously and dynamic PET scanning was started with the clamp

ongoing. Dynamic scans of thoracic region (0–40 min using 4 × 15, 6 × 20, 2 × 60, 2 × 150 and 6 × 300 s frames), upper abdomen (40–55 min; 3 × 300 s) and thighs (55–70 min; 3 × 300 s) and static data of the neck (10 min; 1 × 600 s) and brain (10 min; 1 × 600 s) were collected. Short low-dose CT scans were obtained before the emission scan of every region. To measure plasma activity, arterialized venous blood samples were taken at 4.5, 7.5, 10, 20 and 30 min from the [^{18}F]FDG injection, and in the middle time points of the upper abdomen, thigh, neck and brain scans. The amount of [^{18}F]FDG lost to urine was determined from a urine collected at the end of the scan and during the scan when necessary, and measured with an isotope dose calibrator (Model VDC-205; Comecer Netherlands, Joure, Netherlands)

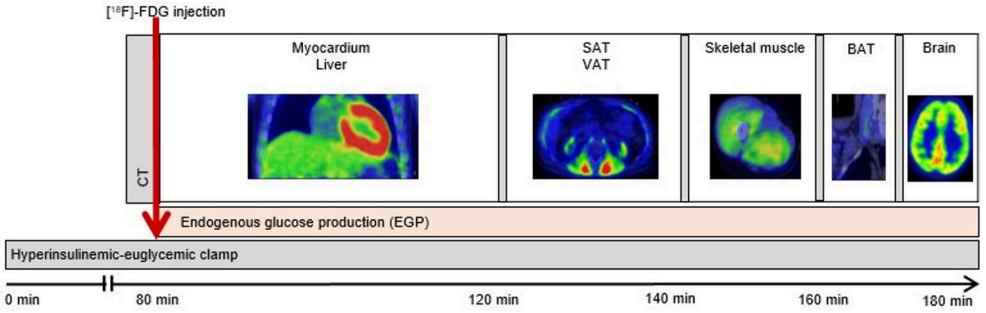

Figure 9 Clinical [^{18}F]FDG PET study design during hyperinsulinemic–euglycemic clamp. BAT, brown adipose tissue; SAT, subcutaneous adipose tissue; VAT, visceral adipose tissue.

4.2.3.2 [^{18}F]FMPEP-d_2 scan

The [^{18}F]FMPEP-d_2 scans were performed with PET/CT (GE Discovery VCT PET/CT, GE Healthcare) after a 6–12 hour fast. Two cannulas were inserted in veins of opposite forearms, one for blood sampling and one for [^{18}F]FMPEP-d_2 injection. Before the scan, fasting blood samples were collected to measure hematocrit and serum endocannabinoid levels. A scout CT was acquired for attenuation correction. 147–215 MBq of [^{18}F]FMPEP-d_2 was injected as an intravenous bolus and dynamic scans of the brain (60 min using 3 × 60 s, 5 × 180s and 7 × 360 s frames), neck (12 min; 4 × 180 s frames), abdomen (9 min; 3 × 180 s) and a late scan of the brain (9 min; 3 × 180 s) were conducted. Before each scanning region, CT scans were acquired for photon attenuation and anatomical reference. Arterialized venous blood samples to measure plasma activity were collected at 0.25, 0.5, 0.75, 1, 1.25, 1.5, 1.75, 2, 2.5, 3, 4.5, 7.5, 11, 15, 20, 25, 30, 35, 40, 45, 50 and 60 min from the [^{18}F]FMPEP-d_2 injection, and at following time points (min from the regional scan start): neck (2 and 6 min), abdomen (4.5 min) and late brain scan (4.5 min). Additional blood samples for [^{18}F]FMPEP-d_2 metabolite analysis were taken before the scan and at 4.5, 11, 15, 20, 30, 45 and 60 min from the radiotracer injection, and

at following time points (min from the regional scan start): neck (2 and 6 min), abdomen (4.5 min) (**Figure 10**).

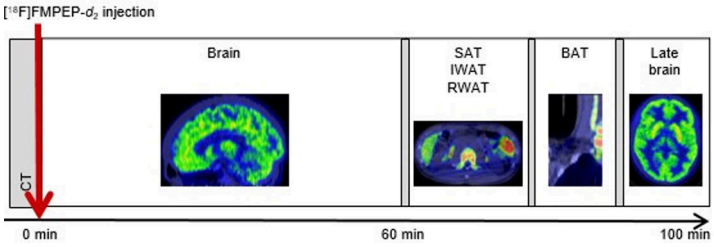

Figure 10 Clinical [^{18}F]FMPEP-d_2 PET study design. BAT, brown adipose tissue; IWAT, intraperitoneal white adipose tissue; RWAT, retroperitoneal adipose tissue; SAT, subcutaneous adipose tissue.

4.2.4 PET image analysis

4.2.4.1 Quantification of glucose uptake with [^{18}F]FDG

Quantification of tissue GU with [^{18}F]FDG is commonly based on three-compartmental model. In this model, [^{18}F]FDG in plasma, [^{18}F]FDG in extracellular space and [^{18}F]FDG-6-P inside the cells are considered as compartments [Phelps et al., 1979] (**Figure 11**).

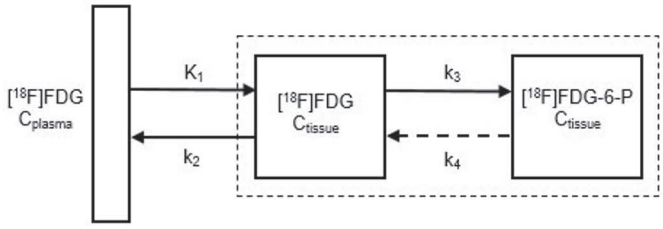

Figure 11 Three-compartment model of [^{18}F]FDG kinetic modelling. K1 and k2 are rates of [^{18}F]FDG transportation, k3 is the rate of [18F]FDG phosphorylation, and k4 the rate of [^{18}F]FDG-6-P dephosphorylation. Modified from Gunn et al., 2001.

Metabolic rate of glucose ($MR_{glucose}$) can be calculated using following formula:

$$MR_{glucose} = \frac{C_{glucose}}{LC} \; x \; \frac{K_1^* \, x \, k_3^*}{k_2^* + k_3^*} \qquad (2)$$

where $C_{glucose}$ is the average plasma glucose concentration from the [^{18}F]FDG injection until the end of the PET scan, LC is a lumped constant that accounts for the differences in transport and phosphorylation rates between [^{18}F]FDG and glucose of

the studied tissue, K_1* is the rate of [^{18}F]FDG membrane transport forward, k_2* is the rate of [^{18}F]FDG membrane transport backward, and k_3* is the rate constant of [^{18}F]FDG phosphorylation.

A direct estimation of the combination of the rate constants can be derived using a graphical method, the Patlak plot [Patlak & Blasberg, 1985], that combines the rate of constants (K_1*, k_2*, k_3*) as the net uptake rate (K_i) for [^{18}F]FDG for the further calculation of $MR_{glucose}$:

$$K_i^* = \frac{K_1^* \, x \, k_3^*}{k_2^* + k_3^*} \tag{3}$$

$$MR_{glucose} = \frac{C_{glucose}}{LC} \, x \, K_i^* \tag{4}$$

The principle of the Patlak plot is that the accumulation of radiotracer in the irreversible compartment in relation to the radiotracer that has been available in plasma reflects the net uptake rate of the radiotracer in the tissue. This takes place when the concentration of the radiotracer in the reversible tissue compartments and in plasma are in dynamic equilibrium. This happens after the early sharp rise in plasma concentration when the radiotracer concentration in reversible tissue compartments start to follow that in plasma. The Patlak plot is useful in other tissues than in brain, where the endothelial wall is very permeable for glucose and [^{18}F]FDG as compared to the BBB The following equation describes the Patlak plot:

$$\frac{C_{tissue}(T)}{C_{plasma}(T)} = K_i \, x \, \frac{\int_0^T C_{plasma}(t)dt}{C_{plasma}(T)} + Int \tag{5}$$

where the tissue concentration of radiotracer in relation to the radiotracer availability in plasma in certain time is calculated by multiplying the net uptake rate (K_i) by integral of plasma radiotracer concentration from injection to the middle of the selected time frame divided by plasma concentration during the frame and added with the intercept (Int) of the slope with the y-axis (**Figure 12**) [Oikonen, 2023].

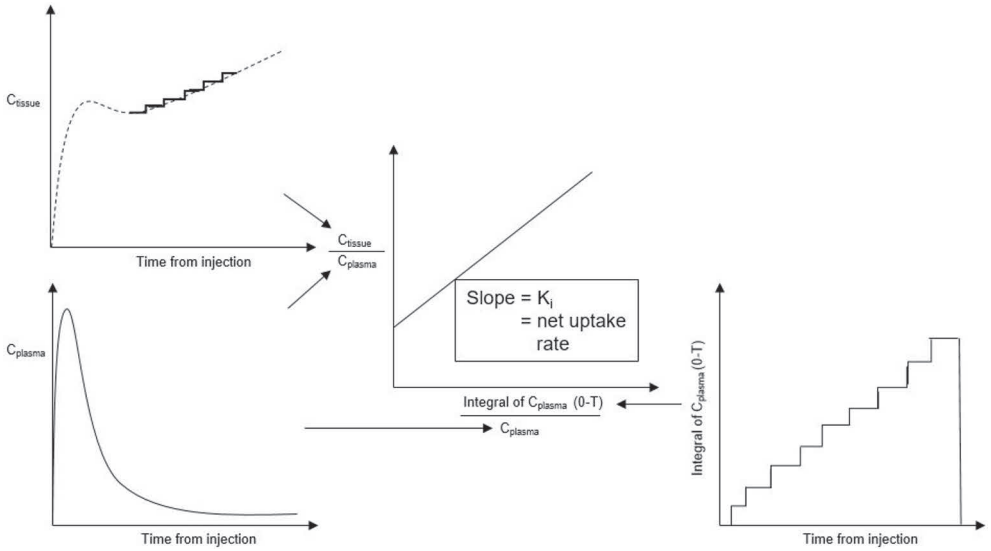

Figure 12 The Patlak plot becomes linear when the equilibrium between the radiotracer concentrations in the reversible compartments and plasma is achieved. The y-axis of the plot comprises of the ratio of concentrations of radiotracer in tissue region of interest and plasma as function of time. The x-axis is the ratio of the integral of plasma radiotracer concentration and the plasma concentration. The slope of the plot´s linear phase represents the tissue net uptake rate of the radiotracer. Based on Oikonen, 2023.

Concentration of [^{18}F]FDG in plasma is measured from blood samples collected during the scan, and can be combined with the PET image-derived activity to form the input function for the analysis of [^{18}F]FDG uptake. Conversion of tissue [^{18}F]FDG uptake to GU is performed multiplying the Ki with the average plasma glucose concentration from [^{18}F]FDG injection to the end of the scanned tissue and divided by tissue density and LC as described in chapter 4.2.5.2.

The Patlak plot is suitable only for dynamic PET scans. For static scans in which activity is measured only in one timepoint, calculation of fractional uptake rate (FUR) of [^{18}F]FDG is preferred. FUR can be calculated with the following equation:

$$FUR = \frac{C_{tissue}(T)}{\int_0^T C_{plasma}(t)dt} \quad (6)$$

FUR is a simple estimate of the Patlak plot slope Ki, with the extension that the distribution volume of [^{18}F]FDG is no longer important at late time after [^{18}F]FDG injection [Thie, 1995]. Tissue GU is obtained by multiplying FUR with the average plasma glucose concentration and dividing by LC. FUR overestimates the net uptake rate of the radiotracer, but at late timepoints (over 60 min after injection) the bias is less than 5%, making FUR a suitable alternative for the Patlak plot [Oikonen, 2021].

4.2.4.2 Quantification of peripheral tissue glucose uptake (II, III)

Carimas software (version 2.9, Turku PET Centre, downloadable at https://turkupetcentre.fi/software/) was used for PET image analyses. Tissue [^{18}F]FDG activity was measured by manually drawing regions of interest (ROI) or volume of interest (VOI) to both quadriceps femoris and hamstrings muscles, right lobe of the liver, supraclavicular BAT depots and several volumes of abdominal SAT and VAT on the fused PET/CT images. Several ROIs and VOIs in several slices of images were drawn avoiding large vessels to minimize the spill over effect due to partial volume effect and motion. In the analysis of myocardium, a segmenting tool implemented in Carimas software was used to include the left ventricular walls and septum in the analysis.

Input function for [^{18}F]FDG was determined by combining PET image derived data from left ventricle from 0 to 4.5 min to the arterialized plasma sampling from 4.5 min to the end of the scan. Dynamic tissue time-activity curves and input functions were then used to determine the fractional uptake (Ki) of [^{18}F]FDG using the Patlat plot or its approximation fractional uptake rate (FUR). Tissue-specific GU was calculated using the following formula:

$$Tissue\ GU = \frac{Ki\ x\ plasma\ glucose}{tissue\ density\ x\ LC}\ x\ 1000 \quad (7)$$

where K_i (or FUR) is the fractional uptake of [^{18}F]FDG (l/min), plasma glucose is the average glucose concentration from [^{18}F]FDG injection to the end of the scanned tissue (mmol/L), tissue density (kg/L) and LC is 1.2 for skeletal muscle, 1.0 for liver and myocardium, and 1.14 for adipose tissue [Bøtker et al., 1997; Iozzo et al., 2007; Kelley et al., 1999; Peltoniemi et al., 2000; Virtanen et al., 2001].

4.2.4.3 Quantification of brain glucose uptake (I, II)

Automated PET image processing pipeline Magia [Karjalainen et al., 2020] (https://github.com/tkkarjal/magia), running on MATLAB (The MathWorks, Inc., Natick, MA, USA), was used for preprocessing and modelling of the PET data. [^{18}F]FDG PET images were first corrected for motion and then coregistered with the MRI images. To define ROIs, Magia uses FreeSurfer (https://surfer.nmr.mgh.harvard.edu/). The ROI-wise kinetic modelling was based on extraction of ROI-wise time-activity curves. Parametric images were spatially normalized to Montreal Neurobiological Institute (MNI) space and then smoothed using a Gaussian kernel (full width at half maximum; FWHM = 8 mm). Insulin-stimulated BGU was quantified using FUR. To quantify the FUR values, the tissue radioactivity values were averaged over the time frames after 40 minutes from [^{18}F]FDG injection (late scan). The input function for [^{18}F]FDG was obtained in the

same manner as in peripheral tissues. The FUR estimates were converted into BGU (µmol/min/100g) with the following equation:

$$BGU = 100\ x\ \frac{avg_{plasma\ glucose}\ x\ FUR}{LC\ x\ density} \quad (8)$$

where $avg_{plasma\ glucose}$ is the average plasma glucose concentration (mmol/L) from the time of [^{18}F]FDG injection to the end of brain scan, LC is lumped constant (0.65) [Wu et al., 2003] and density is grey matter relative density in the brain (1.04) [Snyder et al., 1975].

4.2.4.4 Measurement of endogenous glucose production (EGP) (II, III)

EGP was calculated by subtracting the exogenous glucose infusion rate (GIR) from the rate of disappearance of glucose (Rd) during the hyperinsulinemic-euglycemic clamp using the following formula:

$$EGP = R_d + V_{glucose}\ x\ \frac{\Delta_{glucose}}{\Delta_T} - GIR \quad (9)$$

GIR is corrected by a space correction [DeFronzo et al., 1979], where $V_{glucose}$ is the estimated constant for glucose distribution volume (0.19 l/kg), $\Delta_{glucose}$ is the change in glucose concentration from [^{18}F]FDG injection to the end of sampling (mmol/L), Δ_T is the time from [^{18}F]FDG injection to the end of sampling (min) and GIR is the total amount of infused glucose during the scan (mg/kg).

Glucose disappearance rate (Rd) (µmol/min/kg) was calculated using the following equation:

$$R_d = \frac{MCR_{FDG}\ x\ avg_{plasma\ glucose}}{weight} \quad (10)$$

where MCR_{FDG} (ml/min) is the metabolic clearance rate of [^{18}F]FDG, $avg_{plasma\ glucose}$ is the average plasma glucose concentration (mmol/L) from the time of [^{18}F]FDG injection to the end of sampling, and weight is the subject´s weight (kg).
MCR_{FDG} was the calculated with the following formula:

$$MCR_{FDG} = \frac{dose_{FDG} - urine_{FDG}}{AUC_{FDG}} \quad (11)$$

where $dose_{FDG}$ is the injected [^{18}F]FDG dose (kBq), $urine_{FDG}$ is the amount of radiotracer lost to urine (µmol/min/kg) during the entire scan (kBq), and AUC_{FDG} is the area under the curve representing [^{18}F]FDG from the radiotracer injection to infinity.

4.2.4.5 Quantification of cannabinoid receptor availability in peripheral tissues (III)

CB1R availability in peripheral tissues was quantified both as FUR and volume of distribution (V_T) of the [^{18}F]FMPEP-d_2. Radiometabolite corrected plasma input for image analysis was determined by correcting the plasma time-activity curve (TAC) for the fraction of nonmetabolized radioligand measured using thin layer chromatography and digital autoradiography as previously described elsewhere [Lahesmaa et al., 2018].

To determine the FUR of [^{18}F]FMPEP-d_2, Carimas 2.9 Software was used for the image analysis of abdominal SAT, intraperitoneal (IWAT) and retroperitoneal white adipose tissue (RWAT), BAT and muscle. ROIs of each abdominal adipose tissue depots were manually drawn on the fused PET/CT images to several volumes. BAT ROIs were drawn bilaterally in supraclavicular adipose tissue depots. Only voxels with CT Hounsfield units (HU) within the adipose tissue range -50 to -250 were included. ROIs in the skeletal muscle were drawn bilaterally in the deltoideus muscle. Several ROIs in several slices of images for each tissue were drawn avoiding large vessels, and the average of the ROIs was analysed. FUR in each peripheral tissue was calculated by dividing the tissue radioactivity concentration at time X by the $AUC_{0\text{-}X}$ of the radiometabolite corrected plasma TAC. Only FUR estimation was possible in peripheral tissue, since the PET acquisition of those areas did not start directly after radiotracer injection.

V_T (mL·cm-3) is defined as the ratio of the radioligand concentration in tissue target region to the plasma radioligand concentration at the equilibrium state (Innis et al., 2007). V_T of each peripheral tissue was calculated by dividing the radioactivity concentration in tissue by radiometabolite corrected plasma activity at the time interval of the scanned tissue. The V_T and FUR of [^{18}F]FMPEP-d_2 in peripheral tissues were reciprocally related indicating that the V_T may be suitable for estimating CB1R availability also in the late PET scans.

4.2.4.6 Quantification of cannabinoid receptor availability in brain (I, III)

CB1R availability in the brain was quantified as V_T in 21 bilateral ROIs involved in emotion and food reward processing (Study I), and as V_T in the whole brain (Study III). To process the [^{18}F]FMPEP-d_2 PET data, Magia pipeline was used as described above. The PET images were first smoothed using Gaussian kernel (FWHM = 6 mm) to increase signal-to-noise ratio before model fitting. Then, calculated parametric images were spatially normalized to MNI-space and further smoothed using a Gaussian kernel (FWHM = 6 mm). In study I, V_T was determined using multiple-time graphical analysis for reversible radiotracer uptake described by Logan [Logan, 2000]. In this method, activity concentration-time curves for the tissue and plasma

are combined to form a single Logan plot, where linearity is achieved after intercept is effectively constant, and the slope can be estimated as V_T. Image frames starting at 36 minutes and later after the radiotracer injection were used in the modelling, since Logan plots became linear after 36 minutes. Following equation for the Logan plot and V_T calculation can be presented:

$$\frac{\int_0^T C_{ROI}(t)dt}{C_{ROI}(T)dt} = V_T \, x \, \frac{\int_0^T C_p(t)dt}{C_{ROI}(T)} + Int \quad (12)$$

where $C_{ROI}(T)$ is the activity concentration in tissue at the time T, C_p is the activity concentration in the plasma, and Int is the intercept. Detailed modelling information is provided at Turku PET Centre webpages: http://www.turkupetcentre.net/petanalysis/model_mtga.html#logan

In study II, mean V_T of the whole brain was calculated as the average of all white and grey matter voxels within the MNI space template.

4.3 Anthropometric measurements

Height and weight of the subjects were measured at the Turku PET Centre. Weight was measured in underwear or light hospital clothes in fasting state after urinating. Waist circumference was measured at the midpoint between the lowest ribs and the top of iliac crest, and hip circumference around the largest lateral extension of the hip. Body fat percentage was assessed with an air displacement plethysmograph (the Bod Pod system, software version 5.4.0, COSMED, Inc., Concord, CA, USA) after at least four hours of fasting. Blood pressure was measured in sitting position from upper arm with a digital blood pressure monitor. Two measurements in relaxed state were done and the mean value was used.

4.4 Biochemical analysis (I-III)

Plasma glucose during the clamp was determined in the laboratory of the Turku PET Centre in duplicates using the glucose oxidate method (Analox GM9; Analox Instruments, London, UK). Plasma insulin at fasting and during the clamp were measured using an automated electrochemiluminescence immunoassay (Cobas 8000; Roche Diagnostics), serum free fatty acid (FFA) with an enzymatic colorimetric method (NEFA-HR2, ACS-ACOD; Wako Chemicals, Neuss, Germany; Cobas 8000 c502 and Cobas 800 c702 Analyzer, Roche Diagnostics), plasma glucose at fasting and in oral glucose tolerance test (OGTT) with an enzymatic photometry/hexokinase reaction (Cobas 8000 c 702; Roche Diagnostics) and HbA1c with immunoturbidimetry (Cobas 6000 c 501, Roche Diagnostics) at the Turku University Hospital laboratory. Total plasma cholesterol and HDL and LDL

cholesterol were measured with a direct photometric enzymatic assay (Cobas 8000 c 702, Roche Diagnostics) and plasma triglycerides with a photometric enzymatic assay (GPO-PAP; Cobas 8000 c 702, Roche Diagnostics). Plasma creatinine was measured with a photometric enzymatic assay (Cobas 8000 c 702, Roche Diagnostics) and serum high-sensitivity C-reactive protein (hs-CRP) with immunonefelometry (BN ProSpec System; Siemens Healthineers). Plasma alanine aminotransferase, alkaline phosphatase and gamma-glutamyltransferase (GGT) in fasting state were assessed using a kinetic photometry according to IFCC recommendation (Cobas 8000 c 702, Roche Diagnostics) also at the Turku University Hospital laboratory.

4.5 Metabololic analysis (II, III)

Metabolic biomarkers were quantified from serum samples at fasting state using high-throughput proton NMR metabolomics (Nightingale Health Oyj, Helsinki, Finland). The method affords simultaneous quantification of routine lipids, fatty acids, amino acids, glycolysis related metabolites, ketone bodies, fluid balance and inflammation markers well as lipoprotein subclass profiling with lipid concentrations within 14 subclasses. The experimentation and applications of the NMR metabolomics have been detailed discussed previously [Soininen et al., 2015].

4.6 Measurement of tissue masses (II, III)

The abdominal subcutaneous (SAT) and visceral (VAT) adipose tissue volumes were analyzed from MRI images using sliceOmatic® (Tomovision, Montreal, Quebec, Canada). A whole-body MRI was performed at 3T after a 12-hour fasting using the MRI part of a clinical PET-MRI system (Philips Ingenuity TF PET/MR, Philips, Amsterdam, Netherlands). The abdominal SAT compartment was defined as the fat depot between the skin and the above the abdominal musculature. The abdominal VAT volume was quantified from the combination of the intraperitoneal and retroperitoneal fat compartments [Hung et al., 2014].

The femoral SAT and skeletal muscle mass were analyzed from CT images acquired with PET/CT (GE Discovery VCT PET/CT, GE Healthcare) while performing the [^{18}F]FDG -PET/CT-study, because of artefacts in the MRI images in the femoral region. The tissue volume analysis were performed with Carimas software. A total of 47 slices of CT-derived images covering the length of 15 cm, the height of the scanned femoral area, in the mid-section of the thighs of both lower limbs were used for the analysis. To define the tissue regions, attenuation threshold value of -300 to -10 HU for adipose tissue [Martinez-Tellez et al., 2020] and -29 to +150 HU for skeletal muscle [Aubrey et al., 2014] was used. The MRI and CT

derived tissue volumes were converted to masses using densities of 0.9196 kg/L for adipose tissue [Abate et al., 1994] and 1.0597 kg/L for skeletal muscle [Segal et al., 1986]. Brain volumes were determined from MRI images and converted to mass using a density of 1.04 kg/L [Snyder et al., 1975].

4.7 Statistical analysis

In study I, BGU quantified with [^{18}F]FDG and [^{18}F]FMPEP-d_2, V_T were compared between groups using two-sample t-test. Full-volume data were analyzed with nonparametric testing using SnPM13 (http://www.nisox.org/Software/SnPM13/). $P < 0.05$ was considered as the cluster-defining threshold, and only clusters large enough to be statistically significant (False Discovery rate, FDR $P < 0.05$) were reported. Bayesian hierarchical modelling was applied to estimate effect of the obesity risk factors (BMI, physical exercise and parental risk factors) to BGU, V_T and BP_{ND} in a ROI-level. The modelling was performed with the R package BRMS (https://cran.r-project.org/web/packages/brms/index.html), which uses the efficient Markov chain Monte Carlo sampling tools of RStan (https://mc-stan.org/users/interfaces/rstan).To improve model fit, BGU, V_T and BP_{ND} were log-transformed. Associations between serum endocannabinoids and [^{18}F]FMPEP-d_2 V_T were tested in separate full-volume models. Eight endocannabinoid compounds were analysed, so the results were confirmed with Bonferroni-corrected P value as the cluster-defining threshold (0.05/8 = 0.00625). In all analysis, the age was included as a covariate.

In study II, data are presented as mean ± SD. Differences between groups were studied using independent samples t-test or Wilcoxon rank-sum test as appropriate. Categorical variables were compared with the $\chi 2$ test. SPSS statistical software, version 27 was used in statistical analysis. Associations between BGU and distinct predictor variables were examined with a general linear model and SPM12 (https://www.fil.ion.ucl.ac.uk/spm/software/spm12/). The comparison of correlation coefficients between the groups was performed using two-sample independent t-test. The statistical threshold in SPM analysis was set at a cluster level and corrected with false discovery rate (FDR) with $P < 0.05$. Age was controlled for in the SPM analysis.

In study III, the statistical analyses were performed using IBM SPSS statistical software, version 28.0. All data are presented as mean ± SD. An independent samples t-test or Wilcoxon rank-sum test were used as appropriate, to study between-groups comparisons. Categorical variables were compared with $\chi 2$ test. Correlations between distinct variables were studied using the Pearson or Spearman correlation tests. $P < 0.05$ was considered statistically significant.

5 Results

5.1 Obesity risk associates with increased brain glucose uptake already in early adulthood

5.1.1 Study I-II: Increased brain glucose uptake in subjects with high versus low obesity risk

Insulin-stimulated BGU was globally higher in subjects with high (HR) versus low (LR) obesity risk (**Figure 13**).

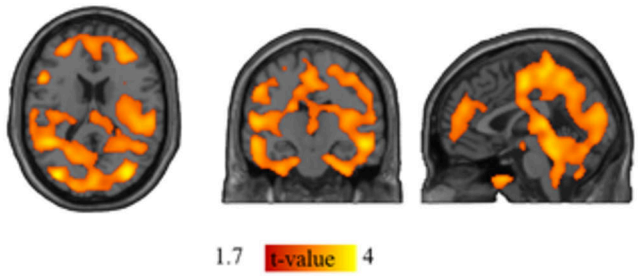

Figure 13 A Statistical parametric mapping (SPM) results from two-sample t test between the HR and the LR group. Colouring show cerebral regions with significantly higher BGU in the high than in the low obesity risk group. Higher T values denote larger differences between the groups. Data are thresholded at $P < 0.05$ and false discovery rate (FDR) corrected at cluster level. Modified from the original publication II.

5.1.2 Study I: Familial obesity risk associates with increased brain glucose uptake

When analysed the association between the three distinct obesity risk factors (BMI, leisure time physical activity and familial obesity risk, including parental overweight, obesity or T2D) and BGU, increased familial obesity risk had the strongest association with increased BGU (**Figure 14**), while the effect of BMI was weaker.

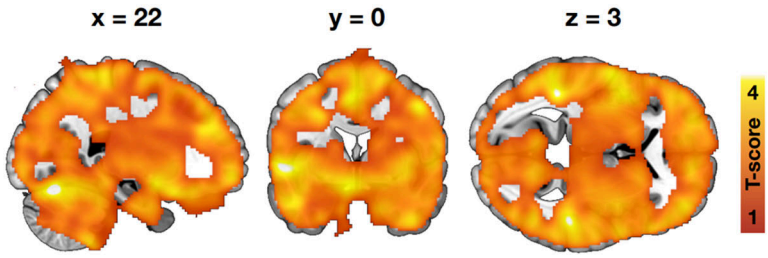

Figure 14 Brain regions (as defined by FDR-corrected SPM one-sample t test) where higher familial obesity risk score was associated with increased BGU in the whole study group. Data are thresholded at $P < 0.05$ and false discovery rate (FDR) corrected at cluster level. Modified from the original publication I.

5.1.3 Study II: Whole-body insulin sensitivity associates negatively with brain glucose uptake

During the clamp, plasma glucose levels were steady with no differences between the groups (5.3 ± 0.3 mmol/L in HR vs. 5.3 ± 0.2 mmol/L in LR group, $P = 0.5$). Steady-state insulin levels were higher (581.7 ± 94.9 ρmol/L in HR vs. 510.5 ± 76.8 in LR ρmol/L, $P = 0.01$) and FFA suppression was smaller (0.05 ± 0.03 mmol/L in HR vs. 0.03 ± 0.01 mmol/L in LR, $P = 0.03$) in the HR as compared to the LR group, and these two measurements were also correlated ($r = –0.41$, $P = 0.009$).

Whole-body insulin sensitivity indexed by the M value and the rate of glucose disappearance (Rd) were lower in the HR than in the LR group (**Figure 15A**).

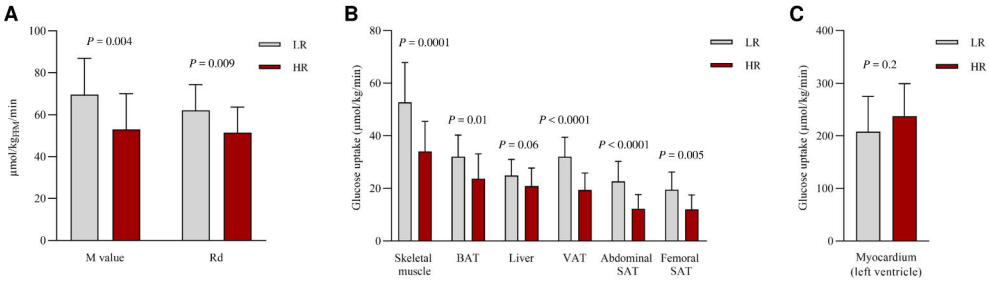

Figure 15 Whole-body and tissue-specific glucose uptake (GU) rates. (**A**) Whole-body insulin sensitivity indexed by the M value and the rate of glucose disappearance (Rd) calculated with the fat-free mass in the low-risk (LR) and in the high-risk (HR) group. (**B**) GU rates in skeletal muscle, brown adipose tissue (BAT), liver, visceral adipose tissue (VAT) and abdominal and femoral subcutaneous adipose tissue (SAT) and (**C**) myocardium in the LR and in the HR group. Bar heights represent sample means and vertical lines sample SD. *P* values for comparison of LR vs HR group. Reproduced from the original publication II.

Similarly, the HR group exhibited lower rates of GU in skeletal muscle, liver, VAT, abdominal and femoral SAT and BAT than the LR group (**Figure 15B**).

Myocardial left ventricle GU rates did not differ between the groups (**Figure 15C**). Insulin-suppressed EGP (–0.6 ± 8.9 μmol/kg_{FFM}/min in HR vs. –2.2 ± 8.9 μmol/kg_{FFM}/min in LR, P = 0.6) did not significantly differ between the groups. M value and Rd correlated negatively with insulin-suppressed FFA levels, and M value positively with Rd and negatively with EGP in both groups and in the whole dataset (**Figure 16**).

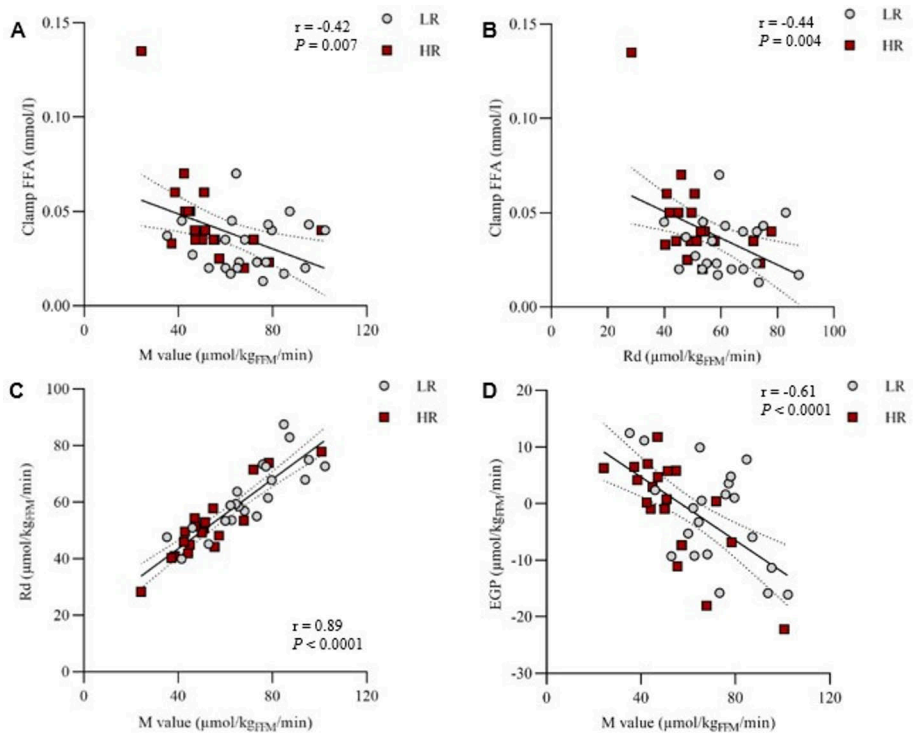

Figure 16 Association between the whole-body insulin sensitivity indexes. (**A**) Association between the M value and free fatty acid (FFA) levels and (**B**) the rate of glucose disappearance (Rd) and FFA levels during the hyperinsulinemic-euclycemic clamp, (**C**) M value and Rd, (**D**) M value and endogenous glucose production (EGP). Modified from the original publication II.

BGU correlated negatively with M value, and the association was driven by the HR group (**Figure 17A**). Furthermore, BGU correlated positively with 2-h plasma glucose level in OGTT among all study subjects and negatively with insulin sensitivity index by Matsuda (Matsuda-ISI) in the HR group (**Figure 17B-C**). BGU in the HR group correlated negatively with skeletal muscle GU and showed a trend toward a negative correlation with BAT GU, whereas no association was found between BGU and liver, VAT or abdominal and femoral SAT GU.

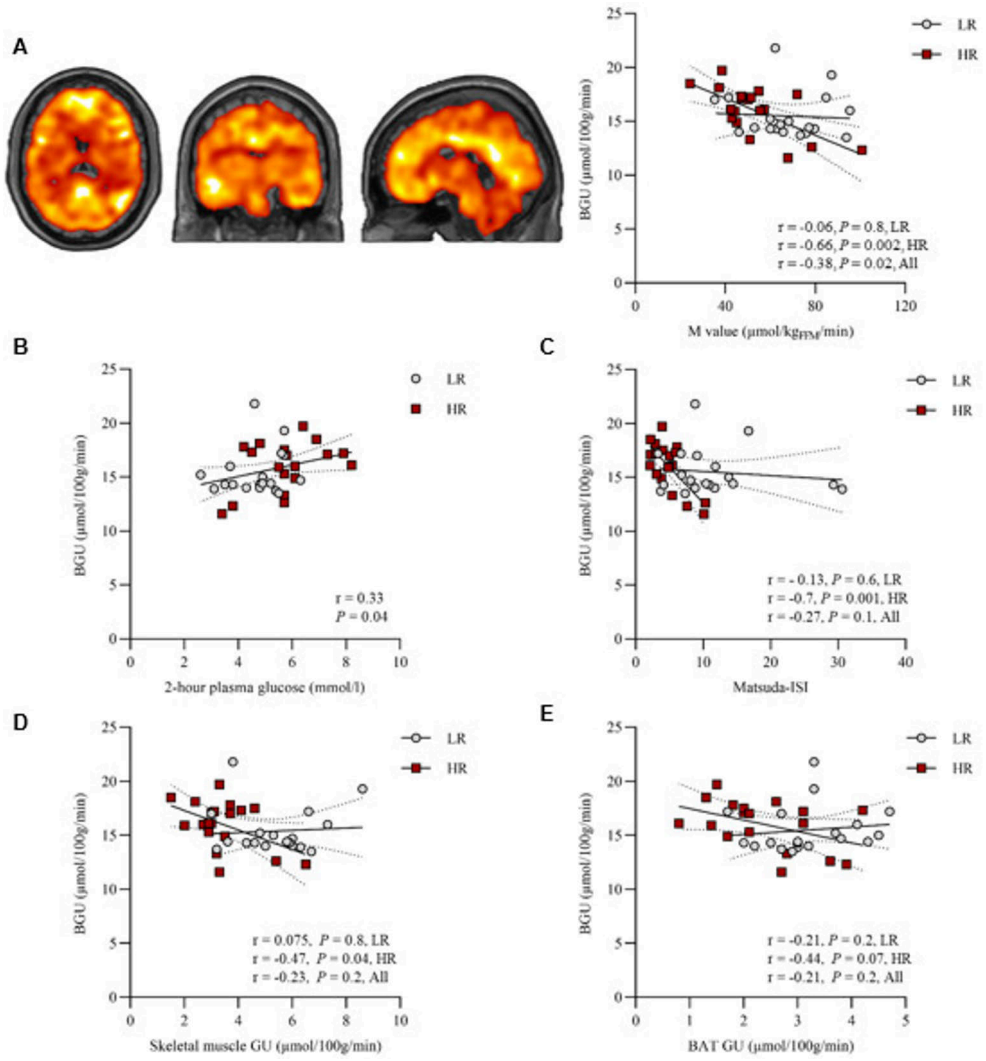

Figure 17 Brain glucose uptake (BGU) in the high-risk (HR) and the low-risk (LR) group. (**A**) Brain clusters (as defined by false discovery rate (FDR) corrected Statistical parametric mapping (SPM) one-sample t test) for the association between BGU and M value and the corresponding scatterplot. Higher T values denote larger differences between the groups (**B**) Association between the BGU and 2-hour plasma glucose level in oral glucose tolerance test, (**C**) BGU and insulin sensitivity index by Matsuda (Matsuda-ISI), (**D**) BGU and skeletal muscle glucose uptake (GU) and (**E**) BGU and brown adipose tissue (BAT) GU in the LR and in the HR group. Scatterplots show global cerebral GU. Modified from the original publication II.

Insulin-suppressed FFA correlated positively with BGU in the ROI level and the association was driven by the HR group (**Table 2**).

Table 2 Associations (Pearson correlations) between the regional insulin-stimulated brain glucose uptake rates and insulin-suppressed free fatty acid (FFA) levels. Associations are shown separately for all study subjects, the low-risk (LR) and the high-risk (HR) group. Significant associations are indicated by bold font. *P < 0.05, **P < 0.001. Modified from original publication II.

ROI	All	LR	HR
Amygdala	**0.36***	-0.02	**0.47***
Caudate	**0.36***	0.05	**0.50***
Cerebellum	**0.34***	0.15	0.38
Dorsal anterior cingulate cortex	**0.34***	0.06	0.43
Hippocampus	**0.28***	-0.004	0.40
Inferior temporal gyrus	**0.33***	0.03	0.39
Insula	0.30	0.04	0.37
Medulla	0.22	-0.064	0.30
Midbrain	0.25	-0.02	0.33
Middle temporal gyrus	**0.35***	0.06	0.41
Nucleus accumbens	**0.34***	0.02	**0.53***
Orbitofrontal cortex	**0.37***	0.12	0.44
Pars opercularis	**0.35***	0.07	0.41
Posterior cingulate cortex	**0.43***	0.21	**0.47***
Pons	0.24	-0.06	0.37
Putamen	**0.32***	-0.005	0.42
Rostral anterior cingulate cortex	**0.36***	0.08	**0.49***
Superior frontal gyrus	**0.40***	0.11	**0.47***
Superior temporal gyrus	0.27	-0.0005	0.33
Temporal pole	**0.32***	0.08	0.40
Thalamus	**0.33***	0.18	0.37

5.1.4 Study II: EGP associates positively with brain glucose uptake

Higher insulin-suppressed EGP associated with insulin-stimulated BGU in the whole dataset. The association was driven by the HR group (**Figure 18**).

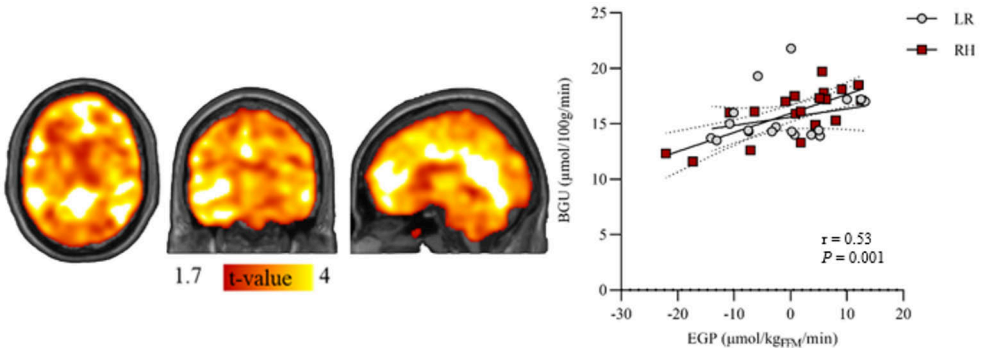

Figure 18 Brain regions (as defined by FDR-corrected SPM one-sample t test) where BGU was associated with EGP in the whole study group. Data are thresholded at $P < 0.05$ and false discovery rate (FDR) corrected at cluster level. Scatterplot shows the association between EGP and global BGU separately for the high-risk (HR) and the low-risk (LR) groups. Modified from the original publication II.

5.2 Obesity risk associates with lower abdominal adipose tissue CB1 receptor availability

5.2.1 Study III: Lower abdominal adipose tissue CB1 receptor availability in subjects with high as compared to low obesity risk

CB1R availability was quantified with [^{18}F]FMPEP-d_2 PET in peripheral tissues including abdominal SAT, IWAT and RWAT, BAT and muscle. CB1R availability, determined as the V_T and FUR of [^{18}F]FMPEP-d_2, of the each abdominal adipose tissue depot was lower in the HR versus LR group. CB1R availability of muscle was numerically lower in HR than in the LR group but did not reach statistically significance. No difference was found in CB1R availability of BAT between the groups (**Figure 19**). Tissue-wise V_T and FUR values were positively associated (r = 0.80, $P < 0.0001$ for abdominal SAT; r = 0.72, $P < 0.0001$ for IWAT; r = 0.78, $P < 0.0001$ for RWAT; r = 0.87, $P < 0.0001$ for BAT; r = 0.58, $P = 0.0002$ for muscle).

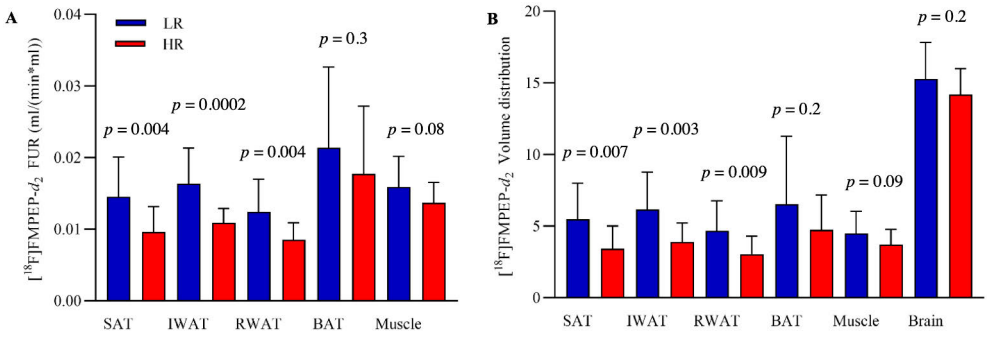

Figure 19 Lower CB1R availability in abdominal SAT, IWAT and RWAT in the high-risk (HR) as compared to the low-risk (LR) group. (**A**) The FUR of [^{18}F]FMPEP-d_2 in abdominal subcutaneous (SAT), intraperitoneal (IWAT) and retroperitoneal white adipose tissue (RWAT), brown adipose tissue (BAT) and muscle in the LR and in the HR group. (**B**) [^{18}F]FMPEP-d_2 VT of SAT, IWAT, RWAT, BAT, muscle and the whole brain in the LR and in the HR group. Modified from the original publication III.

5.2.2 Study III: Lower CB1 receptor availability is associated with decreased insulin sensitivity, higher body adiposity, unfavourable lipid profile and inflammatory markers

CB1R availability of each abdominal adipose tissue depot was positively associated with abdominal adipose tissue insulin sensitivity assessed as tissue-specific GU (**Figure 20A-C** and **Table 3**). CB1R availability of the RWAT also correlated positively also with whole-body insulin sensitivity (M value and Rd), and the CB1R availability of IWAT with Rd. Furthermore, CB1R availability of each abdominal adipose tissue depot correlated negatively with serum insulin-suppressed FFA level (**Table 3**).

CB1R availability of the abdominal adipose tissue correlated negatively with body weight, BMI, total fat and abdominal adipose tissue masses (**Table 3** and **Figure 20D-F**) CB1R availability of muscle correlated negatively with weight, BMI and visceral adipose tissue mass, while CB1R availability of BAT did not correlate with any of these measures (**Table 3**).

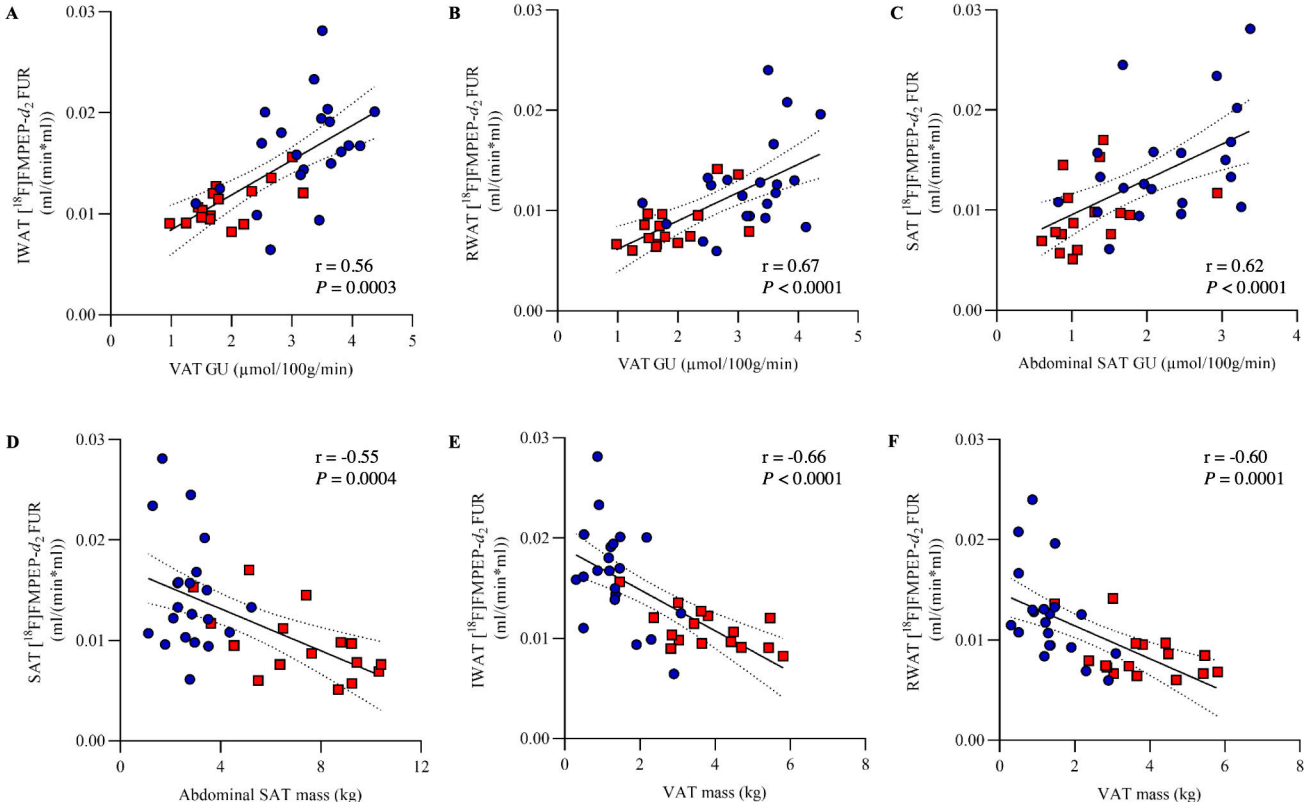

Figure 20 Associations between abdominal adipose tissue cannabinoid receptor type 1 (CB1R) availabilities and tissue glucose uptake (GU) rates and tissue masses. Pearson correlation between [^{18}F]FMPEP-d_2 FUR values of (**A**) abdominal subcutaneous adipose tissue (SAT) and SAT GU, (**B**) intraperitoneal white adipose tissue (WAT) and visceral adipose tissue (VAT) GU, (**C**) retroperitoneal WAT and VAT GU, (**D**) abdominal SAT and abdominal SAT mass, (**E**) intraperitoneal WAT and VAT mass, and (**F**) retroperitoneal WAT and VAT mass in the low-risk (LR; blue circle) and in the high-risk (HR; red square) group. Reproduced from the original publication III.

Table 3 Associations (Pearson correlations) between [^{18}F]FMPEP-d_2 FUR values of abdominal subcutaneous (SAT), intraperitoneal (IWAT) and retroperitoneal white adipose tissue (RWAT), brown adipose tissue (BAT) and muscle, and V_T of the whole brain and anthropometric and metabolic characters, and insulin-stimulated tissue-specific glucose uptake rates. Statistically significant associations are indicated by bold font. *P < 0.05; **P < 0.01; ***P < 0.001; ****P < 0.0001.
[a]Associations with the LR (n = 20) and HR (n = 16) subjects who gave an urine sample.
[b]Associations with the LR (n = 20) and HR (n = 16) subjects who completed the [^{18}F]FDG scan successfully.
[c]Associations with the LR (n = 19) and HR (n = 16) subjects who completed the [^{18}F]FDG scan successfully. Modified from original publication III.

	FUR (ml/(min*ml))			**V_T**		
	SAT	**IWAT**	**RWAT**	**BAT**	**MUSCLE**	**BRAIN**
Age (years)	**-0.49****	**-0.42****	**-0.42****	-0.16	**-0.33***	-0.24
Weight (kg)	**-0.49****	**-0.59*****	**0.57*****	-0.25	**-0.40***	**-0.39***
BMI (kg/m^2)	**-0.49****	**-0.57*****	**-0.59*****	-0.29	**-0.40***	**-0.44****
Body fat (kg)	**-0.56*****	**-0.63******	**-0.65******	-0.13	-0.31	**-0.36***
Body fat (%)	**-0.53*****	**-0.63******	**-0.68******	-0.07	-0.25	**-0.36***
Fat free mass (kg)	-0.15	-0.16	-0.09	-0.32	**-0.35***	-0.08
Abdominal SAT mass (kg)	**-0.55*****	**-0.60*****	**-0.59*****	-0.09	-0.29	-0.28
VAT mass (kg)	**-0.50****	**-0.66******	**-0.60******	-0.10	**-0.33***	**-0.37***
Systolic blood pressure (mmHg)	-0.19	**-0.34***	**-0.35***	0.11	-0.10	**-0.50****
Diastolic blood pressure (mmHg)	-0.07	-0.23	-0.22	0.15	-0.17	**-0.42****
HbA_{1c} (mmol/mol)	-0.23	**-0.37***	-0.20	-0.004	0.09	-0.10
hs-CRP (mg/l)	-0,32	-0.31	-0.26	-0.07	-0.17	-0.28
Fasting serum FFA (mmol/l)	0.078	-0.04	-0.10	0.14	-0.02	-0.25
Clamp serum FFA (mmol/l)	**-0.39***	**-0.39***	**-0.38***	-0.007	-0.13	-0.31
M value (µmol/kg/min)	0.28	-0.27	**0.39***	0.17	0.19	**0.38***
M value (µmol/kg_{FFM}/min)	0.16	0.14	0.24	0.17	0.16	**0.35***
Rd (µmol/kg/min)	0.26	**0.36***	**0.42***	0.14	0.20	0.23
Rd (µmol/kg_{FFM}/min)	0.15	0.20	0.28	0.14	0.18	0.24
EGP (µmol/kg/min)[a]	-0.05	0.08	0.02	0.10	0.06	-0.33
EGP (µmol/kg_{FFM}/min)[a]	-0.12	-0.01	-0.08	0.08	0.05	**-0.43***
GU (µmol/100g/min)						
Abdominal SAT	**0.56*****	**0.64******	**0.60******	0.31	0.24	0.30
VAT	**0.57*****	**0.67******	**0.62******	**0.37***	0.32	0.32
BAT[b]	0.33	**0.43***	**0.50****	0.03	**0.34***	**0.34***
Muscle[c]	0.25	**0.34***	**0.41***	0.18	0.21	0.20
Femoral SAT[c]	**0.41***	**0.45****	**0.51****	0.03	0.11	0.34
Liver	0.15	-0.002	0.02	0.09	-0.02	-0.23

Lower CB1R availability of each abdominal adipose tissue depot associated with unfavourable lipid profile including higher levels of total, non-HDL, remnant, VLDL and LDL cholesterol, triglycerides, free cholesterol, ratio of triglycerides to phosphoglycerides, ApoB and ApoB/ApoA1 ratio. CB1R availability of IWAT and RWAT also correlated negatively with serum fatty acid levels, including omega-6 fatty acids and linoleic acid. CB1R availability of the abdominal SAT correlated positively with HDL cholesterol. Lower CB1R availability of the abdominal adipose tissue associated with higher serum concentration of glycoprotein acetyls (GlycA), a biomarker of systemic inflammation. Lower CB1R availability of muscle associated with higher levels of total, non-HDL, remnant, VLDL and LDL cholesterol, ApoB, ApoB/ApoA1 ratio, and fatty acids. CB1R availability of BAT did not correlate with serum metabolomics (**Figure 21**).

There were no significant association between peripheral tissue CB1R availabilities and serum EC levels. Higher serum EC levels were associated with decreased whole-body insulin sensitivity (M value and Rd) and insulin-suppressed EGP. Higher levels of circulating AA and AEA were associated with lower M value adjusted with fat-free mass (M value$_{FFM}$), and higher AEA concentration also with lower M value, Rd and Rd$_{FFM}$. Higher serum AG (1+2) and DEA levels were associated with higher insulin-suppressed EGP and EGP$_{FFM}$. Serum γ-LEA correlated positively with abdominal SAT GU. (**Table 4**).

Serum AG (1+2) level correlated positively with BMI, while no significant correlations were found between serum EC levels and body weight or adipose tissue masses (**Table 4**).

Higher circulating AG (1+2) level associated with unfavourable lipid profile and higher serum inflammatory markers, including higher total, non-HDL, remnant, VLDL and LDL cholesterol, triglycerides, ApoB, ApoB/apoA1 ratio and fatty acids and GlycA, whereas serum γ –LEA level correlated positively with HDL cholesterol and ApoA1 (**Figure 22**).

Linoleic acid, a precursor for ECs was found to correlate positively with abdominal SAT ($r = 0.40$, $P = 0.004$), VAT ($r = 0.60$, $P = 0.0001$) and total body fat ($r = 0.53$, $P = 0.001$) masses, weight ($r = 0.57$, $P = 0.0003$), and also with BMI ($r = 0.53$, $P = 0.001$).

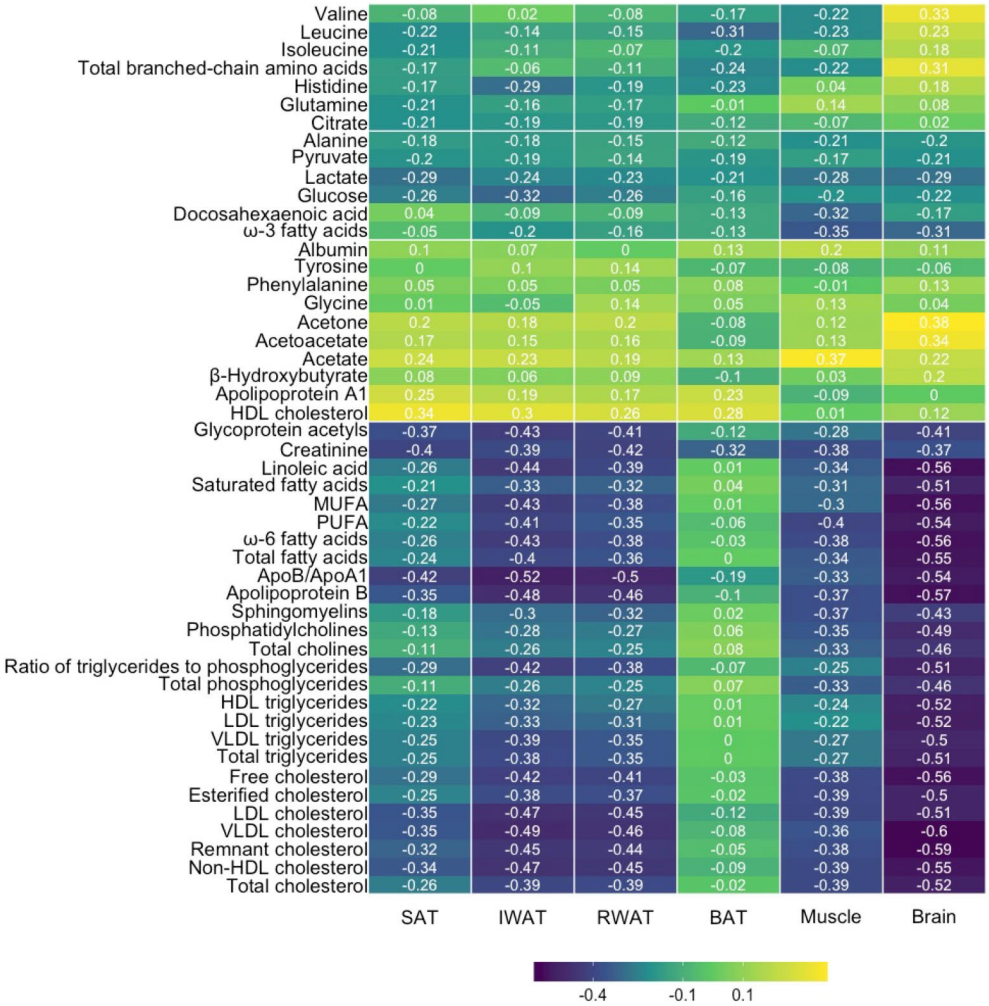

Figure 21 Correlation heart map between CB1R availabilities of abdominal subcutaneous (SAT), intraperitoneal (IWAT) and retroperitoneal white adipose tissue (RWAT), brown adipose tissue (BAT), muscle and the whole brain with serum metabolomics across the whole study sample size. Reproduced from the original publication III.

Table 4 Associations (Pearson correlations) between circulating endocannabinoid concentrations and selective variables of body composition, insulin sensitivity, [^{18}F]FMPEP-d_2 FUR values of abdominal subcutaneous (SAT), intraperitoneal (IWAT) and retroperitoneal white adipose tissue (RWAT), brown adipose tissue (BAT) and muscle, and [^{18}F]FMPEP-d_2 V_T of the whole brain. Statistically significant associations are indicates by bold font. *P < 0.05; **P < 0.01.

[a]Associations with the LR (n = 20) and HR (n = 16) subjects who gave an urine sample.

[b]Associations with the LR (n = 20) and HR (n = 16) subjects who completed the [^{18}F]FDG scan successfully.

[c]Associations with the LR (n = 19) and HR (n = 16) subjects who completed the [^{18}F]FDG scan successfully.

[d]Associations with the LR (n = 20) and HR (n = 16) subjects whose [^{18}F]FMPEP-d_2 image analysis was able to conduct.

Modified from original publication III.

	AA	AEA	AG (1+2)	A-LEA	γ-LEA	DEA	NALS	OEA
Weight (kg)	0.04	0.23	0.26	0.16	0.14	0.09	-0.09	-0.06
BMI (kg/m^2)	0.16	0.22	**0.36***	0.07	0.03	0.10	-0.08	-0.09
Body fat (kg)	0.06	0.24	0.23	0.02	-0.01	0.23	-0.08	0.02
Abdominal SAT mass (kg)	0.05	0.21	0.16	0.02	-0.04	0.24	-0.14	0.04
VAT mass (kg)	0.13	0.26	0.26	-0.02	-0.05	0.24	-0.06	0.09
M value (µmol/kg/min)	-0.31	**-0.43****	-0.24	-0.16	-0.13	-0.33	-0.14	-0.26
M value (µmol/kg$_{FFM}$/min)	**-0.34***	**-0.44****	-0.23	-0.22	-0.20	-0.29	-0-18	-0.29
Rd (µmol/kg/min)	-0.25	**-0.37***	-0.12	-0.02	-0.03	-0.22	-0.10	-0.19
Rd (µmol/kg$_{FFM}$/min)	-0.24	**-0.43****	-0.03	-0.11	-0.12	-0.19	-0.06	-0.19
EGP (µmol/kg/min)[a]	0.28	0.24	**0.40***	0.29	0.25	**0.35***	0.29	0.26
EGP (µmol/kg$_{FFM}$/min)[a]	0.33	0.28	**0.39***	0.22	0.22	**0.41***	0.30	0.30
Clamp serum FFA (mmol/l)	0.03	0.02	0.02	-0.20	-0.15	0.04	-0.18	-0.10
GU (µmol/100g/min)								
Abdominal SAT	0.04	-0.10	-0.01	0.29	**0.37***	-0.17	0.28	0.10
VAT	0.02	-0.12	-0.08	0.23	0.28	-0.26	0.14	-0.04
BAT[b]	-0.14	-0.33	0.10	0.08	0.08	-0.31	-0.03	-0.10
Muscle[c]	-0.19	-0.24	-0.06	-0.03	-0.01	-0.17	0.07	0.03
Femoral SAT[c]	0.00	0.01	-0.05	0.26	0.30	-0.05	0.22	0.22
Liver	0.23	0.01	0.23	-0.25	-0.13	-0.05	0.11	0.03

	AA	AEA	AG (1+2)	A-LEA	γ-LEA	DEA	NALS	OEA
[^{18}F]FMPEP-d_2 FUR (ml/(min*ml))								
SAT	0.24	-0.11	-0.15	0.25	0.32	-0.19	0.23	0.16
IWAT	0.19	-0.12	-0.22	0.26	0.22	-0.21	0.18	0.12
RWAT	0.19	-0.19	-0.20	0.25	0.25	-0.20	0.22	0.14
BAT[d]	-0.004	-0.07	-0.02	0.08	0.15	-0.06	-0.10	0.07
Muscle	-0.01	-0.26	-0.29	0.03	0.03	-0.11	0.09	-0.05
[^{18}F]FMPEP-d_2 V_T of the whole brain	-0.28	-0.20	-0.34*	0.03	-0.05	-0.03	-0.11	-0.03

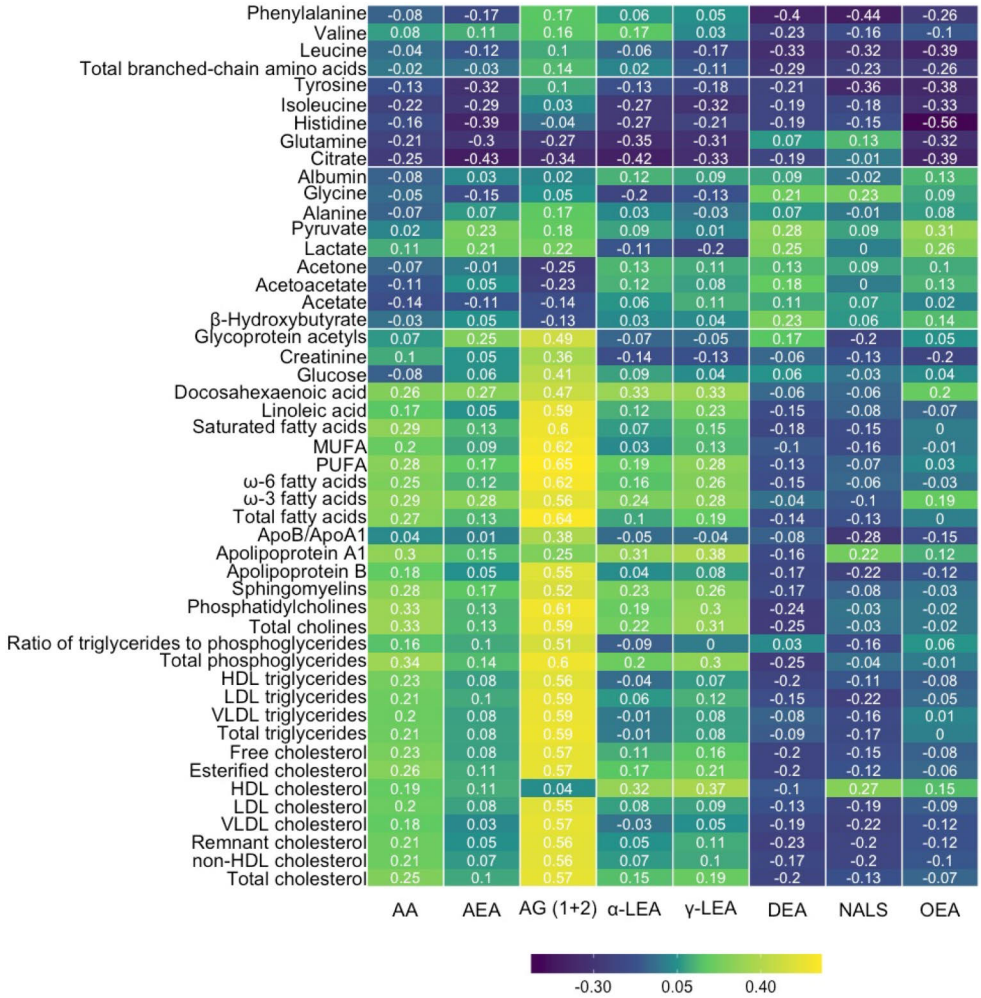

Figure 22 Correlation heart map between serum endocannabinoid levels and serum metabolomics across the whole study sample size. AA = arachidonic acid; AEA = anandamide; AG (1+2) = arachidonoyl glycerol (1 + 2); α-LEA = α-linolenic acid; γ-LEA = γ-linolenic acid; DEA = docosatetraenoyl ethanolamide; NALS = N-arachidonoyl-Lserine; OEA = oleyl ethanolamide. Reproduced from the original publication III.

5.3 Obesity risk associates with central CB1 receptor availability

5.3.1 Study I: Familial obesity risk is associated with lower brain CB1 receptor availability

CB1R availability in brain, analysed in 21 bilateral regions involved in emotion and food reward processing, did not statistically differ between the HR and LR group. Higher familial obesity risk and BMI was associated with lower CB1R availability in the brain (**Figure 23**). Higher serum AEA level was associated with lower CB1R availability in ventral striatum (**Figure 24**), while no significant associations were found between the other seven studied circulating ECs and brain CB1R availability.

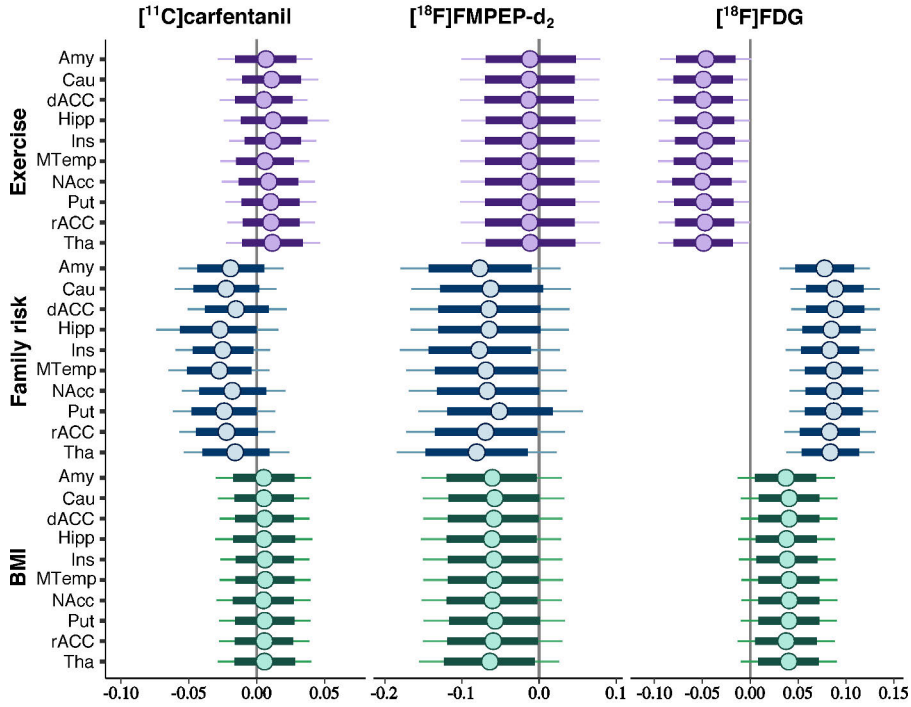

Figure 23 Effects of the obesity risk factors on brain CB1R availability. Posterior distributions of the regression coefficients for exercise, family risk and body mass index (BMI) on log-transformed volume of distribution V_T of the [^{18}F]FMPEP-d_2 in representative regions of interest, with age as a covariate. The colored circles represent posterior means, the thick horizontal bars 80% posterior intervals, and the thin bars 95% posterior intervals. The width of posterior intervals expresses the level of uncertainty of the estimate. Shown are also the effects of the obesity risk factors on binding potential of the [^{18}F]Carfentanil and brain glucose uptake quantified with the [^{18}F]FDG. Amy, amygdala; Cau, caudate; dACC, dorsal anterior cingulate cortex; Hipp, hippocampus; Ins, insula; MTemp, middle temporal gyrus; NAcc, nucleus accubens; Put, putamen; rACC rostral anterior cingulate cortex; Tha, thalamus. Reproduced from the original publication I.

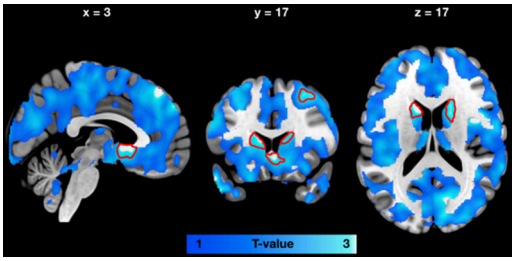

Figure 24 Brain regions (as defined by FDR-corrected SPM one-sample t test) where circulating anandamide (AEA) level was associated with lowered CB1R availability in the whole study group. Data are thresholded at P < 0.05 and false discovery rate (FDR) corrected at cluster level. The areas marked with red indicate clusters significant with Bonferroni-corrected cluster-defining *P* value (0,05/8 = 0.00625). Reproduced from the original publication I.

5.3.2 Study III: Lower whole-body insulin sensitivity, higher body adiposity and unfavourable lipid profile is associated with lower whole-brain CB1 receptor availability

Mean CB1R availability in the whole-brain did not differ statistically between the HR and the LR group (**Figure 25**). Lower CB1R availability of the whole brain associated with decreased whole-body insulin sensitivity indexed by M value and higher insulin-suppressed EGP adjusted with fat-free mass (**Figure 26**). Lower CB1R availability of the whole brain associated also with higher body weight, BMI, total body fat mass and visceral adipose tissue mass (**Table 3**).

Lower CB1R availability in the whole brain was associated with unfavourable lipid profile including higher levels of with total, non-HDL, remnant, VLDL and LDL cholesterol, triglycerides, free cholesterol, ratio of triglycerides to phosphoglycerides, ApoB and ApoB/ApoA1 ratio (**Figure 21**).

Serum AG (1+2) concentration associated negatively with the whole-brain CB1R availability (r = -0.34, *P* = 0.04).

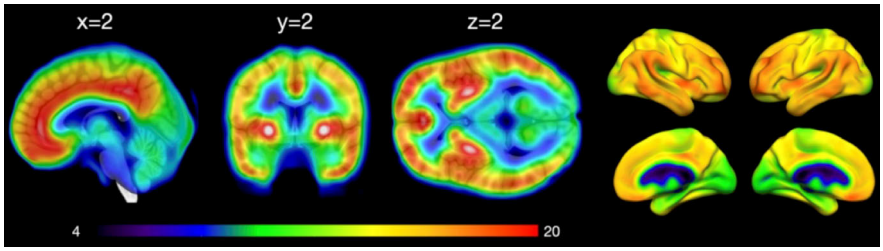

Figure 25 Mean volume of distribution (V_T) for the [^{18}F]FMPEP-d_2 scans in the brain in the whole study population. Modified from the original publication III.

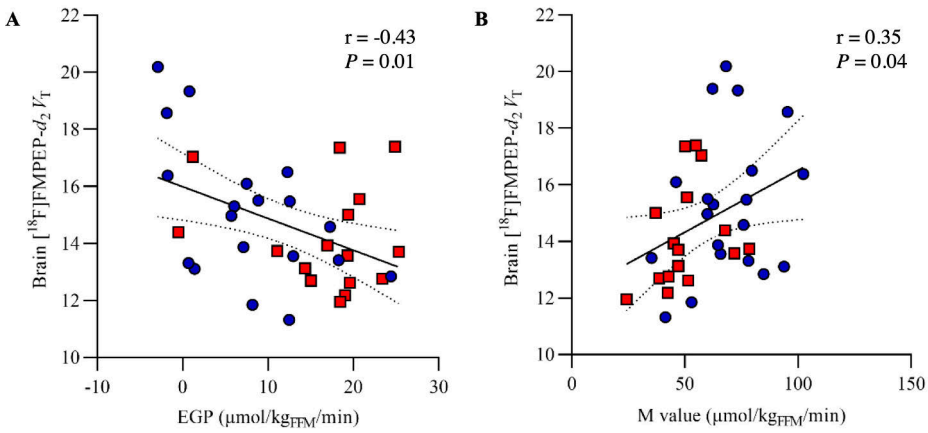

Figure 26 Association between the mean cannabinoid receptor type 1 (CB1R) availability in the whole-brain and insulin-suppressed hepatic endogenous glucose production (EGP) and whole-body insulin sensitivity indexed by M value adjusted with fat-free-mass (FFM). Pearson correlation between [^{18}F]FMPEP-d_2 V_T values of the whole-brain and (A) EGP and (B) M value. Reproduced from the original publication III.

6 Discussion

6.1 Impaired brain insulin sensitivity in the pre-obese state

The aim of this thesis was to examine brain and peripheral tissue insulin signalling and ECS in healthy non-obese young men. We showed that altered brain insulin action and crosstalk between periphery, as well as ECS deregulation may precede obesity.

In Study I, we showed increased insulin-stimulated BGU in subjects with high as compared to low obesity risk. Whole-body and peripheral tissue GU rates in turn were lower in high versus low obesity risk subjects, and there was a negative correlation between insulin-stimulated BGU and whole-body GU (Study II). Our results are in line with previous published data in animals and humans with obesity [Bahri et al., 2018; Rebelos et al., 2021; Tuulari et al., 2013]. In addition to obesity, other insulin resistant states including impaired glucose tolerance and T2D are associated with higher insulin-stimulated BGU when compared with healthy populations [J. W. Eriksson et al., 2021; Hirvonen et al., 2011; Latva-Rasku et al., 2018]. It is thus suggested that the increased BGU is a manifestation of brain insulin resistance. Brain insulin signalling has several pivotal effects on the regulation of body energy homeostasis at central and peripheral levels, including feeding behaviour, energy expenditure and thermogenesis, WAT and hepatic lipid metabolism, and whole-body insulin sensitivity via suppression of hepatic EGP and stimulation of peripheral tissue GU. In the presence of brain insulin resistance, the physiological brain insulin actions are attenuated or even diminished, predisposing to increased homeostatic and hedonic food intake, further weight gain, as well as altered lipid and glucose fluxes. Accumulating evidence suggest that overnutrition and diet-induced hypothalamic inflammation are constitutive factors for the development of brain insulin resistance [Kullmann, Kleinridders, et al., 2020; Scherer et al., 2021]. Especially diet rich with SFAs associate with impaired insulin effect in the brain [Tschritter et al., 2009]. In addition, genetic background, maternal metabolism during pregnancy and advancing age are known to affect brain insulin sensitivity [Heni et al., 2015]. Interestingly, in Study I, we also found an association between higher familial obesity risk and increased insulin-simulated BGU.

Concerning the pre-obese and otherwise healthy state of our young subjects, we suggest our findings indicate that alterations in brain insulin signalling are relatively early events in metabolic disturbances.

Study II revealed associations between enlarged body fat mass, particularly accumulation of fat in abdominal but not femoral WAT depots, and increased BGU under insulin stimulation. Whereas visceral adiposity has long been acknowledged as a consistent indicator for metabolic diseases [Després & Lemieux, 2006], femoral SAT seems to have a protective role [Goodpaster et al., 2005; Goss & Gower, 2012]. A previous study showed an association between brain insulin sensitivity, adiposity and body fat distribution; hypothalamic insulin sensitivity correlated negatively with the ratio of VAT to SAT mass [Kullmann, Valenta, et al., 2020]. It however remains unsolved, whether the increased visceral adiposity plays a role in the pathogenesis of brain insulin resistance or is it a consequence of impaired brain insulin action.

As a potential manifestation of dysregulated organ crosstalk, we observed positive correlation between insulin-suppressed hepatic EGP as well as serum FFA levels and BGU (Study II). Preclinical and clinical studies have demonstrated that insulin action in the brain modulates both hepatic and WAT metabolism [Lewis et al., 2021; Scherer et al., 2021]. Central insulin action has direct effect on hepatic EGP by reducing gluconeogenic enzyme expression and indirect effects by suppressing WAT lipolysis and thus substrate fluxes to liver [Lewis et al., 2021]. It has been shown an association between increased insulin-stimulated BGU and insulin-suppressed EGP in subjects with morbid obesity [Rebelos et al., 2019] and AKT2 gene variant [Latva-Rasku et al., 2018], but not in lean subjects. We suggest our result to accord the view of defective organ crosstalk and reflect early metabolic dysregulation.

6.2 Lower Abdominal adipose tissue CB1 receptor availability associates with metabolic dysregulation in the pre-obese state

In Study III, young healthy subjects with overweight and risk for obesity exhibited lower abdominal adipose tissue CB1R availability as compared to subjects with low obesity risk. Accordingly, lower CB1R availability was associated with decreased insulin sensitivity, higher body adiposity, unfavourable lipid profile and inflammatory markers. Accumulating evidence indicates that ECS is dysregulated in obesity and associated metabolic disorders. It is suggested that the dysregulated ECS might even contribute to the development of obesity, while it modulates the body energy homeostasis at multiple sites [Gatta-Cherifi & Cota, 2016; Quarta et al., 2011].

ECS in WAT, and also in other tissues, has been studied mainly by assessing the tissue EC levels and the gene expression of CB1R and the main EC metabolizing enzymes. Higher levels of ECs in VAT has been found in both rodents and humans with obesity [D'Eon et al., 2008; Matias et al., 2006]. Reduced EC levels in SAT depots in obesity [Bennetzen et al., 2011; Matias et al., 2006] have been argued to reflect the differing nature of the SAT and VAT depots [You et al., 2011]. Lower expression of CB1R in VAT and SAT has been measured in subjects with obesity as compared to lean subjects [Bennetzen et al., 2011; Blüher et al., 2006; Engeli et al., 2005; Kempf et al., 2007], and increases in the CB1R expression followed by weight loss [Bennetzen et al., 2011]. However, there are also contradictory findings [You et al., 2011]. Some studies have reported obesity-related increases in CB1R as well as FAAH expression levels in both VAT and SAT [Bensaid et al., 2003; Pagano et al., 2007; Yan et al., 2007] or a positive correlation between the VAT CB1R expression and VAT area or adipocyte hypertrophy [Bordicchia et al., 2010; Yan et al., 2007]. The expression of EC degrading enzymes, especially the key enzyme FAAH, are differently affected by obesity, adipose tissue depot, and weight loss [Bennetzen et al., 2011; Blüher et al., 2006; Bordicchia et al., 2010; Engeli et al., 2005; Sarzani et al., 2009; You et al., 2011]. Despite mixed results, it is generally agreed that the biological action of activation of the ECS in WAT is to promote adipocyte differentiation, fatty acid *de novo* lipogenesis, triglyceride accumulation, and to reduce lipolysis and mitochondrial function, favouring thus white instead of beige or brown adipocytes, and inhibition of CB1Rs reverses these actions [Silvestri & Di Marzo, 2013]. ECS overactivity in WAT in turn is one hallmark of obesity [Quarta et al., 2011; Simon & Cota, 2017].

Thus far, only few studies have quantified peripheral tissue CB1R availability in humans using [^{18}F]FMPEP-d_2 PET. Unlike measuring CB1R expression in tissue biopsies, [^{18}F]FMPEP-d_2 PET does not display the total amount of CB1Rs in the tissue. Instead, [^{18}F]FMPEP-d_2 binds to CB1Rs that are not occupied with their natural ligands ECs. A previous study showed lower [^{18}F]FMPEP-d_2 binding, that is lower availability of unoccupied CB1Rs in abdominal VAT and SAT in healthy males with obesity (BMI: 32.9 ± 4.6 kg/m^2) as compared with lean (BMI: 24.9 ± 1.7 kg/m^2) males [Lahesmaa et al., 2018]. We observed convergent results; lower CB1R availability in abdominal WAT depots in healthy overweight subjects with obesity risk as compared to lean subjects with no obesity risk. This might be explained by lower total count of CB1Rs, increased WAT EC levels due to increased EC biosynthesis and/or decreased degradation. Indeed, EC production and degradation in white adipocytes appears to be negatively regulated by insulin and leptin. Insulin and leptin resistance, as observed in overweight and prolonged consumption of HFD, are associated with upregulated EC biosynthesis that in turn may predispose to

further accumulation of WAT and weight gain and a cycle promoting overactive ECS tone [Silvestri & Di Marzo, 2013].

Consistent with current understanding, the lower CB1R availability in abdominal WAT depots in the HR subjects we found, likely reflecting dysregulated ECS tone, correlated negatively with weight, BMI, total body fat and VAT and abdominal SAT masses. Although the skeletal muscle CB1R availability did not reach statistical difference between the HR and LR group, it correlated negatively with weight, BMI and VAT mass as well. Abdominal adipose tissue and skeletal muscle CB1R availability associated with unfavourable lipid profile. Abdominal SAT CB1R availability correlated positively with HDL cholesterol, which may represent the metabolic difference of distinct WAT depots. Interestingly, adipose tissue CB1R availability correlated negatively with fatty acids, including omega-6 PUFAs and linoleic acid. Excessive dietary linoleic acid has been implicated in the pathogenesis of weight gain and obesity in which one presented mechanism is an increased synthesis one ECs from linoleic acid leading to ECS overactivation [Naughton et al., 2016]. As a further indication of metabolic disturbance, we observed a negative correlation between WAT CB1R availabilities and GlycA, a composite biomarker of systemic inflammation and cardiometabolic risk [Connelly et al., 2017]. In previous studies, obesity-related ECS activation has been found to accompany WAT inflammation [Kempf et al., 2007]. Also HFD consumption and obesity initiate WAT inflammation manifested with secretion of inflammatory cytokines [Kawai et al., 2021].

CB1R availability in abdominal WAT depots correlated positively with the VAT and SAT insulin sensitivity assessed as insulin-stimulated GU and serum insulin-suppressed FFA levels, and the CB1R availability in intraperitoneal and retroperitoneal WAT depots also with the whole-body insulin sensitivity. This accords with the previous studies in which pharmacological blockade of CB1Rs in DIO mice induced correction of insulin resistance via enhanced expression of GLUT4 and glycolytic enzymes [Jbilo et al., 2005]. Concerning the skeletal muscle, we did not find associations between the tissue CB1R availability and insulin sensitivity. As WAT is a metabolically highly active and insulin sensitive tissue, it might be that the observed association between WAT ECS tone and insulin sensitivity reflect relatively early alterations in the pathogenesis and of obesity [Roden & Shulman, 2019].

The level of circulating ECs, especially 2-AG, are increased in obesity and particularly with excess VAT. Although the pathological role and the origin of circulating ECs remains unsolved, they are thought to express the overactivity of peripheral ECS, increased synthesis and/or decreased degradation of ECs, which might be modulated also by insulin sensitivity, genetic factors and the gender [Silvestri & Di Marzo, 2013]. According to previous studies, it is suggested that the

circulating level of 2-AG might apply as a biomarker of VAT rather than abdominal SAT, whereas AEA would reflect insulin resistance in SAT. We found positive correlation with AG (1+2) and BMI, but not WAT masses. AG (1+2) and AEA both associated with indices of systemic (M value, Rd and EGP), but not tissue-specific insulin sensitivity. In addition, according to previous studies, higher circulating AG (1+2) level associated with unfavourable lipid profile as well as higher GlycA level. Blocking CB1Rs with the inverse agonist Rimonabant showed an increase in HDL cholesterol, decrease in triglyceride level and ApoB/ApoA1 ratio, a shift towards larger LDL particles and a decrease in C-reactive protein in subjects with obesity, and it was suggested that the improvements would not be only secondary to weight loss [Després et al., 2005]. In sum, our results reflect metabolic dysregulation already in the pre-obese state.

6.3 Central CB1 receptor availability associates with metabolic dysregulation in the pre-obese state

In Study I, we investigated the CB1R availability in 21 bilateral brain regions involved in emotion and food reward based on previous studies [Hirvonen et al., 2012; Tuominen et al., 2014; Tuulari et al., 2013]. In Study III, the CB1R availability of the whole brain were assessed. The risk-group comparison showed no significance difference in the brain CB1R availability in either studies. However, the familial obesity risk, comprising of parental overweight/obesity/T2D, correlated negatively with the brain CB1R availability in Study I. Furthermore, higher BMI (Study I and III), total body fat mass and VAT mass (Study III) associated with lower brain CB1R availability.

Previous [^{18}F]FMPEP-d_2 PET study showed lower brain, as well as abdominal VAT and SAT CB1R availability in subjects with obesity as compared to lean subjects [Lahesmaa et al., 2018]. Other studies have shown negative correlation with BMI and brain CB1R availability [Ceccarini et al., 2016; Hirvonen et al., 2012]. Interestingly, the link between the lower CB1R availability and higher BMI was observed in brain areas involved in homeostatic energy balance regulation including the hypothalamus and brainstem. In subjects with eating disorders, such as anorexia or bulimia nervosa, the negative correlation between the CB1R availability and BMI has also been observed in the mesolimbic reward system [Ceccarini et al., 2016]. Subjects with anorexia nervosa have however increased overall cerebral CB1R availability as compared to healthy subjects [Gérard et al., 2011]. Earlier autoradiography studies have found lower CB1R availability in several extrahypothalamic brain regions in DIO mice than in lean mice, and the CB1R availability correlated negatively with total calorie intake and consumption of highly

palatable food [Harrold et al., 2002]. As upregulated EC levels are measured in several brain regions, including the hypothalamus [Higuchi et al., 2011] and hippocampus [Massa et al., 2010] in rodent models of obesity and prolonged HFD consumption, it is suggested that the lower cerebral CB1R availability results from increased cerebral EC levels due to overactive ECS [Engeli, 2008]. A HFD, typically rich in omega-6 and poor in omega-3 PUFAs, increased AEA [Berger et al., 2001] and 2-AG [Watanabe et al., 2003] levels in animal models. When considering the pre-obese state of our participants, our results indicate comparable effects.

Of the studied serum ECs, AEA level correlated negatively with CB1R availability in the ventral striatum (Study I), while AG (1+2) level had negative relationship with the CB1R availability in the whole brain (Study III). A recent study showed likewise negative correlation between serum EC levels, including AEA and AG (1+2), and central CB1R availability in healthy subjects with mild overweight (BMI 25.3 ± 3.7 kg/m^2) [Dickens et al., 2020]. Our result confirm that ECS is dysregulated already in the pre-obese state. Circulating EC levels might reflect the peripheral ECS tone, or even be a causative factor of metabolic deregulation [Silvestri & Di Marzo, 2013]. Accordingly, when studied the metabolomics, unfavourable lipid profile and higher levels of circulating fatty acids, including omega-6 PUFAs and linoleic acid associated with decreased brain CB1R availability (Study III).

Whole-body insulin sensitivity (M value) correlated positively and insulin-suppressed EGP negatively with the whole brain CB1R availability (Study III). It has been proposed that insulin downregulates ECS, whereas in conditions of insulin resistance, such as obesity, sustained hyperinsulinemia and hyperglycaemia results in an increase in adipocyte size and number and hypertrophic pancreatic β-cells, and ECS upregulation. It is suggested that this modulation of ECS by insulin might concern other tissues as well [Matias & Di Marzo, 2007]. As insulin resistance is a common feature of obesity, it might be that insulin resistance promotes or worsens ECS deregulation that in turn further enhances weight gain [Matias & Di Marzo, 2007; Quarta et al., 2011]. A link between cerebral EC signalling and hepatic insulin sensitivity was found in a study, where central CB1R activation led to impaired insulin-induced suppression of hepatic EGP without alterations in hepatic insulin signalling [O'Hare et al., 2011]. Furthermore, when exposed rats for three day HFD, a model of early insulin resistance characterized by hepatic and hypothalamic insulin resistance [Ono et al., 2008], blocking the brain CB1Rs restored the hepatic insulin sensitivity [O'Hare et al., 2011]. The study demonstrates that upregulated cerebral ECS tone may induce hepatic insulin resistance. We suggest our result to be in line with the presented preclinical data demonstrating the crosstalk between the brain and peripheral ECS and insulin action.

6.4 Strengths and limitations

The strength of the current study is the application of the dynamic multi-tracer PET imaging that enables quantification of the brain and peripheral tissue metabolism and receptor binding *in vivo*. Combining PET with hyperinsulinemic–euglycemic clamp, the golden standard method for assessing whole-body insulin sensitivity, allows simultaneous assessment of hepatic EGP. In addition to PET and clamp studies, the characteristics of the subjects´ were carefully determined using MRI and CT imaging, as well as air displacement plethysmograph (the Bod Pod system) for quantifying body adiposity, and blood sampling to measure several metabolic biomarkers and circulating ECs. These comprehensive measurements allow modelling of the brain-periphery interactions. The new whole-body PET scanner Quadra in Turku PET Centre enables simultaneous dynamic imaging of the whole-body, and using Quadra in further studies would allow even more precise studying of the brain-periphery interactions.

As a limitation, our studies comprised only males. Therefore, the results may not be directly generalized to females. There have been divergent results concerning the effects of sex on brain glucose metabolism and insulin sensitivity [Feng et al., 2022; Gur et al., 1995]. Also, studies applying IN insulin administration have suggested sex-dependent differences in the effects of central insulin on appetite and body weight, although the feeding states in those studies differed [Flint et al., 2007; Hallschmid et al., 2004, 2012; Jauch-Chara et al., 2012]. According to previous large-scale cohort study however, insulin-stimulated BGU was not significantly affected by sex [Rebelos et al., 2021]. According to ECS, it seems that estrogen negatively modulates CB1R-induced changes in appetite, body temperature and activity of POMC neurons [Kellert et al., 2009]. Furthermore, there is a bidirectional interaction between the ECS and gonadal hormones. EC signalling in the hypothalamus and anterior pituitary reduces the release of gonadal hormones, which in turn, particularly estrogen, alter ECS-related protein expression and response to ECs [Gorzalka & Dang, 2012]. Whether this interaction has an impact on feeding behaviour or results in sex-dependent differences on ECS function apparently needs further investigation.

The subjects in the high obesity risk group were older than the low-risk subjects. Age is known to be a predictor of brain insulin sensitivity; cerebral insulin signalling decreases with advancing age, as happens in the periphery as well [Kullmann et al., 2016]. However, the effects of age were controlled in the statistical analyses whenever possible Again, in the study consisting of subjects with wide age range (women 23–80 and men 20–69 years), showed that although the whole-body insulin sensitivity was the best predictor of insulin-stimulated BGU, age associated negatively with BGU. The association was strongest in the limbic and temporal lobes, a trend toward a negative correlation was found in the frontal and parietal

lobes, while no correlation in occipital lobes [Rebelos et al., 2021]. In BGU analysis in Study I and II, the age was used as a covariate with unchanged results.

Hepatic EGP values in Study II and III were mainly negative in both high and low-risk group indicating EGP suppression under insulin stimulation. Wide range, and also negative EGP values has been shown in previous study in subjects without diabetes, reflecting the amount of lean body mass [Natali et al., 2000]. Similarly, one previous study presented a progressive decline in insulin suppression of hepatic EGP with increasing VAT mass and hepatic lipid content (HLC) [Gastaldelli et al., 2007]. A recent study comprising of lean non-Asian Indian subjects, showed 95% percentile of HCL to be 1.85%, lower than the previously determined upper normal level 5.56% [Szczepaniak et al., 2005]. Although we did not measure the HLC, we assume it under 1.85% in our subjects thus explaining the effective suppression of EGP.

PET has a limited spatial resolution, typically 4–5 mm resulting in partial volume effect (PVE) that limits studying very small regions, such as hypothalamus, with PET. Motion artefact is another concern when scanning moving structures with PET [Cherry & Dahlbom, 2006]. To limit the effect of spillover due to PVE and motion we carefully draw several ROIs and VOIs in several slices of images avoiding large vessels. In [^{18}F]FDG analysis, the mean K_i values were then extracted from each tissue and used in the analysis.

In study I and II, we investigated CB1R binding with PET and CB1R inverse agonist [^{18}F]FMPEP-d_2. As the method quantifies the amount of available CB1Rs that are not occupied with their natural ligands, it is not possible to measure the total amount and density of CB1Rs or their affinity. Therefore, changes in the CB1R availability may result from alterations in EC levels, receptor density or affinity, or mixture of them. A previous study in mice model of Alzheimer´s disease demonstrated altered brain CB1R availability with unchanged CB1R availability [Takkinen et al., 2018] suggesting that the altered receptor availability represent alterations in EC levels or receptor affinity. Rodent models of obesity have detected reduced CB1R and EC degrading enzyme gene expression in WAT accompanied with increased circulating EC levels indicating a negative feedback loop regulation [Engeli et al., 2005].

Importantly, as our study design is cross-sectional, we cannot ascertain the causality of the observed effects; whether the detected metabolic differences and receptor availabilities between the two risk groups are a cause or a consequence of obesity risk and how do they interact.

6.5 Clinical implications and future aspects

Obesity is a complex disease, characterized by defective interactions between the brain and periphery, altered interorgan substrate fluxes and handling, and deregulated neural signalling pathways. Our results show that these alterations are already present in non-obese subjects with overweight. Concerning the obesity epidemic, understanding the pathogenic pathways predisposing to weight gain is essential, as it would enable launching early interventions and discovering new and maybe more individualized therapeutic targets to treat obesity.

Previous studies from our centre and others have discussed the methods investigating brain insulin sensitivity, and the term brain insulin resistance [Kullmann, Kleinridders, et al., 2020; Latva-Rasku, 2020; Rebelos, 2020]. By applying different methods distinct study groups have gained evidence of disturbances in central insulin action in metabolic diseases, and the term brain insulin resistance has been approved. Available imaging methods for investigating brain insulin action in humans include [^{18}F]FDG PET, MEG and fMRI. Hyperinsulinemic-euglycemic clamp enables assessing of brain glucose handling under insulin-stimulation in relation to other tissues, while intranasal insulin administration allows more selective evaluation of the central and peripheral effects of insulin within the CNS. IN administered insulin spreads throughout the brain and only small proportion is absorbed into circulation, while during the clamp, the insulin effect is systemic [Kullmann, Kleinridders, et al., 2020]. Combining these different approaches would allow building comprehensive understanding of brain insulin action, but this approach is precluded by the methodological complexity and necessity of highly trained personnel and adequate equipment.

The studies of this thesis are part of PROSPECT research project (Clinicaltrials.gov, NCT03106688), in which we have studied the brain and whole-body insulin sensitivity, central u-opioid (MOR) receptor, as well as CB1R availability in brain and peripheral tissues. Radiation exposure limits the further PET studies in the same population. However, fMRI with IN insulin administration would provide complementary information about the effects of insulin on certain brain regions as compared to insulin-stimulated BGU acquired with [^{18}F]FDG PET during clamp. It would be interesting to test whether the effect of insulin in specific brain regions´ activity is weaker in subjects with high as compared to low obesity risk, and does the effect associate with VAT mass, as in previous study in subjects with obesity [Kullmann et al., 2015]. Considering the better resolution of MRI than PET/CT, the assessment of insulin action within the hypothalamus would be of special interest, as this structure cannot be accurately delineated and quantified with PET. Simultaneous hyperinsulinemic-euglycemic clamp would allow assessment of potential improvements in the whole-body insulin sensitive and risk-group differences, as well as confirm the association of central insulin action and whole-

body insulin sensitivity that we found in Study II. Investigating the relationship between central insulin and hepatic EGP, that we also found in Study II, with IN insulin application would be interesting but would require exposing the subjects to radiation when using [^{18}F]FDG PET. Follow-up study within the ongoing PROSPECT project will determine the change in BMI and body composition and their relation to the baseline results in PET studies. Moreover, further studies and effort is needed to resolve the causality between defects in brain insulin signalling and obesity and associated metabolic diseases.

According to ECS, the next interesting step would be determining CB1R and EC expression from tissue, particularly WAT biopsies to determine whether the lower CB1R availability in high as compared to low obesity risk subjects we found in Study III, results from altered CBR1 density or EC level. For such a study, it would be reasonable to recruit a new sample of participants, both male and female subjects with and without obesity, perform [^{18}F]FMPEP-d_2 PET study, and obtain the tissue biopsies at the same visit before the scan, so that the tissue CB1R and EC levels would represent the same metabolic state. Quantifying circulating ECs would offer a chance to compare the serum and tissue EC levels as well. Better understanding of the contribution of WAT CB1Rs in the regulation of whole-body energy metabolism would also profit targeting treatment of obesity. Concerning the brain CB1Rs, and their interaction with central insulin signalling, and other neural signal networks, requires further investigations too.

7 Conclusions

The thesis aimed to investigate obesity risk factors focusing in brain and peripheral tissue insulin sensitivity and endocannabinoid system applying PET imaging. The main findings of the thesis were the following:

1. Brain insulin sensitivity, quantified as insulin-simulated brain glucose uptake, is decreased already in non-obese state, in the presence of overweight. Decreased brain insulin sensitivity associates with decreased whole-body and skeletal muscle insulin sensitivity, and decreased suppression of hepatic EGP and white adipose tissue lipolysis. Familial obesity risk, including parental overweight/obesity/T2D, associates with decreased brain insulin sensitivity. These results add to the current knowledge on the development of obesity, suggesting that altered brain insulin signalling and impaired crosstalk between the brain and peripheral organs may exist already in subjects with overweight and risk factors for obesity.
2. Subjects with overweight and risk factors for developing obesity have lower abdominal adipose tissue CB1R availability as compared to lean subjects. The lower CB1R availability in abdominal adipose tissue depots associates with decreased adipose tissue insulin sensitivity, enlarged body fat mass, unfavorable lipid profile and higher inflammatory markers. Of the circulating endocannabinoids and relates structures, the levels of arachidonic acid, anandamide and arachidonoyl glycerol correlated negatively with whole-body insulin sensitivity. Serum arachidonoyl glycerol level associated also with reduced suppression of hepatic EGP, higher BMI, unfavorable lipid profile and higher levels of systemic inflammatory markers. These results indicate that endocannabinoid system dysregulation in white adipose tissue may be an early manifestation of metabolic disorders, including dyslipidemia, insulin resistance and abdominal obesity.
3. Lower cerebral CB1R availability associates with decreased whole-body insulin sensitivity, decreased suppression of hepatic EGP, as well as higher weight, BMI, enlarged visceral adipose tissue mass and unfavorable lipid

profile. Reduced CB1R availability in cerebral pathways regulating food intake associates with higher level of circulating anandamide, whereas globally decreased brain CB1R availability associates with higher serum arachidonoyl glycerol level. These findings suggest that alterations in brain endocannabinoid signaling take place early, and may even represent the pathological process in the development of obesity comprising of defective crosstalk between the brain and peripheral endocannabinoid and insulin signalling.

Acknowledgements

This study was carried out at the Turku PET Centre, and within the Finnish Centre of Excellence in Cardiovascular and Metabolic Diseases, supported by Academy of Finland, University of Turku, Turku University Hospital and Åbo Akademi University during the years 2017–2023. For financial support I wish to thank Jalmari and Rauha Ahokas Foundation, Turunmaa Duodecim Society, Turku University Hospital Foundation for Education and Research, The Diabetes Research Foundation, Orion Research Foundation and The State Research Funding.

I express my sincerely gratitude to my supervisors Professor Pirjo Nuutila and Professor Lauri Nummenmaa for the opportunity to conduct my doctoral thesis work under your guidance. Pirjo, I admire your knowledge and groundbreaking work in the field of metabolic research and PET imaging. I have felt privileged to be involved in your research group. Lauri, I am grateful for your excellent guidance and encouraging attitude, as well as careful language check of this thesis. You both have had trust on the PROSPECT project and encouraged me to accomplish this challenging journey.

I wish a warm thank to Docent Kirsi Timonen for accepting the invitation to be my opponent. I´m very much looking forward to meeting you. I appreciate the work of Professor Hubert Preissl and Docent Sanni Söderlund for reviewing this thesis and giving me valuable feedback. I acknowledge Professor Kirsi Pietiläinen and Docent Marco Bucci for being in my doctoral follow-up group and Marco Bucci also for the expertise in brain modelling and being one of my co-authors.

I express the warmest thanks to Tatu Kantonen, with whom I have shared the PROSPECT project. Thank you for your companionship, precise work and determined attitude. Despite some setbacks we encountered, I have had a strong trust that together we would manage the early mornings and long days with the PET studies. I am remarkably thankful for the study participants. This thesis would not have been possible without your commitment. I wish to thank all the co-authors that I have had an opportunity to work with. Thank you Eleni Rebelos, Aino Latva-Rasku, Prince Dadson, Tomi Karjalainen, Kari Kalliokoski, Kirsi Laitinen, Noora Houttu, Merja Haaparanta-Solin, Richard Aarnio, Vesa Oikonen, Alex Dickens, Annie von Eyken, Anna K. Kirjavainen, Semi Helin, Jussi Hirvonen, Johan Rajander

and Tapani Rönnemaa. A special thanks to Sanna Laurila, Minna Lahesmaa-Hatting, Aino Latva-Rasku and Miikka Honka for teaching me the basics of the PET image analysis. Eleni, I wish to thank you also for the great collaboration and guidance in so many practical issues. Aino, I appreciate your support and experience that you have shared as well. Prince, I wish to thank you for your encouragement and positivity.

I thank docent Jarna Hannukainen and study nurse Mia Koutu for getting me started with the clamp studies, Heikki Laurikainen for guiding me and Tatu with [^{18}F]FMPEP-d_2 studies and Lihua Sun for the help with PROSPECT´s fMRI studies. I wish to thank study nurse Sanna Himanen for the precious help with the PROSPECT´s follow-up visits as well as the inspiring ideas that you have shared. I want to thank also all the other people with whom I have shared the PET analysis room during these years and the whole Nummenmaa lab team.

I have had a privilege to work in the Turku PET Centre that is extremely innovative place to conduct research. I express my gratitude to Professor Juhani Knuuti for allowing this possibility. Heartfelt thanks to the wonderful staff of the PET Centre. Minna Aatsinki, Sanna Suominen, Heidi Partanen, Eija Salo, Anne-Mari Jokinen, Hannele Lehtinen, Virva Saunavaara, Tuula Tolvanen, Mika Teräs as well as all the other great laboratory technicians, radiochemists, radiographers and physicians. Thank you all for your excellent and dedicated work, guidance and kindness. It has been pleasure to work with you. I am extremely thankful to Vesa Oikonen for the help with data analysis and modelling. I wish my warm thank also to Rami Mikkola and Marko Tättäläinen for helping with IT issues, Sauli Piirola and Timo Laitinen for providing PET software tools and support with them, and Lenita Saloranta and Minna Kangasperko for the assistance with administrative matters.

I wish to thank my superiors in the clinics for granting me time of for research. Thank you Markus Juonala and Minna Soinio in Turku and Tuula Pekkarinen in Pori. I wish my warmest thanks to my colleagues in the department of endocrinology in Turku and Pori. Thank you for your support Minna Soinio, Pia Hakanen, Lassi Nelimarkka, Heidi Immonen, Antti Autere, Nelli Tuomola, Aku Virta, Aino Latva-Rasku, Matti Vuori, Tyko Hellsten, Tuula Pekkarinen, Pirkko Korsoff and Hanna Laine.

Finally, I wish to thank my dear parents and my dear sister for your endless love and support. I am grateful for your encouragement over these years. I know I can always turn to you.

Turku, December 2023
Laura Pekkarinen

References

Abate, N., Burns, D., Peshock, R. M., Garg, A., & Grundy, S. M. (1994). Estimation of adipose tissue mass by magnetic resonance imaging: Validation against dissection in human cadavers. *Journal of Lipid Research*, *35*(8), 1490–1496. https://doi.org/10.1016/s0022-2275(20)40090-2

Afshin, A., Forouzanfar, M. H., Reitsma, M. B., Sur, P., Estep, K., Lee, A., Marczak, L., Mokdad, A. H., Moradi-Lakeh, M., Naghavi, M., Salama, J. S., Vos, T., Abate, K. H., Abbafati, C., Ahmed, M. B., Al-Aly, Z., Alkerwi, A., Al-Raddadi, R., Amare, A. T., … Murray, C. J. L. (2017). Health Effects of Overweight and Obesity in 195 Countries over 25 Years. *The New England Journal of Medicine*, *377*(1), 13–27. https://doi.org/10.1056/NEJMoa1614362

Aimé, P., Hegoburu, C., Jaillard, T., Degletagne, C., Garcia, S., Messaoudi, B., Thevenet, M., Lorsignol, A., Duchamp, C., Mouly, A.-M., & Julliard, A. K. (2012). A physiological increase of insulin in the olfactory bulb decreases detection of a learned aversive odor and abolishes food odor-induced sniffing behavior in rats. *PloS One*, *7*(12), e51227. https://doi.org/10.1371/journal.pone.0051227

Anjana, R. M., Lakshminarayanan, S., Deepa, M., Farooq, S., Pradeepa, R., & Mohan, V. (2009). Parental history of type 2 diabetes mellitus, metabolic syndrome, and cardiometabolic risk factors in Asian Indian adolescents. *Metabolism*, *58*(3), 344–350. https://doi.org/https://doi.org/10.1016/j.metabol.2008.10.006

Aubrey, J., Esfandiari, N., Baracos, V. E., Buteau, F. A., Frenette, J., Putman, C. T., & Mazurak, V. C. (2014). Measurement of skeletal muscle radiation attenuation and basis of its biological variation. *Acta Physiologica (Oxford, England)*, *210*(3), 489–497. https://doi.org/10.1111/apha.12224

Bady, I., Marty, N., Dallaporta, M., Emery, M., Gyger, J., Tarussio, D., Foretz, M., & Thorens, B. (2006). Evidence from glut2-null mice that glucose is a critical physiological regulator of feeding. *Diabetes*, *55*(4), 988–995. https://doi.org/10.2337/diabetes.55.04.06.db05-1386

Bahri, S., Horowitz, M., & Malbert, C. H. (2018). Inward Glucose Transfer Accounts for Insulin-Dependent Increase in Brain Glucose Metabolism Associated with Diet-Induced Obesity. *Obesity*, *26*(8), 1322–1331. https://doi.org/10.1002/oby.22243

Bamshad, M., Song, C. K., & Bartness, T. J. (1999). CNS origins of the sympathetic nervous system outflow to brown adipose tissue. *The American Journal of Physiology*, *276*(6), R1569-78. https://doi.org/10.1152/ajpregu.1999.276.6.R1569

Banks, W. A., Owen, J. B., & Erickson, M. A. (2012). Insulin in the brain: There and back again. In *Pharmacology and Therapeutics* (Vol. 136, Issue 1, pp. 82–93). https://doi.org/10.1016/j.pharmthera.2012.07.006

Baufeld, C., Osterloh, A., Prokop, S., Miller, K. R., & Heppner, F. L. (2016). High-fat diet-induced brain region-specific phenotypic spectrum of CNS resident microglia. *Acta Neuropathologica*, *132*(3), 361–375. https://doi.org/10.1007/s00401-016-1595-4

Baye, T. M., Zhang, Y., Smith, E., Hillard, C. J., Gunnell, J., Myklebust, J., James, R., Kissebah, A. H., Olivier, M., & Wilke, R. A. (2008). Genetic variation in cannabinoid receptor 1 (CNR1) is associated with derangements in lipid homeostasis, independent of body mass index. *Pharmacogenomics*, *9*(11), 1647–1656. https://doi.org/10.2217/14622416.9.11.1647

Beddows, C. A., & Dodd, G. T. (2021). Insulin on the brain: The role of central insulin signalling in energy and glucose homeostasis. *Journal of Neuroendocrinology*, *33*(4), e12947. https://doi.org/10.1111/jne.12947

Bellocchio, L., Lafenêtre, P., Cannich, A., Cota, D., Puente, N., Grandes, P., Chaouloff, F., Piazza, P. V., & Marsicano, G. (2010). Bimodal control of stimulated food intake by the endocannabinoid system. *Nature Neuroscience*, *13*(3), 281–283. https://doi.org/10.1038/nn.2494

Bénard, G., Massa, F., Puente, N., Lourenço, J., Bellocchio, L., Soria-Gómez, E., Matias, I., Delamarre, A., Metna-Laurent, M., Cannich, A., Hebert-Chatelain, E., Mulle, C., Ortega-Gutiérrez, S., Martín-Fontecha, M., Klugmann, M., Guggenhuber, S., Lutz, B., Gertsch, J., Chaouloff, F., … Marsicano, G. (2012). Mitochondrial CB_1 receptors regulate neuronal energy metabolism. *Nature Neuroscience*, *15*(4), 558–564. https://doi.org/10.1038/nn.3053

Bender, D., Munk, O. L., Feng, H. Q., & Keiding, S. (2001). Metabolites of (18)F-FDG and 3-O-(11)C-methylglucose in pig liver. *Journal of Nuclear Medicine : Official Publication, Society of Nuclear Medicine*, *42*(11), 1673–1678.

Benedict, C., Brede, S., Schiöth, H. B., Lehnert, H., Schultes, B., Born, J., & Hallschmid, M. (2011). Intranasal insulin enhances postprandial thermogenesis and lowers postprandial serum insulin levels in healthy men. *Diabetes*, *60*(1), 114–118. https://doi.org/10.2337/db10-0329

Benedict, C., Kern, W., Schultes, B., Born, J., & Hallschmid, M. (2008). Differential sensitivity of men and women to anorexigenic and memory-improving effects of intranasal insulin. *The Journal of Clinical Endocrinology and Metabolism*, *93*(4), 1339–1344. https://doi.org/10.1210/jc.2007-2606

Bennetzen, M. F., Wellner, N., Ahmed, S. S., Ahmed, S. M., Diep, T. A., Hansen, H. S., Richelsen, B., & Pedersen, S. B. (2011). Investigations of the human endocannabinoid system in two subcutaneous adipose tissue depots in lean subjects and in obese subjects before and after weight loss. *International Journal of Obesity (2005)*, *35*(11), 1377–1384. https://doi.org/10.1038/ijo.2011.8

Bensaid, M., Gary-Bobo, M., Esclangon, A., Maffrand, J. P., Le Fur, G., Oury-Donat, F., & Soubrié, P. (2003). The cannabinoid CB1 receptor antagonist SR141716 increases Acrp30 mRNA expression in adipose tissue of obese fa/fa rats and in cultured adipocyte cells. *Molecular Pharmacology*, *63*(4), 908–914. https://doi.org/10.1124/mol.63.4.908

Berge, K., Piscitelli, F., Hoem, N., Silvestri, C., Meyer, I., Banni, S., & Di Marzo, V. (2013). Chronic treatment with krill powder reduces plasma triglyceride and anandamide levels in mildly obese men. *Lipids in Health and Disease*, *12*, 78. https://doi.org/10.1186/1476-511X-12-78

Berger, A., Crozier, G., Bisogno, T., Cavaliere, P., Innis, S., & Di Marzo, V. (2001). Anandamide and diet: inclusion of dietary arachidonate and docosahexaenoate leads to increased brain levels of the corresponding N-acylethanolamines in piglets. *Proceedings of the National Academy of Sciences of the United States of America*, *98*(11), 6402–6406. https://doi.org/10.1073/pnas.101119098

Berglund, E. D., Liu, T., Kong, X., Sohn, J.-W., Vong, L., Deng, Z., Lee, C. E., Lee, S., Williams, K. W., Olson, D. P., Scherer, P. E., Lowell, B. B., & Elmquist, J. K. (2014). Melanocortin 4 receptors in autonomic neurons regulate thermogenesis and glycemia. *Nature Neuroscience*, *17*(7), 911–913. https://doi.org/10.1038/nn.3737

Berthoud, H.-R. (2004). Mind versus metabolism in the control of food intake and energy balance. *Physiology & Behavior*, *81*(5), 781–793. https://doi.org/10.1016/j.physbeh.2004.04.034

Bessell, E. M., Foster, A. B., & Westwood, J. H. (1972). The use of deoxyfluoro-D-glucopyranoses and related compounds in a study of yeast hexokinase specificity. *The Biochemical Journal*, *128*(2), 199–204. https://doi.org/10.1042/bj1280199

Blüher, M. (2019). Obesity: global epidemiology and pathogenesis. *Nature Reviews. Endocrinology*, *15*(5), 288–298. https://doi.org/10.1038/s41574-019-0176-8

Blüher, M., Engeli, S., Klöting, N., Berndt, J., Fasshauer, M., Bátkai, S., Pacher, P., Schön, M. R., Jordan, J., & Stumvoll, M. (2006). Dysregulation of the peripheral and adipose tissue endocannabinoid system in human abdominal obesity. *Diabetes*, *55*(11), 3053–3060. https://doi.org/10.2337/db06-0812

Bódis, K., & Roden, M. (2018). Energy metabolism of white adipose tissue and insulin resistance in humans. *European Journal of Clinical Investigation*, *48*(11), e13017. https://doi.org/10.1111/eci.13017

Boersma, G. J., Johansson, E., Pereira, M. J., Heurling, K., Skrtic, S., Lau, J., Katsogiannos, P., Panagiotou, G., Lubberink, M., Kullberg, J., Ahlström, H., & Eriksson, J. W. (2018). Altered Glucose Uptake in Muscle, Visceral Adipose Tissue, and Brain Predict Whole-Body Insulin Resistance and may Contribute to the Development of Type 2 Diabetes: A Combined PET/MR Study. *Hormone and Metabolic Research = Hormon- Und Stoffwechselforschung = Hormones et Metabolisme*, *50*(8), 627–639. https://doi.org/10.1055/a-0643-4739

Bolli, G. B., & Fanelli, C. G. (1999). Physiology of glucose counterregulation to hypoglycemia. *Endocrinology and Metabolism Clinics of North America*, *28*(3), 467–493, v. https://doi.org/10.1016/s0889-8529(05)70083-9

Bordicchia, M., Battistoni, I., Mancinelli, L., Giannini, E., Refi, G., Minardi, D., Muzzonigro, G., Mazzucchelli, R., Montironi, R., Piscitelli, F., Petrosino, S., Dessì-Fulgheri, P., Rappelli, A., Di Marzo, V., & Sarzani, R. (2010). Cannabinoid CB1 receptor expression in relation to visceral adipose depots, endocannabinoid levels, microvascular damage, and the presence of the Cnr1 A3813G variant in humans. *Metabolism: Clinical and Experimental*, *59*(5), 734–741. https://doi.org/10.1016/j.metabol.2009.09.018

Born, J., Lange, T., Kern, W., McGregor, G. P., Bickel, U., & Fehm, H. L. (2002). Sniffing neuropeptides: a transnasal approach to the human brain. *Nature Neuroscience*, *5*(6), 514–516. https://doi.org/10.1038/nn849

Bøtker, H. E., Böttcher, M., Schmitz, O., Gee, A., Hansen, S. B., Cold, G. E., Nielsen, T. T., & Gjedde, A. (1997). Glucose uptake and lumped constant variability in normal human hearts determined with [18F]fluorodeoxyglucose. *Journal of Nuclear Cardiology : Official Publication of the American Society of Nuclear Cardiology*, *4*(2 Pt 1), 125–132. https://doi.org/10.1016/s1071-3581(97)90061-1

Boucher, J., Kleinridders, A., & Kahn, C. R. (2014). Insulin receptor signaling in normal and insulin-resistant states. *Cold Spring Harbor Perspectives in Biology*, *6*(1). https://doi.org/10.1101/cshperspect.a009191

Bray, G. A., Kim, K. K., & Wilding, J. P. H. (2017). Obesity: a chronic relapsing progressive disease process. A position statement of the World Obesity Federation. In *Obesity reviews : an official journal of the International Association for the Study of Obesity* (Vol. 18, Issue 7, pp. 715–723). https://doi.org/10.1111/obr.12551

Brito, M. N., Brito, N. A., Baro, D. J., Song, C. K., & Bartness, T. J. (2007). Differential activation of the sympathetic innervation of adipose tissues by melanocortin receptor stimulation. *Endocrinology*, *148*(11), 5339–5347. https://doi.org/10.1210/en.2007-0621

Brochu, M., Starling, R. D., Tchernof, A., Matthews, D. E., Garcia-Rubi, E., & Poehlman, E. T. (2000). Visceral adipose tissue is an independent correlate of glucose disposal in older obese postmenopausal women. *The Journal of Clinical Endocrinology and Metabolism*, *85*(7), 2378–2384. https://doi.org/10.1210/jcem.85.7.6685

Broyd, S. J., Demanuele, C., Debener, S., Helps, S. K., James, C. J., & Sonuga-Barke, E. J. S. (2009). Default-mode brain dysfunction in mental disorders: a systematic review. *Neuroscience and Biobehavioral Reviews*, *33*(3), 279–296. https://doi.org/10.1016/j.neubiorev.2008.09.002

Brüning, J. C., Gautam, D., Burks, D. J., Gillette, J., Schubert, M., Orban, P. C., Klein, R., Krone, W., Müller-Wieland, D., & Kahn, C. R. (2000). Role of brain insulin receptor in control of body weight and reproduction. *Science (New York, N.Y.)*, *289*(5487), 2122–2125. https://doi.org/10.1126/science.289.5487.2122

Brünner, Y. F., Benedict, C., & Freiherr, J. (2013). Intranasal insulin reduces olfactory sensitivity in normosmic humans. *The Journal of Clinical Endocrinology and Metabolism*, *98*(10), E1626-30. https://doi.org/10.1210/jc.2013-2061

Cahill, G. F. J., Herrera, M. G., Morgan, A. P., Soeldner, J. S., Steinke, J., Levy, P. L., Reichard, G. A. J., & Kipnis, D. M. (1966). Hormone-fuel interrelationships during fasting. *The Journal of Clinical Investigation*, *45*(11), 1751–1769. https://doi.org/10.1172/JCI105481

Cannon, B., & Nedergaard, J. (2004). Brown adipose tissue: function and physiological significance. *Physiological Reviews*, *84*(1), 277–359. https://doi.org/10.1152/physrev.00015.2003

Cardinal, P., André, C., Quarta, C., Bellocchio, L., Clark, S., Elie, M., Leste-Lasserre, T., Maitre, M., Gonzales, D., Cannich, A., Pagotto, U., Marsicano, G., & Cota, D. (2014). CB1 cannabinoid receptor in SF1-expressing neurons of the ventromedial hypothalamus determines metabolic responses to diet and leptin. *Molecular Metabolism*, *3*(7), 705–716. https://doi.org/10.1016/j.molmet.2014.07.004

Carpentier, A. C., Blondin, D. P., Virtanen, K. A., Richard, D., Haman, F., & Turcotte, É. E. (2018). Brown Adipose Tissue Energy Metabolism in Humans. *Frontiers in Endocrinology*, *9*, 447. https://doi.org/10.3389/fendo.2018.00447

Cazettes, F., Cohen, J. I., Yau, P. L., Talbot, H., & Convit, A. (2011). Obesity-mediated inflammation may damage the brain circuit that regulates food intake. *Brain Research*, *1373*, 101–109. https://doi.org/10.1016/j.brainres.2010.12.008

Ceccarini, J., Weltens, N., Ly, H. G., Tack, J., Van Oudenhove, L., & Van Laere, K. (2016). Association between cerebral cannabinoid 1 receptor availability and body mass index in patients with food intake disorders and healthy subjects: a [(18)F]MK-9470 PET study. *Translational Psychiatry*, *6*(7), e853. https://doi.org/10.1038/tp.2016.118

Cederberg, H., Stančáková, A., Kuusisto, J., Laakso, M., & Smith, U. (2015). Family history of type 2 diabetes increases the risk of both obesity and its complications: is type 2 diabetes a disease of inappropriate lipid storage? *Journal of Internal Medicine*, *277*(5), 540–551. https://doi.org/https://doi.org/10.1111/joim.12289

Chambers, A. P., Vemuri, V. K., Peng, Y., Wood, J. T., Olszewska, T., Pittman, Q. J., Makriyannis, A., & Sharkey, K. A. (2007). A neutral CB1 receptor antagonist reduces weight gain in rat. *American Journal of Physiology. Regulatory, Integrative and Comparative Physiology*, *293*(6), R2185-93. https://doi.org/10.1152/ajpregu.00663.2007

Chen, M., Woods, S. C., & Porte, D. J. (1975). Effect of cerebral intraventricular insulin on pancreatic insulin secretion in the dog. *Diabetes*, *24*(10), 910–914. https://doi.org/10.2337/diab.24.10.910

Cherry, S. ., & Dahlbom, M. (2006). *PET: Physics, Instrumentation, and Scanners*. Spinger New York.

Chong, B., Jayabaskaran, J., Kong, G., Chan, Y. H., Chin, Y. H., Goh, R., Kannan, S., Ng, C. H., Loong, S., Kueh, M. T. W., Lin, C., Anand, V. V., Lee, E. C. Z., Chew, H. S. J., Tan, D. J. H., Chan, K. E., Wang, J.-W., Muthiah, M., Dimitriadis, G. K., … Chew, N. W. S. (2023). Trends and predictions of malnutrition and obesity in 204 countries and territories: an analysis of the Global Burden of Disease Study 2019. *EClinicalMedicine*, *57*, 101850. https://doi.org/10.1016/j.eclinm.2023.101850

Christen, T., Sheikine, Y., Rocha, V. Z., Hurwitz, S., Goldfine, A. B., Di Carli, M., & Libby, P. (2010). Increased glucose uptake in visceral versus subcutaneous adipose tissue revealed by PET imaging. *JACC: Cardiovascular Imaging*, *3*(8), 843–851. https://doi.org/10.1016/j.jcmg.2010.06.004

Cluny, N. L., Chambers, A. P., Vemuri, V. K., Wood, J. T., Eller, L. K., Freni, C., Reimer, R. A., Makriyannis, A., & Sharkey, K. A. (2011). The neutral cannabinoid CB_1 receptor antagonist AM4113 regulates body weight through changes in energy intake in the rat. *Pharmacology, Biochemistry, and Behavior*, *97*(3), 537–543. https://doi.org/10.1016/j.pbb.2010.10.013

Cluny, N. L., Vemuri, V. K., Chambers, A. P., Limebeer, C. L., Bedard, H., Wood, J. T., Lutz, B., Zimmer, A., Parker, L. A., Makriyannis, A., & Sharkey, K. A. (2010). A novel peripherally restricted cannabinoid receptor antagonist, AM6545, reduces food intake and body weight, but does not cause malaise, in rodents. *British Journal of Pharmacology*, *161*(3), 629–642. https://doi.org/10.1111/j.1476-5381.2010.00908.x

Colombo, G., Agabio, R., Diaz, G., Lobina, C., Reali, R., & Gessa, G. L. (1998). Appetite suppression and weight loss after the cannabinoid antagonist SR 141716. *Life Sciences*, *63*(8), PL113-7. https://doi.org/10.1016/s0024-3205(98)00322-1

Connelly, M. A., Otvos, J. D., Shalaurova, I., Playford, M. P., & Mehta, N. N. (2017). GlycA, a novel biomarker of systemic inflammation and cardiovascular disease risk. *Journal of Translational Medicine*, *15*(1), 219. https://doi.org/10.1186/s12967-017-1321-6

Connolly, L., Coveleskie, K., Kilpatrick, L. A., Labus, J. S., Ebrat, B., Stains, J., Jiang, Z., Tillisch, K., Raybould, H. E., & Mayer, E. A. (2013). Differences in brain responses between lean and obese women to a sweetened drink. *Neurogastroenterology and Motility*, *25*(7), 579-e460. https://doi.org/10.1111/nmo.12125

Coomans, C. P., Biermasz, N. R., Geerling, J. J., Guigas, B., Rensen, P. C. N., Havekes, L. M., & Romijn, J. A. (2011). Stimulatory effect of insulin on glucose uptake by muscle involves the central nervous system in insulin-sensitive mice. *Diabetes*, *60*(12), 3132–3140. https://doi.org/10.2337/db10-1100

Coomans, C. P., Geerling, J. J., Guigas, B., van den Hoek, A. M., Parlevliet, E. T., Ouwens, D. M., Pijl, H., Voshol, P. J., Rensen, P. C. N., Havekes, L. M., & Romijn, J. A. (2011). Circulating insulin stimulates fatty acid retention in white adipose tissue via KATP channel activation in the central nervous system only in insulin-sensitive mice. *Journal of Lipid Research*, *52*(9), 1712–1722. https://doi.org/10.1194/jlr.M015396

Coppin, G. (2016). The anterior medial temporal lobes: Their role in food intake and body weight regulation. *Physiology & Behavior*, *167*, 60–70. https://doi.org/10.1016/j.physbeh.2016.08.028

Cota, D., Marsicano, G., Tschöp, M., Grübler, Y., Flachskamm, C., Schubert, M., Auer, D., Yassouridis, A., Thöne-Reineke, C., Ortmann, S., Tomassoni, F., Cervino, C., Nisoli, E., Linthorst, A. C. E., Pasquali, R., Lutz, B., Stalla, G. K., & Pagotto, U. (2003). The endogenous cannabinoid system affects energy balance via central orexigenic drive and peripheral lipogenesis. *The Journal of Clinical Investigation*, *112*(3), 423–431. https://doi.org/10.1172/JCI17725

D'Eon, T. M., Pierce, K. A., Roix, J. J., Tyler, A., Chen, H., & Teixeira, S. R. (2008). The role of adipocyte insulin resistance in the pathogenesis of obesity-related elevations in endocannabinoids. *Diabetes*, *57*(5), 1262–1268. https://doi.org/10.2337/db07-1186

Dash, S., Xiao, C., Morgantini, C., Koulajian, K., & Lewis, G. F. (2015). Intranasal insulin suppresses endogenous glucose production in humans compared with placebo in the presence of similar venous insulin concentrations. *Diabetes*, *64*(3), 766–774. https://doi.org/10.2337/db14-0685

De Souza, C. T., Araujo, E. P., Bordin, S., Ashimine, R., Zollner, R. L., Boschero, A. C., Saad, M. J. A., & Velloso, L. A. (2005). Consumption of a fat-rich diet activates a proinflammatory response and induces insulin resistance in the hypothalamus. *Endocrinology*, *146*(10), 4192–4199. https://doi.org/10.1210/en.2004-1520

Debons, A. F., Krimsky, I., & From, A. (1970). A direct action of insulin on the hypothalamic satiety center. *The American Journal of Physiology*, *219*(4), 938–943. https://doi.org/10.1152/ajplegacy.1970.219.4.938

DeFronzo, R. A., Tobin, J. D., & Andres, R. (1979). Glucose clamp technique: a method for quantifying insulin secretion and resistance. *The American Journal of Physiology*, *237*(3), E214-23. https://doi.org/10.1152/ajpendo.1979.237.3.E214

DeFronzo, R. A., & Tripathy, D. (2009). Skeletal muscle insulin resistance is the primary defect in type 2 diabetes. *Diabetes Care*, *32 Suppl 2*(Suppl 2), S157-63. https://doi.org/10.2337/dc09-S302

Deitmer, J. W., Theparambil, S. M., Ruminot, I., Noor, S. I., & Becker, H. M. (2019). Energy Dynamics in the Brain: Contributions of Astrocytes to Metabolism and pH Homeostasis. *Frontiers in Neuroscience*, *13*, 1301. https://doi.org/10.3389/fnins.2019.01301

Després, J.-P., Golay, A., & Sjöström, L. (2005). Effects of rimonabant on metabolic risk factors in overweight patients with dyslipidemia. *The New England Journal of Medicine*, *353*(20), 2121–2134. https://doi.org/10.1056/NEJMoa044537

Després, J.-P., & Lemieux, I. (2006). Abdominal obesity and metabolic syndrome. *Nature*, *444*(7121), 881–887. https://doi.org/10.1038/nature05488

Dhuria, S. V, Hanson, L. R., & Frey, W. H. 2nd. (2010). Intranasal delivery to the central nervous system: mechanisms and experimental considerations. *Journal of Pharmaceutical Sciences*, *99*(4), 1654–1673. https://doi.org/10.1002/jps.21924

Di Marzo, V. (2008a). Endocannabinoids: synthesis and degradation. *Reviews of Physiology, Biochemistry and Pharmacology*, *160*, 1–24. https://doi.org/10.1007/112_0505

Di Marzo, V. (2008b). The endocannabinoid system in obesity and type 2 diabetes. In *Diabetologia* (Vol. 51, Issue 8, pp. 1356–1367). https://doi.org/10.1007/s00125-008-1048-2

Di Marzo, V. (2008c). The endocannabinoid system in obesity and type 2 diabetes. *Diabetologia*, *51*(8), 1356–1367. https://doi.org/10.1007/s00125-008-1048-2

Di Marzo, V., Goparaju, S. K., Wang, L., Liu, J., Bátkai, S., Járai, Z., Fezza, F., Miura, G. I., Palmiter, R. D., Sugiura, T., & Kunos, G. (2001). Leptin-regulated endocannabinoids are involved in maintaining food intake. *Nature*, *410*(6830), 822–825. https://doi.org/10.1038/35071088

Di Marzo, V., Ligresti, A., & Cristino, L. (2009). The endocannabinoid system as a link between homoeostatic and hedonic pathways involved in energy balance regulation. *International Journal of Obesity (2005)*, *33 Suppl 2*, S18-24. https://doi.org/10.1038/ijo.2009.67

Dickens, A. M., Borgan, F., Laurikainen, H., Lamichhane, S., Marques, T., Rönkkö, T., Veronese, M., Lindeman, T., Hyötyläinen, T., Howes, O., Hietala, J., & Orešič, M. (2020). Links between central CB1-receptor availability and peripheral endocannabinoids in patients with first episode psychosis. *NPJ Schizophrenia*, *6*(1), 21. https://doi.org/10.1038/s41537-020-00110-7

Diggs-Andrews, K. A., Zhang, X., Song, Z., Daphna-Iken, D., Routh, V. H., & Fisher, S. J. (2010). Brain insulin action regulates hypothalamic glucose sensing and the counterregulatory response to hypoglycemia. *Diabetes*, *59*(9), 2271–2280. https://doi.org/10.2337/db10-0401

Donohue, S. R., Krushinski, J. H., Pike, V. W., Chernet, E., Phebus, L., Chesterfield, A. K., Felder, C. C., Halldin, C., & Schaus, J. M. (2008). Synthesis, ex vivo evaluation, and radiolabeling of potent 1,5-diphenylpyrrolidin-2-one cannabinoid subtype-1 receptor ligands as candidates for in vivo imaging. *Journal of Medicinal Chemistry*, *51*(18), 5833–5842. https://doi.org/10.1021/jm800416m

Dorfman, M. D., & Thaler, J. P. (2015). Hypothalamic inflammation and gliosis in obesity. *Current Opinion in Endocrinology, Diabetes, and Obesity*, *22*(5), 325–330. https://doi.org/10.1097/MED.0000000000000182

Dutta, B. J., Singh, S., Seksaria, S., Das Gupta, G., & Singh, A. (2022). Inside the diabetic brain: Insulin resistance and molecular mechanism associated with cognitive impairment and its possible therapeutic strategies. *Pharmacological Research*, *182*, 106358. https://doi.org/10.1016/j.phrs.2022.106358

EASO. (2015). The European Association for the Study of Obesity (EASO). 2015 Milan Declaration. A Call to Action on Obesity. https://easo.org/2015-milan-declaration-a-call-to-action-on-obesity/

Engeli, S. (2008). Peripheral Metabolic Effects of Endocannabinoids and Cannabinoid Receptor Blockade. *Obesity Facts*, *1*(1), 8–15. https://doi.org/10.1159/000114255

Engeli, S., Böhnke, J., Feldpausch, M., Gorzelniak, K., Janke, J., Bátkai, S., Pacher, P., Harvey-White, J., Luft, F. C., Sharma, A. M., & Jordan, J. (2005). Activation of the peripheral endocannabinoid system in human obesity. *Diabetes*, *54*(10), 2838–2843. https://doi.org/10.2337/diabetes.54.10.2838

Eny, K. M., Wolever, T. M. S., Fontaine-Bisson, B., & El-Sohemy, A. (2008). Genetic variant in the glucose transporter type 2 is associated with higher intakes of sugars in two distinct populations. *Physiological Genomics*, *33*(3), 355–360. https://doi.org/10.1152/physiolgenomics.00148.2007

Eraso-Pichot, A., Pouvreau, S., Olivera-Pinto, A., Gomez-Sotres, P., Skupio, U., & Marsicano, G. (2023). Endocannabinoid signaling in astrocytes. *Glia*, *71*(1), 44–59. https://doi.org/10.1002/glia.24246

Eriksson, J. W., Visvanathar, R., Kullberg, J., Strand, R., Skrtic, S., Ekström, S., Lubberink, M., Lundqvist, M. H., Katsogiannos, P., Pereira, M. J., & Ahlström, H. (2021). Tissue-specific glucose partitioning and fat content in prediabetes and type 2 diabetes: Whole-body PET/MRI during hyperinsulinemia. *European Journal of Endocrinology*. https://doi.org/10.1530/EJE-20-1359

Eriksson, O., Mikkola, K., Espes, D., Tuominen, L., Virtanen, K., Forsbäck, S., Haaparanta-Solin, M., Hietala, J., Solin, O., & Nuutila, P. (2015). The Cannabinoid Receptor-1 Is an Imaging Biomarker of Brown Adipose Tissue. *Journal of Nuclear Medicine*, *56*(12), 1937 LP – 1941. https://doi.org/10.2967/jnumed.115.156422

Esterson, Y. B., Carey, M., Boucai, L., Goyal, A., Raghavan, P., Zhang, K., Mehta, D., Feng, D., Wu, L., Kehlenbrink, S., Koppaka, S., Kishore, P., & Hawkins, M. (2016). Central Regulation of Glucose Production May Be Impaired in Type 2 Diabetes. *Diabetes*, *65*(9), 2569–2579. https://doi.org/10.2337/db15-1465

Faber, C. L., Deem, J. D., Campos, C. A., Taborsky, G. J. J., & Morton, G. J. (2020). CNS control of the endocrine pancreas. *Diabetologia*, *63*(10), 2086–2094. https://doi.org/10.1007/s00125-020-05204-6

Feng, B., Cao, J., Yu, Y., Yang, H., Jiang, Y., Liu, Y., Wang, R., & Zhao, Q. (2022). Gender-Related Differences in Regional Cerebral Glucose Metabolism in Normal Aging Brain. *Frontiers in Aging Neuroscience*, *14*, 809767. https://doi.org/10.3389/fnagi.2022.809767

Filbey, F. M., Myers, U. S., & Dewitt, S. (2012). Reward circuit function in high BMI individuals with compulsive overeating: similarities with addiction. *NeuroImage*, *63*(4), 1800–1806. https://doi.org/10.1016/j.neuroimage.2012.08.073

Filippi, B. M., Yang, C. S., Tang, C., & Lam, T. K. T. (2012). Insulin activates Erk1/2 signaling in the dorsal vagal complex to inhibit glucose production. *Cell Metabolism*, *16*(4), 500–510. https://doi.org/10.1016/j.cmet.2012.09.005

FinTerveys2017. (2018). Terveys, Toimintakyky Ja Hyvinvointi Suomessa : FinTerveys 2017 - Tutkimus. https://urn.fi/URN:ISBN:978-952-343-105-8

Flint, A., Gregersen, N. T., Gluud, L. L., Møller, B. K., Raben, A., Tetens, I., Verdich, C., & Astrup, A. (2007). Associations between postprandial insulin and blood glucose responses, appetite sensations and energy intake in normal weight and overweight individuals: a meta-analysis of test meal studies. *The British Journal of Nutrition*, *98*(1), 17–25. https://doi.org/10.1017/S000711450768297X

Fox, C. S., Massaro, J. M., Hoffmann, U., Pou, K. M., Maurovich-Horvat, P., Liu, C.-Y., Vasan, R. S., Murabito, J. M., Meigs, J. B., Cupples, L. A., D'Agostino, R. B. S., & O'Donnell, C. J. (2007). Abdominal visceral and subcutaneous adipose tissue compartments: association with metabolic risk factors in the Framingham Heart Study. *Circulation*, *116*(1), 39–48. https://doi.org/10.1161/CIRCULATIONAHA.106.675355

Fu, Z., Gilbert, E. R., & Liu, D. (2013). Regulation of insulin synthesis and secretion and pancreatic Beta-cell dysfunction in diabetes. *Current Diabetes Reviews*, *9*(1), 25–53.

Gancheva, S., Koliaki, C., Bierwagen, A., Nowotny, P., Heni, M., Fritsche, A., Häring, H.-U., Szendroedi, J., & Roden, M. (2015). Effects of intranasal insulin on hepatic fat accumulation and energy metabolism in humans. *Diabetes*, *64*(6), 1966–1975. https://doi.org/10.2337/db14-0892

García-Cáceres, C., Quarta, C., Varela, L., Gao, Y., Gruber, T., Legutko, B., Jastroch, M., Johansson, P., Ninkovic, J., Yi, C. X., Le Thuc, O., Szigeti-Buck, K., Cai, W., Meyer, C. W., Pfluger, P. T., Fernandez, A. M., Luquet, S., Woods, S. C., Torres-Alemán, I., … Tschöp, M. H. (2016). Astrocytic Insulin Signaling Couples Brain Glucose Uptake with Nutrient Availability. *Cell*, *166*(4), 867–880. https://doi.org/10.1016/j.cell.2016.07.028

Gastaldelli, A., Cusi, K., Pettiti, M., Hardies, J., Miyazaki, Y., Berria, R., Buzzigoli, E., Sironi, A. M., Cersosimo, E., Ferrannini, E., & Defronzo, R. A. (2007). Relationship between hepatic/visceral fat and hepatic insulin resistance in nondiabetic and type 2 diabetic subjects. *Gastroenterology*, *133*(2), 496–506. https://doi.org/10.1053/j.gastro.2007.04.068

Gatta-Cherifi, B., & Cota, D. (2016). New insights on the role of the endocannabinoid system in the regulation of energy balance. *International Journal of Obesity*, *40*(2), 210–219. https://doi.org/10.1038/ijo.2015.179

Gérard, N., Pieters, G., Goffin, K., Bormans, G., & Van Laere, K. (2011). Brain type 1 cannabinoid receptor availability in patients with anorexia and bulimia nervosa. *Biological Psychiatry*, *70*(8), 777–784. https://doi.org/10.1016/j.biopsych.2011.05.010

Goodpaster, B. H., Krishnaswami, S., Harris, T. B., Katsiaras, A., Kritchevsky, S. B., Simonsick, E. M., Nevitt, M., Holvoet, P., & Newman, A. B. (2005). Obesity, regional body fat distribution, and the metabolic syndrome in older men and women. *Archives of Internal Medicine*, *165*(7), 777–783. https://doi.org/10.1001/archinte.165.7.777

Gorzalka, B. B., & Dang, S. S. (2012). Minireview: Endocannabinoids and gonadal hormones: bidirectional interactions in physiology and behavior. *Endocrinology*, *153*(3), 1016–1024. https://doi.org/10.1210/en.2011-1643

Goss, A. M., & Gower, B. A. (2012). Insulin sensitivity is associated with thigh adipose tissue distribution in healthy postmenopausal women. *Metabolism: Clinical and Experimental*, *61*(12), 1817–1823. https://doi.org/10.1016/j.metabol.2012.05.016

Gueye, A. B., Pryslawsky, Y., Trigo, J. M., Poulia, N., Delis, F., Antoniou, K., Loureiro, M., Laviolette, S. R., Vemuri, K., Makriyannis, A., & Le Foll, B. (2016). The CB1 Neutral Antagonist AM4113 Retains the Therapeutic Efficacy of the Inverse Agonist Rimonabant for Nicotine Dependence and Weight Loss with Better Psychiatric Tolerability. *The International Journal of Neuropsychopharmacology*, *19*(12). https://doi.org/10.1093/ijnp/pyw068

Guillemot-Legris, O., & Muccioli, G. G. (2017). Obesity-Induced Neuroinflammation: Beyond the Hypothalamus. *Trends in Neurosciences*, *40*(4), 237–253. https://doi.org/10.1016/j.tins.2017.02.005

Gur, R. C., Mozley, L. H., Mozley, P. D., Resnick, S. M., Karp, J. S., Alavi, A., Arnold, S. E., & Gur, R. E. (1995). Sex differences in regional cerebral glucose metabolism during a resting state. *Science (New York, N.Y.)*, *267*(5197), 528–531. https://doi.org/10.1126/science.7824953

Hallschmid, M., Benedict, C., Schultes, B., Born, J., & Kern, W. (2008). Obese men respond to cognitive but not to catabolic brain insulin signaling. *International Journal of Obesity (2005)*, *32*(2), 275–282. https://doi.org/10.1038/sj.ijo.0803722

Hallschmid, M., Benedict, C., Schultes, B., Fehm, H.-L., Born, J., & Kern, W. (2004). Intranasal insulin reduces body fat in men but not in women. *Diabetes*, *53*(11), 3024–3029. https://doi.org/10.2337/diabetes.53.11.3024

Hallschmid, M., Higgs, S., Thienel, M., Ott, V., & Lehnert, H. (2012). Postprandial administration of intranasal insulin intensifies satiety and reduces intake of palatable snacks in women. *Diabetes*, *61*(4), 782–789. https://doi.org/10.2337/db11-1390

Hamacher, K., Coenen, H. H., & Stöcklin, G. (1986). Efficient stereospecific synthesis of no-carrier-added 2-[18F]-fluoro-2-deoxy-D-glucose using aminopolyether supported nucleophilic substitution. *Journal of Nuclear Medicine : Official Publication, Society of Nuclear Medicine*, *27*(2), 235–238.

Hariri, A. R., Gorka, A., Hyde, L. W., Kimak, M., Halder, I., Ducci, F., Ferrell, R. E., Goldman, D., & Manuck, S. B. (2009). Divergent effects of genetic variation in endocannabinoid signaling on human threat- and reward-related brain function. *Biological Psychiatry*, *66*(1), 9–16. https://doi.org/10.1016/j.biopsych.2008.10.047

Harrold, J. A., Elliott, J. C., King, P. J., Widdowson, P. S., & Williams, G. (2002). Down-regulation of cannabinoid-1 (CB-1) receptors in specific extrahypothalamic regions of rats with dietary obesity: a role for endogenous cannabinoids in driving appetite for palatable food? *Brain Research*, *952*(2), 232–238. https://doi.org/10.1016/s0006-8993(02)03245-6

Haslam, D. W., & James, W. P. T. (2005). Obesity. *Lancet (London, England)*, *366*(9492), 1197–1209. https://doi.org/10.1016/S0140-6736(05)67483-1

Havrankova, J., Roth, J., & Brownstein, M. (1978). Insulin receptors are widely distributed in the central nervous system of the rat. *Nature*, *272*(5656), 827–829. https://doi.org/10.1038/272827a0

Heni, M., Kullmann, S., Ketterer, C., Guthoff, M., Bayer, M., Staiger, H., Machicao, F., Häring, H.-U., Preissl, H., Veit, R., & Fritsche, A. (2014). Differential effect of glucose ingestion on the neural processing of food stimuli in lean and overweight adults. *Human Brain Mapping*, *35*(3), 918–928. https://doi.org/10.1002/hbm.22223

Heni, M., Kullmann, S., Ketterer, C., Guthoff, M., Linder, K., Wagner, R., Stingl, K. T., Veit, R., Staiger, H., Häring, H.-U., Preissl, H., & Fritsche, A. (2012). Nasal insulin changes peripheral insulin sensitivity simultaneously with altered activity in homeostatic and reward-related human brain regions. *Diabetologia*, *55*(6), 1773–1782. https://doi.org/10.1007/s00125-012-2528-y

Heni, M., Kullmann, S., Preissl, H., Fritsche, A., & Häring, H.-U. (2015). Impaired insulin action in the human brain: causes and metabolic consequences. *Nature Reviews. Endocrinology*, *11*(12), 701–711. https://doi.org/10.1038/nrendo.2015.173

Heni, M., Wagner, R., Kullmann, S., Gancheva, S., Roden, M., Peter, A., Stefan, N., Preissl, H., Häring, H. U., & Fritsche, A. (2017). Hypothalamic and striatal insulin action suppresses endogenous glucose production and may stimulate glucose uptake during hyperinsulinemia in lean but not in overweight men. *Diabetes*, *66*(7). https://doi.org/10.2337/db16-1380

Heni, M., Wagner, R., Kullmann, S., Veit, R., Mat Husin, H., Linder, K., Benkendorff, C., Peter, A., Stefan, N., Häring, H.-U., Preissl, H., & Fritsche, A. (2014). Central insulin administration improves whole-body insulin sensitivity via hypothalamus and parasympathetic outputs in men. *Diabetes*, *63*(12), 4083–4088. https://doi.org/10.2337/db14-0477

Henquin, J.-C. (2021). Non-glucose modulators of insulin secretion in healthy humans: (dis)similarities between islet and in vivo studies. *Metabolism: Clinical and Experimental*, *122*, 154821. https://doi.org/10.1016/j.metabol.2021.154821

Higuchi, S., Ohji, M., Araki, M., Furuta, R., Katsuki, M., Yamaguchi, R., Akitake, Y., Matsuyama, K., Irie, K., Mishima, K., Mishima, K., Iwasaki, K., & Fujiwara, M. (2011). Increment of hypothalamic 2-arachidonoylglycerol induces the preference for a high-fat diet via activation of cannabinoid 1 receptors. *Behavioural Brain Research*, *216*(1), 477–480. https://doi.org/10.1016/j.bbr.2010.08.042

Hill, J. O., Wyatt, H. R., & Peters, J. C. (2012). Energy balance and obesity. *Circulation*, *126*(1), 126–132. https://doi.org/10.1161/CIRCULATIONAHA.111.087213

Hirvonen, J. (2015). In vivo imaging of the cannabinoid CB1 receptor with positron emission tomography. *Clinical Pharmacology and Therapeutics*, *97*(6), 565–567. https://doi.org/10.1002/cpt.116

Hirvonen, J., Goodwin, R. S., Li, C.-T., Terry, G. E., Zoghbi, S. S., Morse, C., Pike, V. W., Volkow, N. D., Huestis, M. A., & Innis, R. B. (2012). Reversible and regionally selective downregulation of brain cannabinoid CB1 receptors in chronic daily cannabis smokers. *Molecular Psychiatry*, *17*(6), 642–649. https://doi.org/10.1038/mp.2011.82

Hirvonen, J., Virtanen, K. A., Nummenmaa, L., Hannukainen, J. C., Honka, M. J., Bucci, M., Nesterov, S. V., Parkkola, R., Rinne, J., Iozzo, P., & Nuutila, P. (2011). Effects of insulin on brain glucose metabolism in impaired glucose tolerance. *Diabetes*. https://doi.org/10.2337/db10-0940

Horton, R. W., Meldrum, B. S., & Bachelard, H. S. (1973). Enzymic and cerebral metabolic effects of 2-deoxy-D-glucose. *Journal of Neurochemistry*, *21*(3), 507–520. https://doi.org/10.1111/j.1471-4159.1973.tb05996.x

Hsiao, W.-C., Shia, K.-S., Wang, Y.-T., Yeh, Y.-N., Chang, C.-P., Lin, Y., Chen, P.-H., Wu, C.-H., Chao, Y.-S., & Hung, M.-S. (2015). A novel peripheral cannabinoid receptor 1 antagonist, BPR0912, reduces weight independently of food intake and modulates thermogenesis. *Diabetes, Obesity & Metabolism*, *17*(5), 495–504. https://doi.org/10.1111/dom.12447

Hung, C.-S., Lee, J.-K., Yang, C.-Y., Hsieh, H.-R., Ma, W.-Y., Lin, M.-S., Liu, P.-H., Shih, S.-R., Liou, J.-M., Chuang, L.-M., Chen, M.-F., Lin, J.-W., Wei, J.-N., & Li, H.-Y. (2014). Measurement of

visceral fat: should we include retroperitoneal fat? *PloS One*, *9*(11), e112355. https://doi.org/10.1371/journal.pone.0112355

Iozzo, P., Jarvisalo, M. J., Kiss, J., Borra, R., Naum, G. A., Viljanen, A., Viljanen, T., Gastaldelli, A., Buzzigoli, E., Guiducci, L., Barsotti, E., Savunen, T., Knuuti, J., Haaparanta-Solin, M., Ferrannini, E., & Nuutila, P. (2007). Quantification of liver glucose metabolism by positron emission tomography: validation study in pigs. *Gastroenterology*, *132*(2), 531–542. https://doi.org/10.1053/j.gastro.2006.12.040

Iwen, K. A., Scherer, T., Heni, M., Sayk, F., Wellnitz, T., Machleidt, F., Preissl, H., Häring, H.-U., Fritsche, A., Lehnert, H., Buettner, C., & Hallschmid, M. (2014). Intranasal insulin suppresses systemic but not subcutaneous lipolysis in healthy humans. *The Journal of Clinical Endocrinology and Metabolism*, *99*(2), E246-51. https://doi.org/10.1210/jc.2013-3169

Jais, A., & Brüning, J. C. (2017). Hypothalamic inflammation in obesity and metabolic disease. *The Journal of Clinical Investigation*, *127*(1), 24–32. https://doi.org/10.1172/JCI88878

Jastreboff, A. M., Kotz, C. M., Kahan, S., Kelly, A. S., & Heymsfield, S. B. (2019). Obesity as a Disease: The Obesity Society 2018 Position Statement. *Obesity (Silver Spring, Md.)*, *27*(1), 7–9. https://doi.org/10.1002/oby.22378

Jauch-Chara, K., Friedrich, A., Rezmer, M., Melchert, U. H., G Scholand-Engler, H., Hallschmid, M., & Oltmanns, K. M. (2012). Intranasal insulin suppresses food intake via enhancement of brain energy levels in humans. *Diabetes*, *61*(9), 2261–2268. https://doi.org/10.2337/db12-0025

Jbilo, O., Ravinet-Trillou, C., Arnone, M., Buisson, I., Bribes, E., Péleraux, A., Pénarier, G., Soubrié, P., Le Fur, G., Galiègue, S., & Casellas, P. (2005). The CB1 receptor antagonist rimonabant reverses the diet-induced obesity phenotype through the regulation of lipolysis and energy balance. *FASEB Journal : Official Publication of the Federation of American Societies for Experimental Biology*, *19*(11), 1567–1569. https://doi.org/10.1096/fj.04-3177fje

Jebb, S. A., & Moore, M. S. (1999). Contribution of a sedentary lifestyle and inactivity to the etiology of overweight and obesity: current evidence and research issues. *Medicine and Science in Sports and Exercise*, *31*(11 Suppl), S534-41. https://doi.org/10.1097/00005768-199911001-00008

Jensen, M. D., Ryan, D. H., Apovian, C. M., Ard, J. D., Comuzzie, A. G., Donato, K. A., Hu, F. B., Hubbard, V. S., Jakicic, J. M., Kushner, R. F., Loria, C. M., Millen, B. E., Nonas, C. A., Pi-Sunyer, F. X., Stevens, J., Stevens, V. J., Wadden, T. A., Wolfe, B. M., Yanovski, S. Z., … Tomaselli, G. F. (2014). 2013 AHA/ACC/TOS guideline for the management of overweight and obesity in adults: a report of the American College of Cardiology/American Heart Association Task Force on Practice Guidelines and The Obesity Society. *Circulation*, *129*(25 Suppl 2), S102-38. https://doi.org/10.1161/01.cir.0000437739.71477.ee

Jimenez-Blasco, D., Busquets-Garcia, A., Hebert-Chatelain, E., Serrat, R., Vicente-Gutierrez, C., Ioannidou, C., Gómez-Sotres, P., Lopez-Fabuel, I., Resch-Beusher, M., Resel, E., Arnouil, D., Saraswat, D., Varilh, M., Cannich, A., Julio-Kalajzic, F., Bonilla-Del Río, I., Almeida, A., Puente, N., Achicallende, S., … Marsicano, G. (2020). Glucose metabolism links astroglial mitochondria to cannabinoid effects. *Nature*, *583*(7817), 603–608. https://doi.org/10.1038/s41586-020-2470-y

Juhola, J., Magnussen, C. G., Viikari, J. S. A., Kähönen, M., Hutri-Kähönen, N., Jula, A., Lehtimäki, T., Åkerblom, H. K., Pietikäinen, M., Laitinen, T., Jokinen, E., Taittonen, L., Raitakari, O. T., & Juonala, M. (2011). Tracking of serum lipid levels, blood pressure, and body mass index from childhood to adulthood: the Cardiovascular Risk in Young Finns Study. *The Journal of Pediatrics*, *159*(4), 584–590. https://doi.org/10.1016/j.jpeds.2011.03.021

Jung, K.-M., Lin, L., & Piomelli, D. (2022). The endocannabinoid system in the adipose organ. *Reviews in Endocrine & Metabolic Disorders*, *23*(1), 51–60. https://doi.org/10.1007/s11154-020-09623-z

Juonala, M., Juhola, J., Magnussen, C. G., Würtz, P., Viikari, J. S. A., Thomson, R., Seppälä, I., Hernesniemi, J., Kähönen, M., Lehtimäki, T., Hurme, M., Telama, R., Mikkilä, V., Eklund, C., Räsänen, L., Hintsanen, M., Keltikangas-Järvinen, L., Kivimäki, M., & Raitakari, O. T. (2011). Childhood environmental and genetic predictors of adulthood obesity: the cardiovascular risk in

young Finns study. *The Journal of Clinical Endocrinology and Metabolism*, *96*(9), E1542-9. https://doi.org/10.1210/jc.2011-1243

Kahn, S. E., Hull, R. L., & Utzschneider, K. M. (2006). Mechanisms linking obesity to insulin resistance and type 2 diabetes. *Nature*, *444*(7121), 840–846. https://doi.org/10.1038/nature05482

Karczewska-Kupczewska, M., Tarasów, E., Nikolajuk, A., Stefanowicz, M., Matulewicz, N., Otziomek, E., Górska, M., Straczkowski, M., & Kowalska, I. (2013). The effect of insulin infusion on the metabolites in cerebral tissues assessed with proton magnetic resonance spectroscopy in young healthy subjects with high and low insulin sensitivity. *Diabetes Care*, *36*(9), 2787–2793. https://doi.org/10.2337/dc12-1437

Karjalainen, T., Tuisku, J., Santavirta, S., Kantonen, T., Bucci, M., Tuominen, L., Hirvonen, J., Hietala, J., Rinne, J. O., & Nummenmaa, L. (2020). Magia: Robust Automated Image Processing and Kinetic Modeling Toolbox for PET Neuroinformatics . In *Frontiers in Neuroinformatics* (Vol. 14, p. 3). https://www.frontiersin.org/article/10.3389/fninf.2020.00003

Kawai, T., Autieri, M. V, & Scalia, R. (2021). Adipose tissue inflammation and metabolic dysfunction in obesity. *American Journal of Physiology. Cell Physiology*, *320*(3), C375–C391. https://doi.org/10.1152/ajpcell.00379.2020

Kellert, B. A., Nguyen, M. C., Nguyen, C., Nguyen, Q. H., & Wagner, E. J. (2009). Estrogen rapidly attenuates cannabinoid-induced changes in energy homeostasis. *European Journal of Pharmacology*, *622*(1–3), 15–24. https://doi.org/10.1016/j.ejphar.2009.09.001

Kelley, D. E., Williams, K. V, Price, J. C., & Goodpaster, B. (1999). Determination of the lumped constant for [18F] fluorodeoxyglucose in human skeletal muscle. *Journal of Nuclear Medicine : Official Publication, Society of Nuclear Medicine*, *40*(11), 1798–1804.

Kempf, K., Hector, J., Strate, T., Schwarzloh, B., Rose, B., Herder, C., Martin, S., & Algenstaedt, P. (2007). Immune-mediated Activation of the Endocannabinoid System in Visceral Adipose Tissue in Obesity. *Hormone and Metabolic Research*, *39*(8), 596–600. https://doi.org/10.1055/s-2007-984459

Ketterer, C., Tschritter, O., Preissl, H., Heni, M., Häring, H.-U., & Fritsche, A. (2011). *Insulin sensitivity of the human brain*.

King, G. L., & Johnson, S. M. (1985). Receptor-mediated transport of insulin across endothelial cells. *Science (New York, N.Y.)*, *227*(4694), 1583–1586. https://doi.org/10.1126/science.3883490

Kishore, P., Boucai, L., Zhang, K., Li, W., Koppaka, S., Kehlenbrink, S., Schiwek, A., Esterson, Y. B., Mehta, D., Bursheh, S., Su, Y., Gutierrez-Juarez, R., Muzumdar, R., Schwartz, G. J., & Hawkins, M. (2011). Activation of K(ATP) channels suppresses glucose production in humans. *The Journal of Clinical Investigation*, *121*(12), 4916–4920. https://doi.org/10.1172/JCI58035

Kleinendorst, L., Massink, M. P. G., Cooiman, M. I., Savas, M., van der Baan-Slootweg, O. H., Roelants, R. J., Janssen, I. C. M., Meijers-Heijboer, H. J., Knoers, N. V. A. M., Ploos van Amstel, H. K., van Rossum, E. F. C., van den Akker, E. L. T., van Haaften, G., van der Zwaag, B., & van Haelst, M. M. (2018). Genetic obesity: next-generation sequencing results of 1230 patients with obesity. *Journal of Medical Genetics*, *55*(9), 578–586. https://doi.org/10.1136/jmedgenet-2018-105315

Kleinridders, A., Ferris, H. A., Cai, W., & Kahn, C. R. (2014). Insulin action in brain regulates systemic metabolism and brain function. *Diabetes*, *63*(7), 2232–2243. https://doi.org/10.2337/db14-0568

Kleinridders, A., & Pothos, E. N. (2019). Impact of Brain Insulin Signaling on Dopamine Function, Food Intake, Reward, and Emotional Behavior. *Current Nutrition Reports*, *8*(2), 83–91. https://doi.org/10.1007/s13668-019-0276-z

Koch, L., Wunderlich, F. T., Seibler, J., Könner, A. C., Hampel, B., Irlenbusch, S., Brabant, G., Kahn, C. R., Schwenk, F., & Brüning, J. C. (2008). Central insulin action regulates peripheral glucose and fat metabolism in mice. *The Journal of Clinical Investigation*, *118*(6), 2132–2147. https://doi.org/10.1172/JCI31073

Koepsell, H. (2020). Glucose transporters in brain in health and disease. In *Pflugers Archiv European Journal of Physiology* (Vol. 472, Issue 9, pp. 1299–1343). Springer. https://doi.org/10.1007/s00424-020-02441-x

Könner, A. C., & Brüning, J. C. (2012). Selective insulin and leptin resistance in metabolic disorders. *Cell Metabolism*, *16*(2), 144–152. https://doi.org/10.1016/j.cmet.2012.07.004

Könner, A. C., Janoschek, R., Plum, L., Jordan, S. D., Rother, E., Ma, X., Xu, C., Enriori, P., Hampel, B., Barsh, G. S., Kahn, C. R., Cowley, M. A., Ashcroft, F. M., & Brüning, J. C. (2007). Insulin action in AgRP-expressing neurons is required for suppression of hepatic glucose production. *Cell Metabolism*, *5*(6), 438–449. https://doi.org/10.1016/j.cmet.2007.05.004

Könner, A. C., Klöckener, T., & Brüning, J. C. (2009). Control of energy homeostasis by insulin and leptin: targeting the arcuate nucleus and beyond. *Physiology & Behavior*, *97*(5), 632–638. https://doi.org/10.1016/j.physbeh.2009.03.027

Krug, R., Mohwinkel, L., Drotleff, B., Born, J., & Hallschmid, M. (2018). Insulin and Estrogen Independently and Differentially Reduce Macronutrient Intake in Healthy Men. *The Journal of Clinical Endocrinology and Metabolism*, *103*(4), 1393–1401. https://doi.org/10.1210/jc.2017-01835

Kujala, U. M., Leskinen, T., Rottensteiner, M., Aaltonen, S., Ala-Korpela, M., Waller, K., & Kaprio, J. (2022). Physical activity and health: Findings from Finnish monozygotic twin pairs discordant for physical activity. *Scandinavian Journal of Medicine & Science in Sports*, *32*(9), 1316–1323. https://doi.org/10.1111/sms.14205

Kullmann, S., Fritsche, A., Wagner, R., Schwab, S., Häring, H.-U., Preissl, H., & Heni, M. (2017). Hypothalamic insulin responsiveness is associated with pancreatic insulin secretion in humans. *Physiology & Behavior*, *176*, 134–138. https://doi.org/10.1016/j.physbeh.2017.03.036

Kullmann, S., Heni, M., Hallschmid, M., Fritsche, A., Preissl, H., & Häring, H. U. (2016). Brain insulin resistance at the crossroads of metabolic and cognitive disorders in humans. *Physiological Reviews*, *96*(4), 1169–1209. https://doi.org/10.1152/physrev.00032.2015

Kullmann, S., Heni, M., Veit, R., Scheffler, K., Machann, J., Häring, H.-U., Fritsche, A., & Preissl, H. (2015). Selective insulin resistance in homeostatic and cognitive control brain areas in overweight and obese adults. *Diabetes Care*, *38*(6), 1044–1050. https://doi.org/10.2337/dc14-2319

Kullmann, S., Heni, M., Veit, R., Scheffler, K., Machann, J., Häring, H.-U., Fritsche, A., & Preissl, H. (2017). Intranasal insulin enhances brain functional connectivity mediating the relationship between adiposity and subjective feeling of hunger. *Scientific Reports*, *7*(1), 1627. https://doi.org/10.1038/s41598-017-01907-w

Kullmann, S., Kleinridders, A., Small, D. M., Fritsche, A., Häring, H.-U., Preissl, H., & Heni, M. (2020). Central nervous pathways of insulin action in the control of metabolism and food intake. *The Lancet. Diabetes & Endocrinology*, *8*(6), 524–534. https://doi.org/10.1016/S2213-8587(20)30113-3

Kullmann, S., Valenta, V., Wagner, R., Tschritter, O., Machann, J., Häring, H.-U., Preissl, H., Fritsche, A., & Heni, M. (2020). Brain insulin sensitivity is linked to adiposity and body fat distribution. *Nature Communications*, *11*(1), 1841. https://doi.org/10.1038/s41467-020-15686-y

Lahdenpohja, S., Keller, T., Forsback, S., Viljanen, T., Kokkomäki, E., Kivelä, R. V, Bergman, J., Solin, O., & Kirjavainen, A. K. (2020). Automated GMP production and long-term experience in radiosynthesis of CB(1) tracer [(18) F]FMPEP-d(2). *Journal of Labelled Compounds & Radiopharmaceuticals*, *63*(9), 408–418. https://doi.org/10.1002/jlcr.3845

Lahesmaa, M., Eriksson, O., Gnad, T., Oikonen, V., Bucci, M., Hirvonen, J., Koskensalo, K., Teuho, J., Niemi, T., Taittonen, M., Lahdenpohja, S., U Din, M., Haaparanta-Solin, M., Pfeifer, A., Virtanen, K. A., & Nuutila, P. (2018). Cannabinoid Type 1 Receptors Are Upregulated During Acute Activation of Brown Adipose Tissue. *Diabetes*, *67*(7), 1226–1236. https://doi.org/10.2337/db17-1366

Latva-Rasku, A. (2020). *Regulators of central and peripheral insulin sensitivity in humans*. https://urn.fi/URN:ISBN:978-951-29-8112-0

Latva-Rasku, A., Honka, M.-J., Stančáková, A., Koistinen, H. A., Kuusisto, J., Guan, L., Manning, A. K., Stringham, H., Gloyn, A. L., Lindgren, C. M., Collins, F. S., Mohlke, K. L., Scott, L. J., Karjalainen, T., Nummenmaa, L., Boehnke, M., Nuutila, P., & Laakso, M. (2018). A Partial Loss-of-Function Variant in AKT2 Is Associated With Reduced Insulin-Mediated Glucose Uptake in Multiple Insulin-Sensitive Tissues: A Genotype-Based Callback Positron Emission Tomography Study. *Diabetes*, *67*(2), 334–342. https://doi.org/10.2337/db17-1142

Lemaire, C., Damhaut, P., Lauricella, B., Mosdzianowski, C., Morelle, J. L., Monclus, M., Van Naemen, J., Mulleneers, E., Aerts, J., Plenevaux, A., Brihaye, C., & Luxen, A. (2002). Fast F-18 FDG synthesis by alkaline hydrolysis on a low polarity solid phase supports. *Journal of Labelled Compounds and Radiopharmaceuticals*, *45*(5). https://doi.org/10.1002/jlcr.572

Lenard, N. R., & Berthoud, H.-R. (2008). Central and peripheral regulation of food intake and physical activity: pathways and genes. *Obesity (Silver Spring, Md.)*, *16 Suppl 3*(Suppl 3), S11-22. https://doi.org/10.1038/oby.2008.511

Leskinen, T., Sipilä, S., Alen, M., Cheng, S., Pietiläinen, K. H., Usenius, J.-P., Suominen, H., Kovanen, V., Kainulainen, H., Kaprio, J., & Kujala, U. M. (2009). Leisure-time physical activity and high-risk fat: a longitudinal population-based twin study. *International Journal of Obesity (2005)*, *33*(11), 1211–1218. https://doi.org/10.1038/ijo.2009.170

Lewis, G. F., Carpentier, A. C., Pereira, S., Hahn, M., & Giacca, A. (2021). Direct and indirect control of hepatic glucose production by insulin. *Cell Metabolism*, *33*(4), 709–720. https://doi.org/10.1016/j.cmet.2021.03.007

Liu, Y. L., Connoley, I. P., Wilson, C. A., & Stock, M. J. (2005). Effects of the cannabinoid CB1 receptor antagonist SR141716 on oxygen consumption and soleus muscle glucose uptake in Lep(ob)/Lep(ob) mice. *International Journal of Obesity (2005)*, *29*(2), 183–187. https://doi.org/10.1038/sj.ijo.0802847

Locke, A. E., Kahali, B., Berndt, S. I., Justice, A. E., Pers, T. H., Day, F. R., Powell, C., Vedantam, S., Buchkovich, M. L., Yang, J., Croteau-Chonka, D. C., Esko, T., Fall, T., Ferreira, T., Gustafsson, S., Kutalik, Z., Luan, J., Mägi, R., Randall, J. C., … Speliotes, E. K. (2015). Genetic studies of body mass index yield new insights for obesity biology. *Nature*, *518*(7538), 197–206. https://doi.org/10.1038/nature14177

Logan, J. (2000). Graphical analysis of PET data applied to reversible and irreversible tracers. *Nuclear Medicine and Biology*, *27*(7), 661–670. https://doi.org/10.1016/s0969-8051(00)00137-2

Loos, R. J. F., & Yeo, G. S. H. (2022). The genetics of obesity: from discovery to biology. *Nature Reviews. Genetics*, *23*(2), 120–133. https://doi.org/10.1038/s41576-021-00414-z

Lu, R., Aziz, N. A., Diers, K., Stöcker, T., Reuter, M., & Breteler, M. M. B. (2021). Insulin resistance accounts for metabolic syndrome-related alterations in brain structure. *Human Brain Mapping*, *42*(8), 2434–2444. https://doi.org/10.1002/hbm.25377

Lutter, M., & Nestler, E. J. (2009). Homeostatic and hedonic signals interact in the regulation of food intake. *The Journal of Nutrition*, *139*(3), 629–632. https://doi.org/10.3945/jn.108.097618

Manaserh, I. H., Chikkamenahalli, L., Ravi, S., Dube, P. R., Park, J. J., & Hill, J. W. (2019). Ablating astrocyte insulin receptors leads to delayed puberty and hypogonadism in mice. *PLoS Biology*, *17*(3), e3000189. https://doi.org/10.1371/journal.pbio.3000189

Martinez-Tellez, B., Sanchez-Delgado, G., Boon, M. R., Rensen, P. C. N., Llamas-Elvira, J. M., & Ruiz, J. R. (2020). Distribution of Brown Adipose Tissue Radiodensity in Young Adults: Implications for Cold [18F]FDG-PET/CT Analyses. *Molecular Imaging and Biology*, *22*(2), 425–433. https://doi.org/10.1007/s11307-019-01381-y

Martins, C. J. de M., Genelhu, V., Pimentel, M. M. G., Celoria, B. M. J., Mangia, R. F., Aveta, T., Silvestri, C., Di Marzo, V., & Francischetti, E. A. (2015). Circulating Endocannabinoids and the Polymorphism 385C>A in Fatty Acid Amide Hydrolase (FAAH) Gene May Identify the Obesity Phenotype Related to Cardiometabolic Risk: A Study Conducted in a Brazilian Population of Complex Interethnic Admixture. *PloS One*, *10*(11), e0142728. https://doi.org/10.1371/journal.pone.0142728

Massa, F., Mancini, G., Schmidt, H., Steindel, F., Mackie, K., Angioni, C., Oliet, S. H. R., Geisslinger, G., & Lutz, B. (2010). Alterations in the hippocampal endocannabinoid system in diet-induced obese mice. *The Journal of Neuroscience : The Official Journal of the Society for Neuroscience*, *30*(18), 6273–6281. https://doi.org/10.1523/JNEUROSCI.2648-09.2010

Matias, I., & Di Marzo, V. (2007). Endocannabinoids and the control of energy balance. *Trends in Endocrinology & Metabolism*, *18*(1), 27–37. https://doi.org/https://doi.org/10.1016/j.tem.2006.11.006

Matias, I., Gonthier, M.-P., Orlando, P., Martiadis, V., De Petrocellis, L., Cervino, C., Petrosino, S., Hoareau, L., Festy, F., Pasquali, R., Roche, R., Maj, M., Pagotto, U., Monteleone, P., & Di Marzo, V. (2006). Regulation, function, and dysregulation of endocannabinoids in models of adipose and beta-pancreatic cells and in obesity and hyperglycemia. *The Journal of Clinical Endocrinology and Metabolism*, *91*(8), 3171–3180. https://doi.org/10.1210/jc.2005-2679

Matias, I., Petrosino, S., Racioppi, A., Capasso, R., Izzo, A. A., & Di Marzo, V. (2008). Dysregulation of peripheral endocannabinoid levels in hyperglycemia and obesity: Effect of high fat diets. *Molecular and Cellular Endocrinology*, *286*(1-2 Suppl 1), S66-78. https://doi.org/10.1016/j.mce.2008.01.026

Matias, I., Vergoni, A. V., Petrosino, S., Ottani, A., Pocai, A., Bertolini, A., & Di Marzo, V. (2008). Regulation of hypothalamic endocannabinoid levels by neuropeptides and hormones involved in food intake and metabolism: insulin and melanocortins. *Neuropharmacology*, *54*(1), 206–212. https://doi.org/10.1016/j.neuropharm.2007.06.011

Meye, F. J., Trezza, V., Vanderschuren, L. J. M. J., Ramakers, G. M. J., & Adan, R. A. H. (2013). Neutral antagonism at the cannabinoid 1 receptor: a safer treatment for obesity. *Molecular Psychiatry*, *18*(12), 1294–1301. https://doi.org/10.1038/mp.2012.145

Moore, M. C., Coate, K. C., Winnick, J. J., An, Z., & Cherrington, A. D. (2012). Regulation of hepatic glucose uptake and storage in vivo. *Advances in Nutrition (Bethesda, Md.)*, *3*(3), 286–294. https://doi.org/10.3945/an.112.002089

Muccioli, G. G. (2010). Endocannabinoid biosynthesis and inactivation, from simple to complex. *Drug Discovery Today*, *15*(11–12), 474–483. https://doi.org/10.1016/j.drudis.2010.03.007

Müller, C., Voirol, M. J., Stefanoni, N., Surmely, J. F., Jéquier, E., Gaillard, R. C., & Tappy, L. (1997). Effect of chronic intracerebroventricular infusion of insulin on brown adipose tissue activity in fed and fasted rats. *International Journal of Obesity and Related Metabolic Disorders : Journal of the International Association for the Study of Obesity*, *21*(7), 562–566. https://doi.org/10.1038/sj.ijo.0800441

Myers, M. G. J., Affinati, A. H., Richardson, N., & Schwartz, M. W. (2021). Central nervous system regulation of organismal energy and glucose homeostasis. *Nature Metabolism*, *3*(6), 737–750. https://doi.org/10.1038/s42255-021-00408-5

Myers, M. G. J., Leibel, R. L., Seeley, R. J., & Schwartz, M. W. (2010). Obesity and leptin resistance: distinguishing cause from effect. *Trends in Endocrinology and Metabolism: TEM*, *21*(11), 643–651. https://doi.org/10.1016/j.tem.2010.08.002

Natali, A., Toschi, E., Camastra, S., Gastaldelli, A., Groop, L., & Ferrannini, E. (2000). Determinants of postabsorptive endogenous glucose output in non-diabetic subjects. European Group for the Study of Insulin Resistance (EGIR). *Diabetologia*, *43*(10), 1266–1272. https://doi.org/10.1007/s001250051522

Nauck, M. A., & Meier, J. J. (2018). Incretin hormones: Their role in health and disease. *Diabetes, Obesity & Metabolism*, *20 Suppl 1*, 5–21. https://doi.org/10.1111/dom.13129

Naughton, S. S., Mathai, M. L., Hryciw, D. H., & McAinch, A. J. (2016). Linoleic acid and the pathogenesis of obesity. *Prostaglandins & Other Lipid Mediators*, *125*, 90–99. https://doi.org/10.1016/j.prostaglandins.2016.06.003

Norton, L., Shannon, C., Gastaldelli, A., & DeFronzo, R. A. (2022). Insulin: The master regulator of glucose metabolism. *Metabolism: Clinical and Experimental*, *129*, 155142. https://doi.org/10.1016/j.metabol.2022.155142

Nuutila, P., Koivisto, V. A., Knuuti, J., Ruotsalainen, U., Teräs, M., Haaparanta, M., Bergman, J., Solin, O., Voipio-Pulkki, L. M., & Wegelius, U. (1992). Glucose-free fatty acid cycle operates in human heart and skeletal muscle in vivo. *The Journal of Clinical Investigation*, *89*(6), 1767–1774. https://doi.org/10.1172/JCI115780

O'Hare, J. D., Zielinski, E., Cheng, B., Scherer, T., & Buettner, C. (2011). Central endocannabinoid signaling regulates hepatic glucose production and systemic lipolysis. *Diabetes*, *60*(4), 1055–1062. https://doi.org/10.2337/db10-0962

Obici, S., Feng, Z., Karkanias, G., Baskin, D. G., & Rossetti, L. (2002). Decreasing hypothalamic insulin receptors causes hyperphagia and insulin resistance in rats. *Nature Neuroscience*, *5*(6), 566–572. https://doi.org/10.1038/nn0602-861

Obici, S., Feng, Z., Tan, J., Liu, L., Karkanias, G., & Rossetti, L. (2001). Central melanocortin receptors regulate insulin action. *The Journal of Clinical Investigation*, *108*(7), 1079–1085. https://doi.org/10.1172/JCI12954

Obici, S., Zhang, B. B., Karkanias, G., & Rossetti, L. (2002). Hypothalamic insulin signaling is required for inhibition of glucose production. *Nature Medicine*, *8*(12), 1376–1382. https://doi.org/10.1038/nm798

Oikonen, V. (2021). *Fractional uptake rate (FUR)*. http://www.turkupetcentre.net/petanalysis/model_fur.html

Oikonen, V. (2023). *Multiple Time Graphical Analysis (MTGA)*. http://www.turkupetcentre.net/petanalysis/model_mtga.html

Olver, T. D., Grunewald, Z. I., Jurrissen, T. J., MacPherson, R. E. K., LeBlanc, P. J., Schnurbusch, T. R., Czajkowski, A. M., Laughlin, M. H., Rector, R. S., Bender, S. B., Walters, E. M., Emter, C. A., & Padilla, J. (2018). Microvascular insulin resistance in skeletal muscle and brain occurs early in the development of juvenile obesity in pigs. *American Journal of Physiology. Regulatory, Integrative and Comparative Physiology*, *314*(2), R252–R264. https://doi.org/10.1152/ajpregu.00213.2017

Ono, H., Pocai, A., Wang, Y., Sakoda, H., Asano, T., Backer, J. M., Schwartz, G. J., & Rossetti, L. (2008). Activation of hypothalamic S6 kinase mediates diet-induced hepatic insulin resistance in rats. *The Journal of Clinical Investigation*, *118*(8), 2959–2968. https://doi.org/10.1172/JCI34277

Orava, J., Nuutila, P., Lidell, M. E., Oikonen, V., Noponen, T., Viljanen, T., Scheinin, M., Taittonen, M., Niemi, T., Enerbäck, S., & Virtanen, K. A. (2011). Different metabolic responses of human brown adipose tissue to activation by cold and insulin. *Cell Metabolism*, *14*(2), 272–279. https://doi.org/10.1016/j.cmet.2011.06.012

Orava, J., Nuutila, P., Noponen, T., Parkkola, R., Viljanen, T., Enerbäck, S., Rissanen, A., Pietiläinen, K. H., & Virtanen, K. A. (2013). Blunted metabolic responses to cold and insulin stimulation in brown adipose tissue of obese humans. *Obesity (Silver Spring, Md.)*, *21*(11), 2279–2287. https://doi.org/10.1002/oby.20456

Osei-Hyiaman, D., DePetrillo, M., Pacher, P., Liu, J., Radaeva, S., Bátkai, S., Harvey-White, J., Mackie, K., Offertáler, L., Wang, L., & Kunos, G. (2005). Endocannabinoid activation at hepatic CB1 receptors stimulates fatty acid synthesis and contributes to diet-induced obesity. *The Journal of Clinical Investigation*, *115*(5), 1298–1305. https://doi.org/10.1172/JCI23057

Oussaada, S. M., van Galen, K. A., Cooiman, M. I., Kleinendorst, L., Hazebroek, E. J., van Haelst, M. M., Ter Horst, K. W., & Serlie, M. J. (2019). The pathogenesis of obesity. *Metabolism: Clinical and Experimental*, *92*, 26–36. https://doi.org/10.1016/j.metabol.2018.12.012

Pagano, C., Pilon, C., Calcagno, A., Urbanet, R., Rossato, M., Milan, G., Bianchi, K., Rizzuto, R., Bernante, P., Federspil, G., & Vettor, R. (2007). The endogenous cannabinoid system stimulates glucose uptake in human fat cells via phosphatidylinositol 3-kinase and calcium-dependent mechanisms. *The Journal of Clinical Endocrinology and Metabolism*, *92*(12), 4810–4819. https://doi.org/10.1210/jc.2007-0768

Pagotto, U., Marsicano, G., Cota, D., Lutz, B., & Pasquali, R. (2006). The emerging role of the endocannabinoid system in endocrine regulation and energy balance. *Endocrine Reviews*, *27*(1), 73–100. https://doi.org/10.1210/er.2005-0009

Paranjape, S. A., Chan, O., Zhu, W., Horblitt, A. M., McNay, E. C., Cresswell, J. A., Bogan, J. S., McCrimmon, R. J., & Sherwin, R. S. (2010). Influence of insulin in the ventromedial hypothalamus on pancreatic glucagon secretion in vivo. *Diabetes*, *59*(6), 1521–1527. https://doi.org/10.2337/db10-0014

Parlevliet, E. T., Coomans, C. P., Rensen, P. C. N., & Romijn, J. A. (2014). The Brain Modulates Insulin Sensitivity in Multiple Tissues. In P. J. D. Delhanty & A. J. van der Lely (Eds.), *How Gut and Brain Control Metabolism* (Vol. 42, p. 0). S.Karger AG. https://doi.org/10.1159/000358314

Patlak, C. S., & Blasberg, R. G. (1985). Graphical evaluation of blood-to-brain transfer constants from multiple-time uptake data. Generalizations. *Journal of Cerebral Blood Flow and Metabolism : Official Journal of the International Society of Cerebral Blood Flow and Metabolism*, *5*(4), 584–590. https://doi.org/10.1038/jcbfm.1985.87

Peltoniemi, P., Lönnroth, P., Laine, H., Oikonen, V., Tolvanen, T., Grönroos, T., Strindberg, L., Knuuti, J., & Nuutila, P. (2000). Lumped constant for [(18)F]fluorodeoxyglucose in skeletal muscles of obese and nonobese humans. *American Journal of Physiology. Endocrinology and Metabolism*, *279*(5), E1122-30. https://doi.org/10.1152/ajpendo.2000.279.5.E1122

Pereira-Miranda, E., Costa, P. R. F., Queiroz, V. A. O., Pereira-Santos, M., & Santana, M. L. P. (2017). Overweight and Obesity Associated with Higher Depression Prevalence in Adults: A Systematic Review and Meta-Analysis. *Journal of the American College of Nutrition*, *36*(3), 223–233. https://doi.org/10.1080/07315724.2016.1261053

Pertwee, R. G. (2006). The pharmacology of cannabinoid receptors and their ligands: an overview. *International Journal of Obesity (2005)*, *30 Suppl 1*, S13-8. https://doi.org/10.1038/sj.ijo.0803272

Petersen, K. F., Dufour, S., Savage, D. B., Bilz, S., Solomon, G., Yonemitsu, S., Cline, G. W., Befroy, D., Zemany, L., Kahn, B. B., Papademetris, X., Rothman, D. L., & Shulman, G. I. (2007). The role of skeletal muscle insulin resistance in the pathogenesis of the metabolic syndrome. *Proceedings of the National Academy of Sciences of the United States of America*, *104*(31), 12587–12594. https://doi.org/10.1073/pnas.0705408104

Petersen, M. C., & Shulman, G. I. (2018). Mechanisms of Insulin Action and Insulin Resistance. *Physiological Reviews*, *98*(4), 2133–2223. https://doi.org/10.1152/physrev.00063.2017

Phelps, M. E., Huang, S. C., Hoffman, E. J., Selin, C., Sokoloff, L., & Kuhl, D. E. (1979). Tomographic measurement of local cerebral glucose metabolic rate in humans with (F-18)2-fluoro-2-deoxy-D-glucose: validation of method. *Annals of Neurology*, *6*(5), 371–388. https://doi.org/10.1002/ana.410060502

Pischon, T., Boeing, H., Hoffmann, K., Bergmann, M., Schulze, M. B., Overvad, K., van der Schouw, Y. T., Spencer, E., Moons, K. G. M., Tjønneland, A., Halkjaer, J., Jensen, M. K., Stegger, J., Clavel-Chapelon, F., Boutron-Ruault, M.-C., Chajes, V., Linseisen, J., Kaaks, R., Trichopoulou, A., … Riboli, E. (2008). General and abdominal adiposity and risk of death in Europe. *The New England Journal of Medicine*, *359*(20), 2105–2120. https://doi.org/10.1056/NEJMoa0801891

Plum, L., Schubert, M., & Brüning, J. C. (2005). The role of insulin receptor signaling in the brain. In *Trends in Endocrinology and Metabolism* (Vol. 16, Issue 2, pp. 59–65). Elsevier Inc. https://doi.org/10.1016/j.tem.2005.01.008

Pocai, A., Lam, T. K. T., Gutierrez-Juarez, R., Obici, S., Schwartz, G. J., Bryan, J., Aguilar-Bryan, L., & Rossetti, L. (2005). Hypothalamic K(ATP) channels control hepatic glucose production. *Nature*, *434*(7036), 1026–1031. https://doi.org/10.1038/nature03439

Puig, J., Blasco, G., Daunis-I-Estadella, J., Molina, X., Xifra, G., Ricart, W., Pedraza, S., Fernández-Aranda, F., & Fernández-Real, J. M. (2015). Hypothalamic damage is associated with inflammatory markers and worse cognitive performance in obese subjects. *The Journal of Clinical Endocrinology and Metabolism*, *100*(2), E276-81. https://doi.org/10.1210/jc.2014-2682

Qayyum, A., Chen, D. M., Breiman, R. S., Westphalen, A. C., Yeh, B. M., Jones, K. D., Lu, Y., Coakley, F. V, & Callen, P. W. (2009). Evaluation of diffuse liver steatosis by ultrasound, computed tomography, and magnetic resonance imaging: which modality is best? *Clinical Imaging*, *33*(2), 110–115. https://doi.org/10.1016/j.clinimag.2008.06.036

Quarta, C., Mazza, R., Obici, S., Pasquali, R., & Pagotto, U. (2011). Energy balance regulation by endocannabinoids at central and peripheral levels. *Trends in Molecular Medicine*, *17*(9), 518–526. https://doi.org/10.1016/j.molmed.2011.05.002

Radziuk, J., & Pye, S. (2002). Quantitation of basal endogenous glucose production in Type II diabetes: Importance of the volume of distribution. In *Diabetologia*. https://doi.org/10.1007/s00125-002-0841-6

Ramage, L. E., Akyol, M., Fletcher, A. M., Forsythe, J., Nixon, M., Carter, R. N., van Beek, E. J. R., Morton, N. M., Walker, B. R., & Stimson, R. H. (2016). Glucocorticoids Acutely Increase Brown Adipose Tissue Activity in Humans, Revealing Species-Specific Differences in UCP-1 Regulation. *Cell Metabolism*, *24*(1), 130–141. https://doi.org/10.1016/j.cmet.2016.06.011

Ramnanan, C. J., Saraswathi, V., Smith, M. S., Donahue, E. P., Farmer, B., Farmer, T. D., Neal, D., Williams, P. E., Lautz, M., Mari, A., Cherrington, A. D., & Edgerton, D. S. (2011). Brain insulin action augments hepatic glycogen synthesis without suppressing glucose production or gluconeogenesis in dogs. *The Journal of Clinical Investigation*, *121*(9), 3713–3723. https://doi.org/10.1172/JCI45472

Rebelos, E. (2020). *Novel aspects of insulin resistance: focus on the brain. Studies using positron emission tomography*. https://urn.fi/URN:ISBN:978-951-29-8151-9

Rebelos, E., Bucci, M., Karjalainen, T., Oikonen, V., Bertoldo, A., Hannukainen, J. C., Virtanen, K. A., Latva-Rasku, A., Hirvonen, J., Heinonen, I., Parkkola, R., Laakso, M., Ferrannini, E., Iozzo, P., Nummenmaa, L., & Nuutila, P. (2021). Insulin Resistance Is Associated With Enhanced Brain Glucose Uptake During Euglycemic Hyperinsulinemia: A Large-Scale PET Cohort. *Diabetes Care*, *44*(3), 788–794. https://doi.org/10.2337/dc20-1549

Rebelos, E., Immonen, H., Bucci, M., Hannukainen, J. C., Nummenmaa, L., Honka, M. J., Soinio, M., Salminen, P., Ferrannini, E., Iozzo, P., & Nuutila, P. (2019). Brain glucose uptake is associated with endogenous glucose production in obese patients before and after bariatric surgery and predicts metabolic outcome at follow-up. *Diabetes, Obesity and Metabolism*, *21*(2), 218–226. https://doi.org/10.1111/dom.13501

Rebelos, E., Mari, A., Bucci, M., Honka, M.-J., Hannukainen, J. C., Virtanen, K. A., Hirvonen, J., Nummenmaa, L., Heni, M., Iozzo, P., Ferrannini, E., & Nuutila, P. (2020). Brain substrate metabolism and ß-cell function in humans: A positron emission tomography study. *Endocrinology, Diabetes & Metabolism*, *3*(3), e00136. https://doi.org/10.1002/edm2.136

Ren, H., Lu, T. Y., McGraw, T. E., & Accili, D. (2015). Anorexia and impaired glucose metabolism in mice with hypothalamic ablation of Glut4 neurons. *Diabetes*, *64*(2), 405–417. https://doi.org/10.2337/db14-0752

Reno, C. M., Puente, E. C., Sheng, Z., Daphna-Iken, D., Bree, A. J., Routh, V. H., Kahn, B. B., & Fisher, S. J. (2017). Brain GLUT4 Knockout Mice Have Impaired Glucose Tolerance, Decreased Insulin Sensitivity, and Impaired Hypoglycemic Counterregulation. *Diabetes*, *66*(3), 587–597. https://doi.org/10.2337/db16-0917

Repple, J., Opel, N., Meinert, S., Redlich, R., Hahn, T., Winter, N. R., Kaehler, C., Emden, D., Leenings, R., Grotegerd, D., Zaremba, D., Bürger, C., Förster, K., Dohm, K., Enneking, V., Leehr, E. J., Böhnlein, J., Karliczek, G., Heindel, W., … Dannlowski, U. (2018). Elevated body-mass index is associated with reduced white matter integrity in two large independent cohorts. *Psychoneuroendocrinology*, *91*, 179–185. https://doi.org/10.1016/j.psyneuen.2018.03.007

Richard, D., Guesdon, B., & Timofeeva, E. (2009). The brain endocannabinoid system in the regulation of energy balance. *Best Practice & Research. Clinical Endocrinology & Metabolism*, *23*(1), 17–32. https://doi.org/10.1016/j.beem.2008.10.007

Rinaldi-Carmona, M., Barth, F., Héaulme, M., Shire, D., Calandra, B., Congy, C., Martinez, S., Maruani, J., Néliat, G., & Caput, D. (1994). SR141716A, a potent and selective antagonist of the brain cannabinoid receptor. *FEBS Letters*, *350*(2–3), 240–244. https://doi.org/10.1016/0014-5793(94)00773-x

Roden, M., & Shulman, G. I. (2019). The integrative biology of type 2 diabetes. *Nature*, *576*(7785), 51–60. https://doi.org/10.1038/s41586-019-1797-8

Roh, E., Song, D. K., & Kim, M.-S. (2016). Emerging role of the brain in the homeostatic regulation of energy and glucose metabolism. *Experimental & Molecular Medicine*, *48*(3), e216. https://doi.org/10.1038/emm.2016.4

Rolfe, D. F., & Brown, G. C. (1997). Cellular energy utilization and molecular origin of standard metabolic rate in mammals. *Physiological Reviews*, *77*(3), 731–758. https://doi.org/10.1152/physrev.1997.77.3.731

Rosario, W., Singh, I., Wautlet, A., Patterson, C., Flak, J., Becker, T. C., Ali, A., Tamarina, N., Philipson, L. H., Enquist, L. W., Myers, M. G. J., & Rhodes, C. J. (2016). The Brain-to-Pancreatic Islet Neuronal Map Reveals Differential Glucose Regulation From Distinct Hypothalamic Regions. *Diabetes*, *65*(9), 2711–2723. https://doi.org/10.2337/db15-0629

Saltiel, A. R., & Kahn, C. R. (2001). Insulin signalling and the regulation of glucose and lipid metabolism. *Nature*, *414*(6865), 799–806. https://doi.org/10.1038/414799a

Sam, A. H., Salem, V., & Ghatei, M. A. (2011). Rimonabant: From RIO to Ban. *Journal of Obesity*, *2011*, 432607. https://doi.org/10.1155/2011/432607

Samuel, V. T., & Shulman, G. I. (2016). The pathogenesis of insulin resistance: integrating signaling pathways and substrate flux. *The Journal of Clinical Investigation*, *126*(1), 12–22. https://doi.org/10.1172/JCI77812

Sanchez-Alavez, M., Tabarean, I. V, Osborn, O., Mitsukawa, K., Schaefer, J., Dubins, J., Holmberg, K. H., Klein, I., Klaus, J., Gomez, L. F., Kolb, H., Secrest, J., Jochems, J., Myashiro, K., Buckley, P., Hadcock, J. R., Eberwine, J., Conti, B., & Bartfai, T. (2010). Insulin causes hyperthermia by direct inhibition of warm-sensitive neurons. *Diabetes*, *59*(1), 43–50. https://doi.org/10.2337/db09-1128

Sarzani, R., Bordicchia, M., Marcucci, P., Bedetta, S., Santini, S., Giovagnoli, A., Scappini, L., Minardi, D., Muzzonigro, G., Dessì-Fulgheri, P., & Rappelli, A. (2009). Altered pattern of cannabinoid type 1 receptor expression in adipose tissue of dysmetabolic and overweight patients. *Metabolism: Clinical and Experimental*, *58*(3), 361–367. https://doi.org/10.1016/j.metabol.2008.10.009

Scherer, T., Lindtner, C., O'Hare, J., Hackl, M., Zielinski, E., Freudenthaler, A., Baumgartner-Parzer, S., Tödter, K., Heeren, J., Krššák, M., Scheja, L., Fürnsinn, C., & Buettner, C. (2016). Insulin Regulates Hepatic Triglyceride Secretion and Lipid Content via Signaling in the Brain. *Diabetes*, *65*(6), 1511–1520. https://doi.org/10.2337/db15-1552

Scherer, T., O'Hare, J., Diggs-Andrews, K., Schweiger, M., Cheng, B., Lindtner, C., Zielinski, E., Vempati, P., Su, K., Dighe, S., Milsom, T., Puchowicz, M., Scheja, L., Zechner, R., Fisher, S. J., Previs, S. F., & Buettner, C. (2011). Brain insulin controls adipose tissue lipolysis and lipogenesis. *Cell Metabolism*, *13*(2), 183–194. https://doi.org/10.1016/j.cmet.2011.01.008

Scherer, T., Sakamoto, K., & Buettner, C. (2021). Brain insulin signalling in metabolic homeostasis and disease. *Nature Reviews. Endocrinology*, *17*(8), 468–483. https://doi.org/10.1038/s41574-021-00498-x

Schmid, V., Kullmann, S., Gfrörer, W., Hund, V., Hallschmid, M., Lipp, H.-P., Häring, H.-U., Preissl, H., Fritsche, A., & Heni, M. (2018). Safety of intranasal human insulin: A review. *Diabetes, Obesity & Metabolism*, *20*(7), 1563–1577. https://doi.org/10.1111/dom.13279

Schneiter, P., Gillet, M., Chioléro, R., Wauters, J. P., Berger, M., & Tappy, L. (2000). Postprandial hepatic glycogen synthesis in liver transplant recipients. *Transplantation*, *69*(5), 978–981. https://doi.org/10.1097/00007890-200003150-00052

Segal, S. S., White, T. P., & Faulkner, J. A. (1986). Architecture, composition, and contractile properties of rat soleus muscle grafts. *The American Journal of Physiology*, *250*(3 Pt 1), C474-9. https://doi.org/10.1152/ajpcell.1986.250.3.C474

Seong, J., Kang, J. Y., Sun, J. S., & Kim, K. W. (2019). Hypothalamic inflammation and obesity: a mechanistic review. *Archives of Pharmacal Research*, *42*(5), 383–392. https://doi.org/10.1007/s12272-019-01138-9

Sewaybricker, L. E., Huang, A., Chandrasekaran, S., Melhorn, S. J., & Schur, E. A. (2023). The Significance of Hypothalamic Inflammation and Gliosis for the Pathogenesis of Obesity in Humans. *Endocrine Reviews*, *44*(2), 281–296. https://doi.org/10.1210/endrev/bnac023

Shin, A. C., Filatova, N., Lindtner, C., Chi, T., Degann, S., Oberlin, D., & Buettner, C. (2017). Insulin Receptor Signaling in POMC, but Not AgRP, Neurons Controls Adipose Tissue Insulin Action. *Diabetes*, *66*(6), 1560–1571. https://doi.org/10.2337/db16-1238

Silventoinen, K., & Konttinen, H. (2020). Obesity and eating behavior from the perspective of twin and genetic research. *Neuroscience and Biobehavioral Reviews*, *109*, 150–165. https://doi.org/10.1016/j.neubiorev.2019.12.012

Silvestri, C., & Di Marzo, V. (2013). The endocannabinoid system in energy homeostasis and the etiopathology of metabolic disorders. *Cell Metabolism*, *17*(4), 475–490. https://doi.org/10.1016/j.cmet.2013.03.001

Simon, V., & Cota, D. (2017). MECHANISMS IN ENDOCRINOLOGY: Endocannabinoids and metabolism: past, present and future. *European Journal of Endocrinology*, *176*(6), R309–R324. https://doi.org/10.1530/EJE-16-1044

Sink, K. S., McLaughlin, P. J., Wood, J. A. T., Brown, C., Fan, P., Vemuri, V. K., Peng, Y., Olszewska, T., Thakur, G. A., Makriyannis, A., Parker, L. A., & Salamone, J. D. (2008). The novel cannabinoid CB1 receptor neutral antagonist AM4113 suppresses food intake and food-reinforced behavior but does not induce signs of nausea in rats. *Neuropsychopharmacology : Official Publication of the American College of Neuropsychopharmacology*, *33*(4), 946–955. https://doi.org/10.1038/sj.npp.1301476

Snyder, W., Cook, M., Nasset, E., Karhausen, L., Howells, G., & Tipton, I. (1975). *Report of the Task Group on Reference Man. A report prepaired by a task group of committee 2 of the international commission on radiological protection*. Pergamon Press.

Soininen, P., Kangas, A. J., Würtz, P., Suna, T., & Ala-Korpela, M. (2015). Quantitative serum nuclear magnetic resonance metabolomics in cardiovascular epidemiology and genetics. *Circulation. Cardiovascular Genetics*, *8*(1), 192–206. https://doi.org/10.1161/CIRCGENETICS.114.000216

Song, C. K., Jackson, R. M., Harris, R. B. S., Richard, D., & Bartness, T. J. (2005). Melanocortin-4 receptor mRNA is expressed in sympathetic nervous system outflow neurons to white adipose tissue. *American Journal of Physiology. Regulatory, Integrative and Comparative Physiology*, *289*(5), R1467-76. https://doi.org/10.1152/ajpregu.00348.2005

Sparks, J. D., & Dong, H. H. (2009). FoxO1 and hepatic lipid metabolism. *Current Opinion in Lipidology*, *20*(3), 217–226. https://doi.org/10.1097/MOL.0b013e32832b3f4c

Spiegelman, B. M., & Flier, J. S. (2001). Obesity and the regulation of energy balance. *Cell*, *104*(4), 531–543. https://doi.org/10.1016/s0092-8674(01)00240-9

Stoeckel, L. E., Weller, R. E., Cook, E. W. 3rd, Twieg, D. B., Knowlton, R. C., & Cox, J. E. (2008). Widespread reward-system activation in obese women in response to pictures of high-calorie foods. *NeuroImage*, *41*(2), 636–647. https://doi.org/10.1016/j.neuroimage.2008.02.031

Stouffer, M. A., Woods, C. A., Patel, J. C., Lee, C. R., Witkovsky, P., Bao, L., Machold, R. P., Jones, K. T., de Vaca, S. C., Reith, M. E. A., Carr, K. D., & Rice, M. E. (2015). Insulin enhances striatal dopamine release by activating cholinergic interneurons and thereby signals reward. *Nature Communications*, *6*, 8543. https://doi.org/10.1038/ncomms9543

Szczepaniak, L. S., Nurenberg, P., Leonard, D., Browning, J. D., Reingold, J. S., Grundy, S., Hobbs, H. H., & Dobbins, R. L. (2005). Magnetic resonance spectroscopy to measure hepatic triglyceride

content: prevalence of hepatic steatosis in the general population. *American Journal of Physiology. Endocrinology and Metabolism*, *288*(2), E462-8. https://doi.org/10.1152/ajpendo.00064.2004

Takkinen, J. S., López-Picón, F. R., Kirjavainen, A. K., Pihlaja, R., Snellman, A., Ishizu, T., Löyttyniemi, E., Solin, O., Rinne, J. O., & Haaparanta-Solin, M. (2018). [(18)F]FMPEP-d(2) PET imaging shows age- and genotype-dependent impairments in the availability of cannabinoid receptor 1 in a mouse model of Alzheimer's disease. *Neurobiology of Aging*, *69*, 199–208. https://doi.org/10.1016/j.neurobiolaging.2018.05.013

Tam, J., Cinar, R., Liu, J., Godlewski, G., Wesley, D., Jourdan, T., Szanda, G., Mukhopadhyay, B., Chedester, L., Liow, J.-S., Innis, R. B., Cheng, K., Rice, K. C., Deschamps, J. R., Chorvat, R. J., McElroy, J. F., & Kunos, G. (2012). Peripheral cannabinoid-1 receptor inverse agonism reduces obesity by reversing leptin resistance. *Cell Metabolism*, *16*(2), 167–179. https://doi.org/10.1016/j.cmet.2012.07.002

Tam, J., Szanda, G., Drori, A., Liu, Z., Cinar, R., Kashiwaya, Y., Reitman, M. L., & Kunos, G. (2017). Peripheral cannabinoid-1 receptor blockade restores hypothalamic leptin signaling. *Molecular Metabolism*, *6*(10), 1113–1125. https://doi.org/10.1016/j.molmet.2017.06.010

Tam, J., Vemuri, V. K., Liu, J., Bátkai, S., Mukhopadhyay, B., Godlewski, G., Osei-Hyiaman, D., Ohnuma, S., Ambudkar, S. V, Pickel, J., Makriyannis, A., & Kunos, G. (2010). Peripheral CB1 cannabinoid receptor blockade improves cardiometabolic risk in mouse models of obesity. *The Journal of Clinical Investigation*, *120*(8), 2953–2966. https://doi.org/10.1172/JCI42551

Tarragon, E., & Moreno, J. J. (2017). Role of Endocannabinoids on Sweet Taste Perception, Food Preference, and Obesity-related Disorders. *Chemical Senses*, *43*(1), 3–16. https://doi.org/10.1093/chemse/bjx062

Terry, G. E., Hirvonen, J., Liow, J.-S., Seneca, N., Tauscher, J. T., Schaus, J. M., Phebus, L., Felder, C. C., Morse, C. L., Pike, V. W., Halldin, C., & Innis, R. B. (2010). Biodistribution and dosimetry in humans of two inverse agonists to image cannabinoid CB1 receptors using positron emission tomography. *European Journal of Nuclear Medicine and Molecular Imaging*, *37*(8), 1499–1506. https://doi.org/10.1007/s00259-010-1411-7

Terry, G. E., Hirvonen, J., Liow, J.-S., Zoghbi, S. S., Gladding, R., Tauscher, J. T., Schaus, J. M., Phebus, L., Felder, C. C., Morse, C. L., Donohue, S. R., Pike, V. W., Halldin, C., & Innis, R. B. (2010). Imaging and quantitation of cannabinoid CB1 receptors in human and monkey brains using (18)F-labeled inverse agonist radioligands. *Journal of Nuclear Medicine : Official Publication, Society of Nuclear Medicine*, *51*(1), 112—120. https://doi.org/10.2967/jnumed.109.067074

Thaler, J. P., Yi, C.-X., Schur, E. A., Guyenet, S. J., Hwang, B. H., Dietrich, M. O., Zhao, X., Sarruf, D. A., Izgur, V., Maravilla, K. R., Nguyen, H. T., Fischer, J. D., Matsen, M. E., Wisse, B. E., Morton, G. J., Horvath, T. L., Baskin, D. G., Tschöp, M. H., & Schwartz, M. W. (2012). Obesity is associated with hypothalamic injury in rodents and humans. *The Journal of Clinical Investigation*, *122*(1), 153–162. https://doi.org/10.1172/JCI59660

Thie, J. A. (1995). Clarification of a fractional uptake concept. In *Journal of nuclear medicine : official publication, Society of Nuclear Medicine* (Vol. 36, Issue 4, pp. 711–712).

Thorens, B. (2015). GLUT2, glucose sensing and glucose homeostasis. *Diabetologia*, *58*(2), 221–232. https://doi.org/10.1007/s00125-014-3451-1

Timper, K., & Brüning, J. C. (2017). Hypothalamic circuits regulating appetite and energy homeostasis: pathways to obesity. *Disease Models & Mechanisms*, *10*(6), 679–689. https://doi.org/10.1242/dmm.026609

Titchenell, P. M., Lazar, M. A., & Birnbaum, M. J. (2017). Unraveling the Regulation of Hepatic Metabolism by Insulin. *Trends in Endocrinology and Metabolism: TEM*, *28*(7), 497–505. https://doi.org/10.1016/j.tem.2017.03.003

Tschritter, O., Preissl, H., Hennige, A. M., Sartorius, T., Grichisch, Y., Stefan, N., Guthoff, M., Düsing, S., Machann, J., Schleicher, E., Cegan, A., Birbaumer, N., Fritsche, A., & Häring, H.-U. (2009). The insulin effect on cerebrocortical theta activity is associated with serum concentrations of

saturated nonesterified Fatty acids. *The Journal of Clinical Endocrinology and Metabolism*, *94*(11), 4600–4607. https://doi.org/10.1210/jc.2009-0469

Tschritter, O., Preissl, H., Hennige, A. M., Stumvoll, M., Porubska, K., Frost, R., Marx, H., Klösel, B., Lutzenberger, W., Birbaumer, N., Häring, H.-U., & Fritsche, A. (2006). The cerebrocortical response to hyperinsulinemia is reduced in overweight humans: a magnetoencephalographic study. *Proceedings of the National Academy of Sciences of the United States of America*, *103*(32), 12103–12108. https://doi.org/10.1073/pnas.0604404103

Tuominen, L., Nummenmaa, L., Keltikangas-Järvinen, L., Raitakari, O., & Hietala, J. (2014). Mapping neurotransmitter networks with PET: an example on serotonin and opioid systems. *Human Brain Mapping*, *35*(5), 1875–1884. https://doi.org/10.1002/hbm.22298

Turkington, T. G. (2001). Introduction to PET instrumentation. *Journal of Nuclear Medicine Technology*, *29*(1), 4–11.

Tuulari, J. J., Karlsson, H. K., Hirvonen, J., Hannukainen, J. C., Bucci, M., Helmiö, M., Ovaska, J., Soinio, M., Salminen, P., Savisto, N., Nummenmaa, L., & Nuutila, P. (2013). Weight loss after bariatric surgery reverses insulin-induced increases in brain glucose metabolism of the morbidly obese. *Diabetes*, *62*(8), 2747–2751. https://doi.org/10.2337/db12-1460

van Schaftingen, E., & Gerin, I. (2002). The glucose-6-phosphatase system. *The Biochemical Journal*, *362*(Pt 3), 513–532. https://doi.org/10.1042/0264-6021:3620513

Virtanen, K. A., Lönnroth, P., Parkkola, R., Peltoniemi, P., Asola, M., Viljanen, T., Tolvanen, T., Knuuti, J., Rönnemaa, T., Huupponen, R., & Nuutila, P. (2002). Glucose uptake and perfusion in subcutaneous and visceral adipose tissue during insulin stimulation in nonobese and obese humans. *The Journal of Clinical Endocrinology and Metabolism*, *87*(8), 3902–3910. https://doi.org/10.1210/jcem.87.8.8761

Virtanen, K. A., Peltoniemi, P., Marjamäki, P., Asola, M., Strindberg, L., Parkkola, R., Huupponen, R., Knuuti, J., Lönnroth, P., & Nuutila, P. (2001). Human adipose tissue glucose uptake determined using [18 F]-fluoro-deoxy-glucose ([18 F]FDG) and PET in combination with microdialysis. In *Diabetologia* (Vol. 44).

Vogt, M. C., Paeger, L., Hess, S., Steculorum, S. M., Awazawa, M., Hampel, B., Neupert, S., Nicholls, H. T., Mauer, J., Hausen, A. C., Predel, R., Kloppenburg, P., Horvath, T. L., & Brüning, J. C. (2014). Neonatal insulin action impairs hypothalamic neurocircuit formation in response to maternal high-fat feeding. *Cell*, *156*(3), 495–509. https://doi.org/10.1016/j.cell.2014.01.008

Waise, T. M. Z., Toshinai, K., Naznin, F., NamKoong, C., Md Moin, A. S., Sakoda, H., & Nakazato, M. (2015). One-day high-fat diet induces inflammation in the nodose ganglion and hypothalamus of mice. *Biochemical and Biophysical Research Communications*, *464*(4), 1157–1162. https://doi.org/10.1016/j.bbrc.2015.07.097

Wajchenberg, B. L. (2000). Subcutaneous and visceral adipose tissue: their relation to the metabolic syndrome. *Endocrine Reviews*, *21*(6), 697–738. https://doi.org/10.1210/edrv.21.6.0415

Wang, G. J., Volkow, N. D., Logan, J., Pappas, N. R., Wong, C. T., Zhu, W., Netusil, N., & Fowler, J. S. (2001). Brain dopamine and obesity. *Lancet (London, England)*, *357*(9253), 354–357. https://doi.org/10.1016/s0140-6736(00)03643-6

Watanabe, S., Doshi, M., & Hamazaki, T. (2003). n-3 Polyunsaturated fatty acid (PUFA) deficiency elevates and n-3 PUFA enrichment reduces brain 2-arachidonoylglycerol level in mice. *Prostaglandins, Leukotrienes, and Essential Fatty Acids*, *69*(1), 51–59. https://doi.org/10.1016/s0952-3278(03)00056-5

Weiss, M., Steiner, D. F., & Philipson, L. H. (2000). *Insulin Biosynthesis, Secretion, Structure, and Structure-Activity Relationships.* (K. R. Feingold, B. Anawalt, M. R. Blackman, A. Boyce, G. Chrousos, E. Corpas, W. W. de Herder, K. Dhatariya, K. Dungan, J. Hofland, S. Kalra, G. Kaltsas, N. Kapoor, C. Koch, P. Kopp, M. Korbonits, C. S. Kovacs, W. Kuohung, B. Laferrère, … D. P. Wilson (Eds.)).

White, H., & Venkatesh, B. (2011). Clinical review: ketones and brain injury. *Critical Care (London, England)*, *15*(2), 219. https://doi.org/10.1186/cc10020

Whitlock, G., Lewington, S., Sherliker, P., Clarke, R., Emberson, J., Halsey, J., Qizilbash, N., Collins, R., & Peto, R. (2009). Body-mass index and cause-specific mortality in 900 000 adults: collaborative analyses of 57 prospective studies. *Lancet (London, England)*, *373*(9669), 1083–1096. https://doi.org/10.1016/S0140-6736(09)60318-4

WHO. (2021). World Health Organization (WHO), Obesity and Overweight. https://www.who.int/news-room/fact-sheets/detail/obesity-and-overweight

Wilson, J. L., & Enriori, P. J. (2015). A talk between fat tissue, gut, pancreas and brain to control body weight. *Molecular and Cellular Endocrinology*, *418 Pt 2*, 108–119. https://doi.org/10.1016/j.mce.2015.08.022

Woods, S. C., & Porte, D. J. (1975). Effect of intracisternal insulin on plasma glucose and insulin in the dog. *Diabetes*, *24*(10), 905–909. https://doi.org/10.2337/diab.24.10.905

Woods, S. C., Seeley, R. J., Baskin, D. G., & Schwartz, M. W. (2003). Insulin and the blood-brain barrier. *Current Pharmaceutical Design*, *9*(10), 795–800. https://doi.org/10.2174/1381612033455323

World Obesity. (2023). The World Obesity Federation (World Obesity), World Obesity Atlas 2023. https://data.worldobesity.org/publications/?cat=19

Wu, H.-M., Bergsneider, M., Glenn, T. C., Yeh, E., Hovda, D. A., Phelps, M. E., & Huang, S.-C. (2003). Measurement of the global lumped constant for 2-deoxy-2-[18F]fluoro-D-glucose in normal human brain using [15O]water and 2-deoxy-2-[18F]fluoro-D-glucose positron emission tomography imaging. A method with validation based on multiple methodologies. *Molecular Imaging and Biology*, *5*(1), 32–41. https://doi.org/10.1016/s1536-1632(02)00122-1

Yan, Z. C., Liu, D. Y., Zhang, L. L., Shen, C. Y., Ma, Q. L., Cao, T. B., Wang, L. J., Nie, H., Zidek, W., Tepel, M., & Zhu, Z. M. (2007). Exercise reduces adipose tissue via cannabinoid receptor type 1 which is regulated by peroxisome proliferator-activated receptor-delta. *Biochemical and Biophysical Research Communications*, *354*(2), 427–433. https://doi.org/10.1016/j.bbrc.2006.12.213

You, T., Disanzo, B. L., Wang, X., Yang, R., & Gong, D. (2011). Adipose tissue endocannabinoid system gene expression: depot differences and effects of diet and exercise. *Lipids in Health and Disease*, *10*, 194. https://doi.org/10.1186/1476-511X-10-194

Zhang, M., Hu, T., Zhang, S., & Zhou, L. (2015). Associations of Different Adipose Tissue Depots with Insulin Resistance: A Systematic Review and Meta-analysis of Observational Studies. *Scientific Reports*, *5*, 18495. https://doi.org/10.1038/srep18495

TURUN
YLIOPISTO
UNIVERSITY
OF TURKU

Painosalama, Turku, Finland 2023

ISBN 978-951-29-9574-5 (PRINT)
ISBN 978-951-29-9575-2 (PDF)
ISSN 0355-9483 (Print)
ISSN 2343-3213 (Online)